

ABSTRACT

Title of Document: GENOME-WIDE ANALYSIS OF CHICKEN MIRNAS AND DNA METHYLATION AND THEIR ROLES IN MAREK'S DISEASE RESISTANCE AND SUSCEPTIBILITY.

Fei Tian,

Doctor of Philosophy, 2012

Directed By: Associate Professor Dr. Jiuzhou Song,
Department of Animal and Avian Sciences

Marek's disease (MD) is a T cell lymphoma in chickens and causes high mortality and morbidity in productive chickens. Two inbred chicken lines, resistant line 6₃ and susceptible line 7₂, with the same MHC haplotype, showed distinct disease outcomes after MDV infection. The current studies aimed to illustrate the role of microRNA (miRNAs) and DNA methylation in MD resistance and susceptibility in chickens. First, to ascertain the function of miRNAs, miRNA microarray experiments

were used to identify miRNAs sensitive to MDV infection in the 2 lines. Most miRNAs were repressed in line 7₂ after MDV infection, while their transcription was steady in line 6₃. The miRNA target genes were identified in chickens. Cellular miRNA *gga-miR-15b* and *gga-let-7i* were reduced in infected line 7₂ chickens and MD tumors. The downregulation of the two miRNAs increased the expression of *ATF2* (activating transcription factor 2) and *DNMT3a* (DNA methyltransferase 3a) in infected line 7₂. These results indicated that miRNAs may play antiviral functions through modulating target gene expression. Next, to characterize the role of miRNAs in MDV infection, the selected chicken miRNAs were overexpressed in MDV infected DF-1 cells. The overexpressions of chicken miRNA *gga-miR-15b* and *gga-let-7i*, by using the retroviral based vector, significantly restricted MDV replications *in vitro*. MDV oncoprotein was repressed, suggesting that chicken miRNAs may limit MDV propagation. Finally, we found deregulation of transcription of *DNA methyltransferases* (DNMTs) in lines 6₃ and 7₂ after MDV infection, which coordinated with the methylation alterations in the 2 lines. Infection induced differential methylation regions (iDMRs) that were identified through genome-wide DNA methylation quantification. Genes overlapping line-specific iDMRs were related with pathways of different functions in these two lines, implying the involvement of DNA methylation in MD- resistance and susceptibility. An *in vitro* study showed that DNA methylation inhibitor repressed viral spread and viral replication. In conclusion, the observed variations of miRNA expression and DNA methylation may be associated with disease predisposition in chickens.

GENOME-WIDE ANALYSIS OF CHICKEN MIRNAS AND DNA
METHYLATION AND THEIR ROLES IN MAREK'S DISEASE
RESISTANCE AND SUSCEPTIBILITY

By

Fei Tian

Dissertation submitted to the Faculty of the Graduate School of the
University of Maryland, College Park, in partial fulfillment
of the requirements for the degree of
Doctor of Philosophy

2012

Advisory Committee:

Associate Professor Dr. Jiuzhou Song, Chair
Research Biologist Dr. George Liu
Associate Professor Dr. Stephen Mount
Professor Dr. Tom Porter
Investigator Dr. Sige Zou

© Copyright by

Fei Tian

2012

Acknowledgements

This dissertation work would have been possible without the expert guidance of my advisor Dr. Jiuzhou Song. I remembered how great I felt when he accepted me as a Ph.D student even I knew nothing about the epigenetics. He always encourages me to try different ideas and gives me consistent support. His guidance is an invaluable experience and will be greatly appreciated throughout my life.

I would like to express my deep appreciation to all my advisory committee, Dr. George Liu, Dr. Stephen Mount, Dr. Tom Porter, and Dr. Sige Zou, for their willingness to serve on the committee and their inspiring ideas, encouraged words and helpful suggestions. Their constructive criticisms greatly improved the dissertation work.

I would like to gratefully acknowledge all the lab members: Dr. Juan Luo, Apratim Mitra, Fei Zhan, Jose and former members Dr. Ying Yu, Dr. Yali Hou Chunping Zhao and Ping Yuan. I could not complete my Ph.D studies without your advice, assistance and encouragement. Your friendship will be treasured throughout my lifetime.

Many thanks go to all my friends in China and here at University of Maryland for their supporting and having confidence on me. Life would be lonely without their concern and friendship.

Finally, I would like to thank my parents, grandparents, and husband. Words cannot express my gratitude and love to them. I want to thank to my parents for letting me studying overseas and their support and understanding. I owe my gratitude

to my grandparents for their encouragement to letting me pursuing my dream. I am indebted to my husband Qien for helping me keep things in perspective and sharing the excited and frustrated moment together.

Table of Contents

Acknowledgements	ii
Table of Contents	iv
List of Tables	vii
List of Figures	viii
List of Abbreviations	x
Chapter 1: Literature Review	1
Introduction.....	1
Marek's disease resistance in chickens.....	2
Pathogenesis of Marek's disease virus infection	2
Immunity to Marek's disease.....	7
Marek's disease resistance and susceptibility.....	10
MicroRNAs in Animal Health	13
MicroRNAs Biogenesis	13
Post-transcriptional repression by miRNAs.....	16
Functions of MicroRNAs in immunology	18
Chicken and MDV microRNAs.....	21
DNA Methylation	24
The regulation of DNA methylation	24
The biological functions of DNA methylation	27
DNA methylation and miRNAs in diseases.....	30
Rationale and significance	33
Chapter 2: MiRNA Expression Signatures Induced by Marek's Disease Virus Infection in Chickens	35
Abstract.....	35
Introduction.....	35
Materials and Methods.....	38
Experimental animals and sample preparation	38
Quantification of MDV genome DNA loads in spleen samples.....	38
MiRNA array profiling and data Analysis.....	39
Quantification of miRNA and mRNA Levels using real-time PCR.....	40
Western blot.....	42
Cell culture, Plasmid constructs, Transfection and Luciferase Reporter Assay	43
Results.....	44
Validation of MDV infection in resistant and susceptible chickens.....	44
MiRNA expression profiles	45
MiRNA Target Identification	50
Discussion	56
Chapter 3: The Functional Analysis of Selected Chicken MicroRNAs on Marek's Disease Virus Infection	62
Abstract.....	62

Introduction.....	62
Materials and Methods.....	64
Vector construction and cell transfection	64
Cell culture and MDV infection	68
Quantification of MDV genomic DNA loads.....	68
Quantification of miRNA and mRNA levels using real-time PCR.....	68
Western blot.....	69
Results.....	70
Validation of miRNA overexpression	70
The expression of target genes in miRNA overexpressed cells.....	72
The virus loads in MDV-infected DF-1 cells with miRNA overexpression	73
Discussion.....	75
Chapter 4: MDV Infection Induced Expression Changes of <i>DNMT</i> Genes Resulting in DNA Methylation Alternations in Marek’s Disease Resistant and Susceptible Chickens	78
Abstract.....	78
Introduction.....	79
Materials and Methods.....	82
Experimental Animals and Sample Preparation	82
DNA preparation and endonuclease digestion.....	82
SOLiD mate-pair library construction	84
DNA sequencing.....	86
Tag mapping and data analysis.....	87
Bisulfite conversion, pyrosequencing and bisulfite sequencing.....	87
Purification and quantification of mRNA levels	88
DNA dot blot.....	89
Cell culture and MDV infection	90
Immunofluorescence.....	91
Results.....	91
The expressions of <i>DNMTs</i> in MDV infected chickens	91
Global mapping of DNA methylation in chickens	92
DNA methylation variations induced by MDV infection.....	95
Methylation variation in CGIs and repetitive regions.....	101
Methylation variations across genes	105
Identification of infection induced differential methylation regions (iDMRs).	108
DNA demethylation.....	112
Methylation inhibition and MDV infection <i>in vitro</i>	114
Discussion.....	115
Chapter 5: Conclusions and Future Directions.....	122
Summary	122
MicroRNAs.....	122
DNA methylation.....	124
Conclusions.....	125

Future Directions	126
Appendices.....	130
Appendix I. Differentially expressed chicken microRNAs between infected and noninfected Line7 ₂ groups	130
Appendix II. Differentially expressed chicken microRNAs between infected Line 6 ₃ and Line7 ₂ groups	132
Appendix III. Differentially expressed MDV microRNAs in chickens of the infected Line 6 ₃ and Line7 ₂ groups.....	134
Appendix IV. Pathways predicted by IPA.....	135
Appendix V The genome browser view of two CGI methylation.	137
Appendix VI The genome browser view of <i>FABP3</i> CGI methylation.	138
Appendix VII. The genome browser view of <i>GATA2</i> promoter methylation.....	139
Appendix VIII The genome browser view of CR1-B methylation.....	140
Appendix IX The genome browser view of <i>GH</i> DMR.....	141
Appendix X. The genome browser view of <i>CDC42</i> DMR.....	142
Bibliography	143

List of Tables

Table 2.1 Real time-PCR.....	42
Table 2.2 Numbers of chicken microRNAs differentially expressed between chicken lines and MDV treatment groups.....	46
Table 3.1 Pre-miRNA sequences.....	66
Table 4.1 PCR Primers	89
Table 4.2 The Global mapping statistics.....	93
Table 4.3 The CpG coverage.	94
Table 4.4 The distributions of annotated CpGs among 4 samples.	95
Table 4.6 Top Networks	112
Table 4.5 Top Canonical Pathways	112

List of Figures

Chapter 1

Figure 1.1 The schematic representation of the sequential events in lymphocyte infected by MDV.	4
Figure 1.2 The schematic figure of chicken B locus.	11
Figure 1.3 MicroRNA Biogenesis.	15
Figure 1.4 Proposed mechanisms for DNA demethylation.	26

Chapter 2

Figure 2.1 Quantification of viral gene copy number and viral gene expression. ...	45
Figure 2.2 Clustering analysis of miRNA expression profiles.	47
Figure 2.3 Expression of chicken and MDV miRNAs in MDV.	49
Figure 2.4 Protein and mRNA quantification of <i>ATF2</i>	52
Figure 2.5 The validation of miRNA- <i>ATF2</i> interaction.	53
Figure 2.6 Protein and mRNA quantification of <i>DNMT3a</i>	54
Figure 2.7 The validation of miRNA- <i>DNMT3a</i> interaction.	55

Chapter 3

Figure 3.1 The expression ALV gag protein.	71
Figure 3.2 The validation of miRNA expression by qRT-PCR.	71
Figure 3.3 Detection of DNMT3a and ATF2 by Western blotting.	73
Figure 3.4 Quantification of viral genome copy numbers.	74
Figure 3.5 Detection of oncoprotein <i>Meq</i> in MDV-infected DF-1 cells by Western blotting.	75

Chapter 4

Figure 4.1 The mRNA Quantification of chicken <i>DNMTs</i>	92
Figure 4.2 The CpG coverage distributions.	94
Figure 4.3 The distributions of annotated CpGs.	95
Figure 4.4 The boxplot of methylation levels for the detected CpGs.	97
Figure 4.5 Quantification of 5mC content by anti-5mC dot blot.	98
Figure 4.6 The classification of CpG based on the methylation levels.	99
Figure 4.7 The genome-wide DNA methylation profiling.	101
Figure 4.8 The CGI methylation status.	103
Figure 4.9 Pryosequencing and bisulfite sequencing confirmation of promoter CGI methylation.	104

Figure 4.10 The CpG methylation in repetitive DNA regions.....	105
Figure 4.11 CpG distribution and DNA methylation pattern in chicken genes....	107
Figure 4.12 The methylation of CGI upstream of <i>FABP3</i>	107
Figure 4.13 The bisulfite sequencing of CpGs upstream of <i>GATA2</i>	108
Figure 4.14 The validation of CR1-B methylation.	109
Figure 4.15 The bisulfite sequencing of iDMR upstream of <i>CDC42</i>	111
Figure 4.16 The quantification of CDC42 mRNA level.....	112
Figure 4.17 Quantification of 5hmC content by anti-5hmC box blot.....	113
Figure 4.18 Quantification of viral genome copy numbers.	114
Figure 4.19 The expression of MDV oncogene Meq.	115

List of Abbreviations

5'AZA	5'-azacytidine
5-aza-CdR	5-aza-2'deoxyctidine
5caC	5'carboxylcytosine
5fC	5'formylcytosine
5hmC	5'-hydroxymethylcytosine
5mC	5'-methylcytosine
ADAR	adenosine deaminases acting on RNA
ADOL	Avian Disease and Oncology Laboratory
AGO	Argonaute
ALV	avian leukosis virus
ATF2	activating transcription factor 2
CDC42	cell division cycle 42
CEF	chicken embryonic fibroblast
CGI	CpG island
CpG	CG dinucleotide
CR1	chicken repeat 1
CTL	cytotoxic T lymphocyte
DAPI	4',6-diamidino-2-phenylindole
DMR	differential methylation region
DNMT	DNA methyltransferase
DPI	days post infection
dsRNA	double-stranded RNA
EBV	Epstein-Barr virus
ESCs	embryonic stem cells
FABP3	Fatty acid binding protein 3
FAR1	fatty acyl CoA reductase 1
FDR	false discovery rate
GATA1	GATA binding protein 1
GH	growth hormone
H3K27me3	histone 3 lysine 27 trimethylation
H3K4me3	histone 3 lysine 4 trimethylation
HCV	hepatitis C virus
HDAC9	histone deacetylase 9
HKMT	histone lysine methyltransferase
HKMT	histone lysine methyltransferase
HSCs	hematopoietic stem cells

HSV-1	herpes simplex virus type 1
HTV	herpesvirus of turkey
iDMR	infection associated differential methylation region
IFN	interferon
IL12A	interleukin 12A
IPA	Ingenuity systems pathway analysis
iPS	induced pluripotent stem
LATs	latency-associated transcripts
LINE	long interspersed nuclear element
LTR	long-terminal repeat
M.O.I	multiplicity of infection
MD	Mareks's disease
MDV	Marek's disease virus
Methyl-MAPS	methylation mapping analysis by paired-end sequencing
MHC	major histocompatibility complex
miRNA	microRNA
NO	nitric oxide
PBL	perioheral blood lymphocytes
PolII	polymerase II
pre-B cell	precursor B cell
pre-miRNA	precursor microRNA
pri-miRNA	primary microRNA
pro-B cell	progenitor B cell
QTL	quantitative trait loci
RISC	RNA-induced silencing complex
RNAi	RNA interference
SAM	S-adenosylmethionine
shRNA	short hairpin RNA
siRNAs	small interfering RNA
ssRNA	single-stranded RNA
TCR	T cell receptor
TE	transposable element
UL	unique long
Us	unique short
UTR	untranslated region
vMDV	virulent MDV
vv+MDV	very virulent plus MDV
vvMDV	very virulent MDV
VZV	varicella-zoster virus

SEM	Standard error of the mean
STD	Standard deviation

Chapter 1: Literature Review

Introduction

Marek's disease virus (MDV) is a highly contagious avian oncovirus. MDV infection induces Marek's disease (MD), a neoplastic lymphoproliferative disease in domestic chickens, and causes up to 100% mortality rate in productive flock and approximately \$1 billion losses to the poultry industry in US annually. Although vaccines against MD have been developed, vaccination has driven MDV virulence upwards. The disadvantages of using vaccines have impelled studies on genetic selection of MD resistant chickens. So far, two different MD resistance mechanisms have been identified in chickens, either dependent or independent of major histocompatibility complex (MHC) haplotype [1]. MHC independent MD resistant line 6₃ and susceptible line 7₂ have been selected since 1930s; however, the detailed molecular basis of MD resistance in these two lines is not clear.

MDV infection has 4 steps, including early cytolitic stage, latency, late cytolitic phase and transformation. The virus targets key components in host immune system at each stage of infection [2-6]. Recent studies from MDV and other oncovirus revealed that viral infection changed the expression signatures of microRNAs (miRNAs) and DNA methylation patterns to induce tumorigenesis [7-9]. MiRNAs, a group of short non-coding RNAs, usually negatively regulate target gene expression. MiRNAs control numerous biological processes, including development, cellular metabolism, cell differentiation, immune responses and oncogenesis [10-14].

MicroRNA expression profiles differ in healthy and malignant tissues, and some miRNAs repress tumor suppressors therefore are defined as oncomirs [9]. DNA methylation is an important epigenetic marker for gene silencing, which plays important roles in regulating reprogramming, X chromosome inactivation, imprinting and tumorigenesis [10, 15, 16].

Although the critical functions of miRNAs and DNA methylation have been delineated in several diseases, little is known about their roles in MD resistance and susceptibility, especially at genome-wide scale. Therefore, the characterization of miRNA and DNA methylation in MD resistance and susceptibility would provide the framework for understanding the genetic and epigenetic effects on disease predisposition.

Marek's disease resistance in chickens

Pathogenesis of Marek's disease virus infection

Marek's disease virus (MDV) family consists of three serotypes, MDV1, MDV2 and herpesvirus of turkeys (HVT). MDV1 is the only oncogenic serotype that causes Marek's disease (MD). MD is characterized as a T cell lymphoma with serious clinical symptoms, such as tumor infiltration, paralysis, and visceral lesions. MDV1 infection usually results in high mortality rate in high-producing chickens thereby causing large economic losses to poultry industry [1]. Vaccines against MD have been applied since the 1970s using HTV or attenuated MDV [17]. However, MDV has evolved since the vaccine utilization. According to MD incidence in

nonvaccinated, HVT- and (HVT+SB-1)-vaccinated chickens, MDV was divided into 4 serotypes based on their virulence: mild MDV (mMDV), Virulent MDV (vMDV), very virulent MDV (vvMDV), and very virulent plus MDV (vv+MDV) [18]. Virulent MDV (vMDV) and vvMDV have become predominant and vv+MDV has been also isolated from bivalent-vaccinated chickens [1]. The current vaccination provides poor protection to chickens. Malignant T cell lymphoma is rapidly developed several weeks after MDV infection. New symptoms, for example acute rash, acute brain oedema and transient paralysis have been observed in most of susceptible chicken population [19].

MDV genome is linear and double-stranded DNA. The genome size of the very virulent strain MDV1 (Md5) is 177,874 bp, with 44.1% GC content, encoding 103 proteins [20]. According to the genome size and the ability to induce lymphoid tumors in chickens, MDV was originally classified as a gamma-herpesvirus, in the same subfamily as Epstein-Barr virus (EBV). With the discovery of the DNA sequence and genome organization, MDV was finally reclassified as an alpha-herpesvirus. MDV genome consists of long and short unique regions (U_L and U_S), each of which is enclosed by inverted internal and terminal repeats. Two putative origins of replication are located at both internal and terminal repeat regions flanking the U_L region; however, little is known about the initiation and temporal regulation of MDV gene expression. The oncogenesis of MDV1 is due to the existence of oncogene Meq, located in MDV EcoRI-Q fragment. Meq protein is 339 amino acids in length, and carries a basic leucine zipper (bZIP) at N-terminal, structurally resembling Jun/Fos oncogene family. It functions as a transactivator, and enhances

the expression of both viral and host gene via chromatin remodeling and transcriptional regulation in MDV infected birds [21].

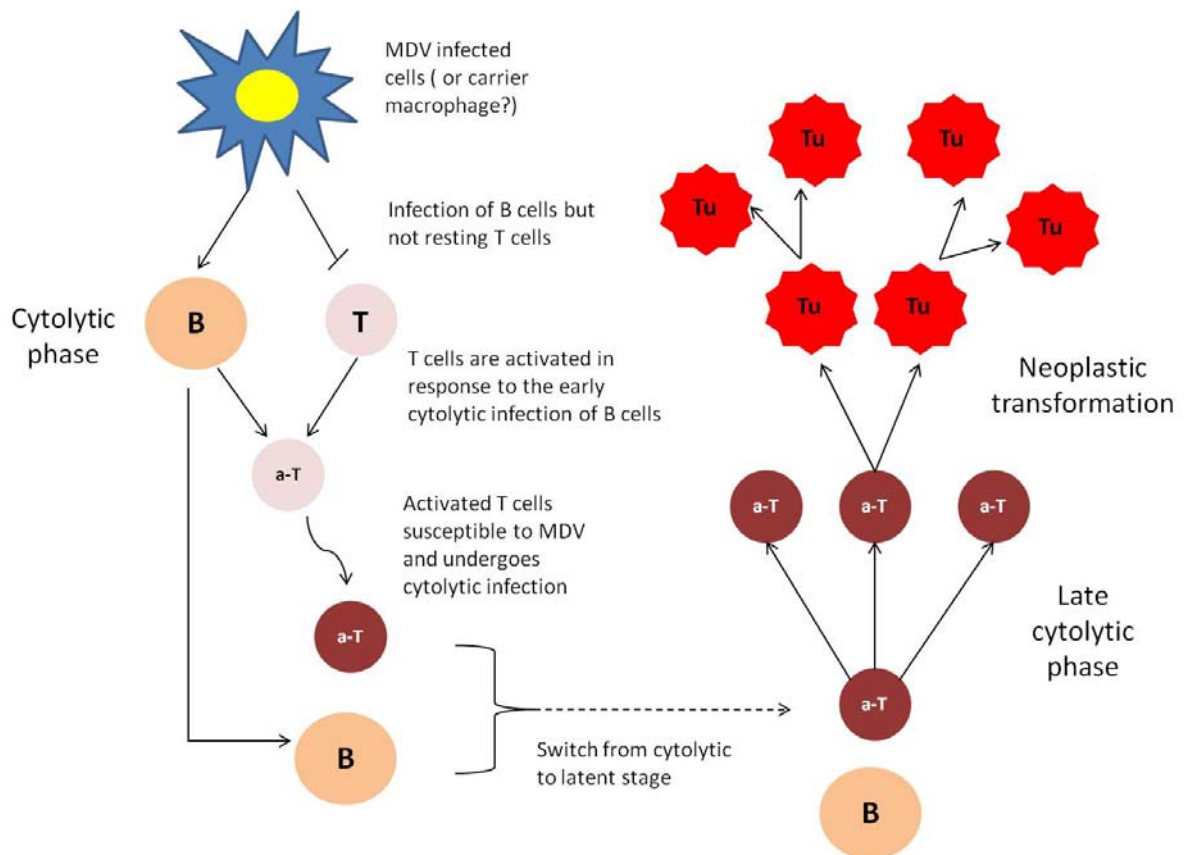


Figure 1.1 A schematic representation of the sequential events in lymphocyte infected by MDV. MDV infected macrophages carries the virus to immune organs (spleen, thymus and bursa), B cells are first infected by MDV, and then the activated T cells. Around 7-8 dpi, infected CD4⁺ T cells enter latency. In susceptible chickens, the latently infected CD4⁺ T cells are reactivated. Neoplastic transformation and proliferation are caused by unknown events, presumably the integration of MDV into the host genome.

MD progression includes 4 steps, and each of them is intricately controlled. (Figure 1.1) [19]. The initial step of MDV infection in chickens occurs through the respiratory tract by inhalation of cell-free virus from the environment. However, the actual sites of virus uptake and cellular mechanisms involved in virus entry have not

yet been identified. Lung-resident macrophages or external macrophages are assumed to pick up virus and carry it to lymphoid organs, preferentially in spleen, thymus and bursa [22]. In these immune organs, MDV meets the primary target cells: first, B lymphocytes and then the activated CD4⁺ T lymphocytes. In spleen, B cells are surrounded by ellipsoid-associated reticular cells (EARCs), where MDV is phagocytosed. T cells are activated by the cytolytic infection of B cells. The close interaction between T cells and B cells, partially due to immune responses, enhances the spread of MDV to T cells, especially activated CD4⁺ T cells. The expressions of viral proteins, such as U_L49 and VP22, are essential for cell-to-cell spread of MDV. The cytolytic infections of B cells and T cells are semi-productive since no cell-free virus but only non-envelope intracellular particles are produced. The rapid viral replication in these cells occurs between 3 to 7 days post infection (DPI) [23]. The significant feature of the early lytic stage is the sustainable downregulation of MHC I molecules on the infected cell surface, which helps virus escape the cytolytic immune surveillance by CD8⁺ T cells [24]. The repressed MHC I representation on the cell surface is directly mediated by the expression of viral gene U_L49.5, which blocks the antigen presentation processing [25, 26].

At 7-8 DPI or slightly later, MDV infection switches from cytolytic stage to latency. During the period of 7 to 14 DPI, MDV undergoes latent phase specifically in the target cells. The primary target cells for latency are mainly activated CD4⁺ T cells, along with a minor population of infected B cells. The viral genome is maintained in host cells but does not produce infectious progeny viruses. MDV latency is very difficult to study since it is hard to establish *in vitro*. Additionally, in

in vivo samples, latent infected cells usually coexist with transformed cells. During latency, transcription is restricted to latency-associated transcripts (LATs) in MDV. The activation of LATs and the repression of other viral genes are associated with the epigenetic markers, including DNA methylation, histone acetylation and histone methylation [4]. The presence of LATs help MDV to establish latent phase and keep the balance between latency and lytic infection in host cells [19, 27]. Some small non-coding miRNAs located upstream of LATs, are also expressed during latency, and may regulate the transition between latent and cytolitic infection [28]. In the latent infected cells, MDV genome exists either as the episomal, the isolated from or integrated into host chromosomes [29, 30]. The hot spots for viral integration have been found. Some evidence suggested that integration sites were different among integration events, and were generally near telomeres of the macro- and intermediate-chromosomes. Very few copies of viral genome are detected in the non-transformed T cells and peripheral blood lymphocytes (PBL) during this phase, i.e. around 5 copies/cell [31]. In resistant chickens, latent infection persisted at a low level in spleen and blood lymphocytes, while the infected PBLs delivered virus to other organs and propagate in kidneys, skin and nerves of susceptible chickens [31].

The reactivation from latency to late cytolitic infection and transformation occur around 2-3 weeks post infection in susceptible chickens. Immunosuppression in susceptible chickens is usually coincident with late cytolitic infection. MDV provokes the reactivation and the transformation by expressing viral oncogene Meq. As a transcriptional factor, Meq represses or activates host and viral gene expression by binding to promoter regions of target genes, as a result, induces morphological

changes and the growth of cells [32, 33]. Due to its similarity to the Jun/Fos family, Meq forms a heterodimer with members of the Jun/Fos family, and binds to AP-1 sites leading to the activation of oncogenic pathway [34, 35]. *In vitro* study shows that cells overexpressing *Meq* has strong antiapoptotic properties with the downregulation of apoptotic genes *Fas* and *DAP5* [33]. *In vivo* analyses demonstrate that the transcription of some immune responsive genes is time-dependent, and is likely activated during the transition from latency to late cytolytic stage [36-38]. For example, proto-oncogene *Bcl-2* was upregulated in the transformed cells, indicating its critical role in the transformation process by MDV [39]. The overexpression of CD30, a tumor necrosis factor receptor II family member, was found in MD tumors, which was similar to Hodgkin's lymphoma disease in human. This fact makes MDV/Chicken a natural model to study virus-induced lymphoma and Hodgkin's disease [19, 40].

Immunity to Marek's disease

MDV infection triggers innate and acquired immune responses during 4 infection stages. Some of the lymphocytes are the effector cells, eliciting immune functions to protect the host from viral infection and disease development, and some of them are the targets for the MDV infection, resulting in cell death or malignant transformation. The spread of virus and viral replication are impaired by effective immune responses. Meanwhile, viral infection induces tumorigenesis and immunosuppression, which restricts the efficiency and the effectiveness of immune responses. Therefore, the outcome of MDV infection is dependent on the balance

between protections elicited by the immune responses and MD tumors provoked by MDV infection.

Innate immunity is the first host response to MDV infection. MDV can be detected within 2 dpi in the spleen of infected chickens, and the innate immune response is stimulated at 3 dpi. Macrophages, natural killer (NK) cells, and other factors such as cytokines and chemokines, are rapidly activated after MDV entering into cells. The mRNA level of interferon (*IFN*)- γ is upregulated in splenocytes, which triggers *MHC class II* expression and inhibits MDV replication *in vitro* and *in vivo* [41, 42]. NK cells are the other population of effector cells in the MDV induced innate immune responses, and provide protection against MDV by producing an additional source of *IFN*- γ in the early cytolytic phase. The increased *IFN*- γ provokes the immune responses by stimulating the transcription of inducible nitric oxide synthase (*iNOS*) and interleukin (*IL*)- 1β in macrophages [43, 44]. Macrophages recognize viral antigens via the pattern recognition receptors. It has been reported that the inhibition of MDV replication *in vitro* is much more effective by the macrophages collected from MDV infected chickens than from uninfected chickens [45]. Depletion of macrophages or their repressed activity in infected chickens increase MD incidence and reduce the survival time [46]. The activated macrophages produce soluble mediators such as nitric oxide (NO) through the upregulation of *iNOS* (inducible nitric oxide synthase). The increased level of circulating NO and that generated by spleen cells are probably responsible for the reduction of the viral replication [38]. In addition, *IFN*- γ also plays a role in the establishment and maintenance of latency. The increased *IFN*- γ and *IL*-8 facilitate the expression of IL-8

receptor on the activated T cells which allows the establishment of latency [1]. Some undiscovered soluble factors may also contribute to the induction of acquired immune responses, especially released by the cytotoxic T lymphocytes (CTLs).

CTL is the major component of acquired immunity. Its particular importance in immune responses to MDV is to kill infected cells and prevent the development of the secondary lytic infection and tumor formation. The acquired immune response is detected as early as about 6-7 dpi with the emergence of antibodies and antigen-specific CTL. MDV genome encodes 103 viral proteins, including structural proteins such as glycoproteins *gB*, *gE*, and *gI*. Given the complexity of MDV infection, it is reasonable that antibodies are generated in response to MDV infection. Sera from MDV vaccinated birds provide the protection to chickens, which decreases early mortality rate [47]. Cell lines overexpressing viral antigen *pp38*, *meq* and *gB* were lysed by MDV vaccinated splenocytes, but cells overexpressing other viral genes were not recognized [48]. Among the purified MDV antibodies, *gB* and *gE* homologous antibodies were able to neutralize herpes simplex virus [49, 50]. The maternal antibodies transmitted from vaccinated hens to their offsprings decrease the severity of MD regarding mortality, morbidity and tumor formation. In contrast, it has been observed that the presence of maternal antibodies has deleterious influences on the vaccine efficiency [1]. Depletion of CD8⁺ or T cell receptor (TCR) alpha beta 1⁺ cells significantly reduce the amount of MDV released from the cells [48]. It is likely that CTL is essential for preventing the reactivation and transformation of virus from latent stage.

Marek's disease resistance and susceptibility

MD resistance is observed in natural chicken populations, and numerous studies have used different populations to estimate the heritability of MD resistance in chickens. Heritability estimates range from 0.1 to 0.61 [51, 52]. The inconsistent estimation of MD resistance heritability is likely due to different populations, chicken lines, ages, virus strains and routes of MDV exposure. These studies also reported negative correlations between MD incidence and egg production or egg weights, and positive correlation between MD incidence and age of the first egg or egg gravity. Like other complex traits, it is a challenge to identify exact genes that control MD resistance or susceptibility and balance the MD resistance and production traits.

MD resistance is classified as either MHC dependent or MHC independent. MHC (B system of haplotype) gene is the determining factor for MD resistance [53]. Cell-mediated or humoral immune responses are thought to contribute to MHC linked MD resistance. The genomic structure of the *MHC* locus is shown in Figure 1.2. MD resistance is attributed to genes located in *BF/BL* region of the B locus [54]. The most famous MHC associated resistant and susceptible chickens are the N and P chicken lines, with B²¹ and B¹⁹ haplotypes, respectively. B²¹ haplotype shows the strongest MD resistance regardless of the strains or genetic origins (white leghorn, broiler or red jungle fowl). Besides B²¹ and B¹⁹, haplotypes such as B¹, B⁴/B¹³, B⁵, B¹² and B¹⁵, are related with moderate susceptibility, and haplotypes B², B⁶ and B¹⁴ shows the moderate resistance. Chickens of different haplotypes, when crossed, produce MHC heterozygotes. Studies showed that B²/B²¹ had the greatest MD resistance (9% MD

incidence); chickens with B²/B¹³ and B²/B¹⁴ haplotypes were moderately susceptible (42-43% MD incidence) [55]. Therefore, crossing chickens with different *MHC* haplotypes can improve MD resistance. However, MHC associated MD resistance cannot fully explain the differences in disease incidence observed in commercial flocks [1].

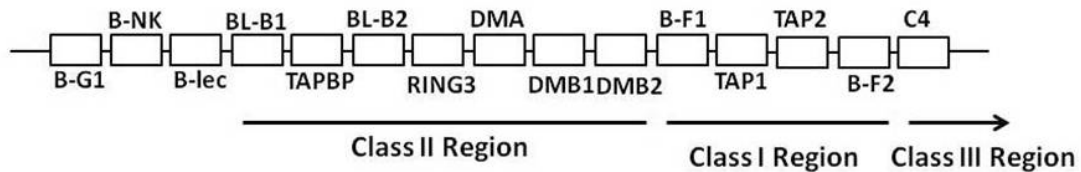


Figure 1.2 A schematic of chicken MHC locus. Open boxes denote the genes with gene names above the line (transcription from left to right) or names below the line (transcription from right to left).

Despite the contribution of MHC haplotypes, it is clear that other genes also have strong influences on the overall level of MD resistance. Chicken line 6 and line 7 are MD resistant and susceptible inbred chickens developed by the Avian Disease and Oncology Laboratory (ADOL) [56]. These two lines share the same B² MHC haplotype, showing moderate resistance to MD. Studies showed that about 99% of line 7₂ chickens generated tumors after infection with vv+MDV whereas almost none of line 6₃ chickens developed MD. MD phenotypic difference between these two lines results from differences in MDV replication and spread as well as the way of infected cells being transformed in hosts. MDV replicated faster in line 6 than in line 7, and the different viral load was detected at 10 dpi [31]. Spleen cells from line 7 had six-fold greater capability to adsorb virus than the corresponding cells from line 6

[57]. The transplantation of thymus from line 7 to line 6 raised the level of susceptibility in the line 6 recipient chickens, and grafting of line 6 thymus to line 7 did not diminish the susceptibility of the recipients [58]. To investigate the mechanism of non-MHC associated MD resistance, a number of approaches were applied to compare the difference between line 6 and line 7 chickens. Quantitative trait loci (QTL) analysis identified genes or regions outside *MHC* locus were linked with MD phenotypic variations. The most striking association was between polymorphisms in growth hormone (*GH*) and MD resistance [59]. Genomic approaches, such as microarray, also uncovered several non-MHC genes that were related to MD resistance and susceptibility [37, 38, 60-64]. Cytokines, some immune related genes and unknown genes showed significant transcriptional variations between line 6 and line 7 before and after MDV infection. The expression of *IL-6* and *IL-18* was significantly higher in splenocytes from infected line 7 than those from line 6. The higher transcriptional level of *IL-2* in line 7 rather than in line 6 was only observed at 21 dpi. *IFN- γ* mRNA was expressed by all infected chickens from 3 to 10 dpi, with the increased MDV loads. No significant differences were observed in transcription of *IL-8* and *IL-15* [65]. Genes, such as T cell receptor beta chain (*TCR- β*), MHC class I and immunologically light chain had two-fold or greater differences in expression in two lines [36]. These results suggested that non-MHC genes may play essential roles in MDV driven immune responses, which causes lymphoma in the susceptible chickens but maintains latency in the resistant birds. However, the important question about how these genes are regulated to modulate MD resistance remains unanswered.

MicroRNAs in Animal Health

MicroRNAs Biogenesis

MicroRNAs (miRNAs) are a newly identified class of single-stranded RNA (ssRNA) molecules ~22 nucleotides in length. They do not encode proteins but regulate gene expression at the post-transcriptional level. The biogenesis of miRNAs is well studied. Basically, miRNAs are generated by RNA endonuclease cleavage of endogenous transcripts with a stem-loop structure. MiRNA genes are transcribed by RNA polymerase II (PolII) or polymerase III (PolIII) into long primary microRNAs (pri-miRNAs) in the nucleus [66]. Same as other PolII transcripts, pri-miRNAs are also capped with 7-methylguanosine at the 5' UTR and polyadenylated at their 3' end, which are the marks of PolII transcription. Lee *et al.* reported that pri-miRNA levels decreased in cells treated with PolII inhibitor α -amanitin, and the immunoprecipitation analysis demonstrated that PolII physically interacted with miRNA promoters [67]. Pri-miRNAs are trimmed by a microprocessor complex formed by RNase III Drosha and GGCR8/Pasha to precursor microRNAs (pre-miRNAs). Typical pri-miRNAs consist of approximately 33 bp stem terminal and ssRNA flanking sequences at both up- and down-stream of the loop. The flanking ssRNAs of pri-miRNAs are essential for the processing, since the flanking regions directly and specifically interact with GGCR8. The cleavage sites depend on the distance from the ssRNA-stem junction [68]. Upon nuclear cleavage by Drosha, one end of the mature miRNA is defined [69]. Pri-miRNAs can be modified by ADAR (adenosine deaminases acting on RNA), an RNA editing enzyme, which converts

adenosine (A) to inosine (I). It has been reported that some miRNAs such as *mir-22* [70], *mir-142*, *mir-143* and *mir-151*[71] as well as *mir-99* [72] are edited by ADAR1 and ADAR2. A-to-I editing in *pri-mir-142* is likely to interfere with miRNA processing, specially the cleavage function of Drosha, and results in the reduction of mature *mir-142* [71]. The processing for some intron-derived miRNAs occurs in a Drosha independent manner, and splicing replaces Drosha cleavage, which indicated that these pre-miRNAs are released from their host transcripts after splicing [66]. After transcription and processing, pre-miRNAs are formed, around 70 nt in length with the imperfect hairpin structure, and exported to the cytoplasm by nuclear transporter receptor complex exportin-5-RanGTP [73] (Figure 1.3.).

Inside the cytoplasm, pre-miRNAs are further cut by another RNase III Dicer to generate ~22 nt miRNA:miRNA*duplex. Dicer was first identified to play an important role in the RNAi pathway, and performs a similar activity in miRNA synthesis. It was proposed that Dicer had particular affinity to 5' phosphate and 3' overhang at the base of hairpin precursors, and cut pri-miRNA to form an imperfect double-stranded RNA (miRNA:miRNA*) [69]. The double-stranded RNA (dsRNA) duplex contains both the mature miRNA strand called the guide strand and the complementary fragment from the opposing arm, called miRNA* or the passenger strand. In principle, two different mature miRNA could be produced from the dsRNA duplex, and load on the RNA-induced silencing complex (RISC). However, RISC incorporation rate of miRNA versus miRNA* is roughly 100-fold due to the different stabilities of the 5' ends [74]. MiRNA and miRNA* selection is based on the thermodynamic properties of the base pairing at the two ends of the duplex to

determine the duplex unwinding, molecule's longevity, and function [75]. The passenger strand, with a more stable 5' end compared to the miRNA guide strand, is usually released and decayed rapidly, but it is not always the byproduct of miRNA synthesis. It also can associate with RISC and function as the guide strand [76-78]. The guide strand (miRNA) with a relatively less stable 5' end preferentially loads into RISC to control target gene expression [76, 79] (Figure 1.3).

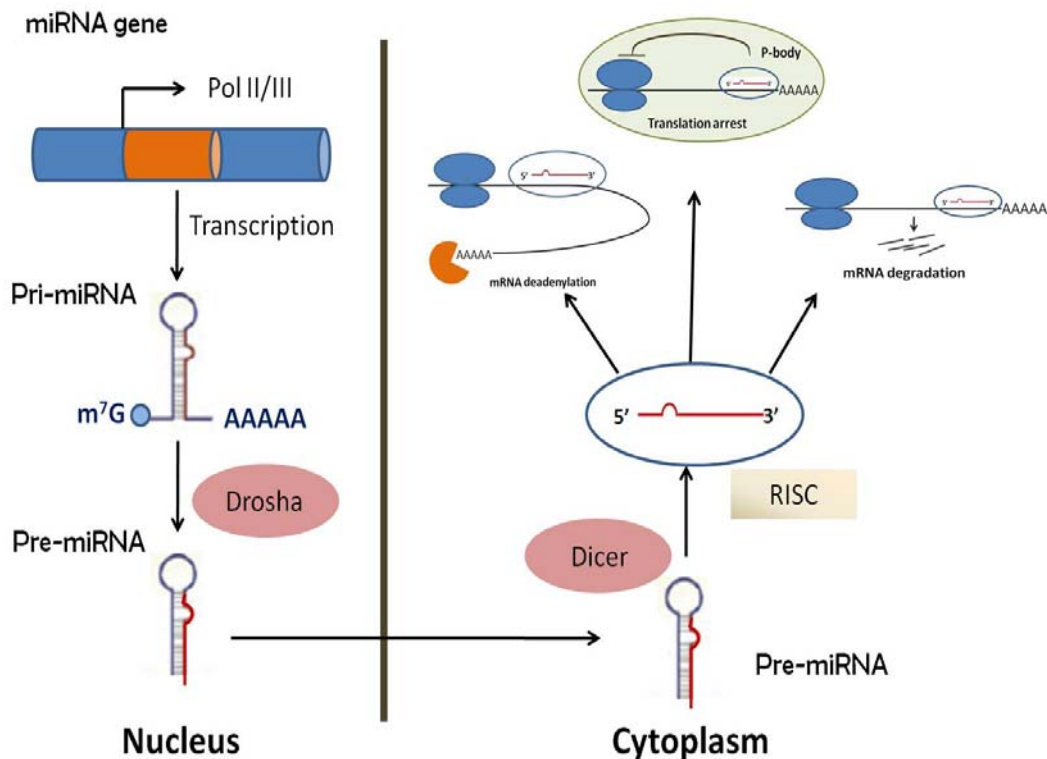


Figure 1.3. MicroRNA Biogenesis. Pri-miRNA is transcribed by Pol II from the genome. Drosha and other processor proteins cleave the pri-miRNA into ~ 70 nt long pre-miRNA. The hairpin structured pre-miRNA is transported from nucleus to cytoplasm in a RanGTP/Exportin dependent manner. In the cytoplasm, pre-miRNA is further cut by Dicer to release stem-loop structured mature miRNA (~ 22 nt). The miRNA is incorporated into an RNA-induced silencing complex, and represses gene expression by translational inhibition, mRNA destabilization or mRNA degradation.

The incorporation of miRNA makes RISC the effector complex in the miRNA

pathway to interact with messenger RNAs (mRNAs) (Figure 1.3). Argonaute (AGO) proteins are the core components in RISC, and are an evolutionarily conserved protein family. Proteins from this family contain PIWI domain and PAZ domain, providing endonucleolytic RNase H activity, which implicates AGO as the slicer [80]. Among AGO proteins, the deletion of AGO2 reduces miRNA expression and activity, suggesting that AGO2 serves as the regulator to coordinate miRNA biogenesis and function [81]. MiRNA target recognition largely depends on sequence complementarity. The seed sequence of miRNAs refers to nucleotides 2~8 that perfectly match to mRNA, and is crucial for target recognition. The less important 3' end of miRNA also contributes to miRNA-mRNA interaction, particularly when the seed sequence match is weak [82]. Most miRNA target prediction methods rely on the base pairing information of the seed sequence to mRNA interacting sites. Meanwhile, it has been found that mRNA fragments that pair to miRNAs and seed regions in miRNAs are conserved among different species, and now are a vital criterion for bioinformatic prediction of miRNA targets [83, 84].

Post-transcriptional repression by miRNAs

MiRNAs usually reduce gene expression at post-transcriptional level. Several models have been proposed to explain miRNA-induced gene repression [76]. MiRNAs direct mRNA destruction when miRNAs perfectly matching to mRNAs, which is common in plants. The molecular basis of the repression in animals is less clear. Generally, early studies reported that miRNAs negatively regulated gene expression by inhibiting translation initiation and elongation through the

incomplementary match to 3' UTR of target mRNA. It is a rare phenomenon in animal kingdom that miRNA causes mRNA degradation via perfectly base-pairing. Mouse *mir-196* was the first example of an animal miRNA resulting in target mRNA cleavage [85]. However, some new evidence has shown that, like in plants, miRNA also reduces mRNA levels by promoting mRNA deadenylation, which is followed by decapping and rapid degradation of mRNA [86, 87]. An alternative possibility is miRNA-dependent mRNA accumulation into processing bodies (P-bodies) for translation repression [76, 78, 88]. Recently, miRNA induced gene expression has been reported. In quiescent cells, AU-rich elements (ARE) in the 3' UTR of *TNF* recruited AGO and fragile X mental retardation-related protein 1 (FXR1), which are associated with the upregulation of TNF α expression by microRNA *mir-369-3* [89]. Another example was that miRNA *let-7i* was shown to activate translation on cell cycle arrest by serum starvation, but it inhibited translation in the proliferative cells [90].

MiRNA recognition sites are not restricted to the 3' UTR of mRNA. *In vitro* studies suggested that 5' UTR miRNA-binding sites were as effective for translation inhibition as those in the 3'UTR [91]. A recent study showed that human *mir-148* decreased *DNA methyltransferase 3b (DNMT3b)* expression through the interaction with the coding region. *Dnmt3b* has 4 different transcript variants, and this miRNA binding region is conserved and present among the other 3 *DNMT3b* splice variants, but absent in *DNMT3b3* transcript [92]. Due to the lack of a putative binding site, *DNMT3b3* was resistant to *mir-148*-mediated translation inhibition. This discovery provides evidence that coding regions are eligible targets of miRNAs, and also

challenge the current miRNA target searching algorithms since most tools confine the search to the 3' UTR regions [93], but ignore the possibility that miRNA target sites may be in other regions of mRNA sequence.

Functions of MicroRNAs in immunology

So far, miRNA control has emerged as essential in regulation of animal development, metabolism, homeostasis, and especially the immune system. Mammalian immune cells are generated from hematopoietic stem cells (HSCs), including a series of ordered events of lineage commitment, differentiation, proliferation and migration [94]. Chen et al. reported HSC specific miRNAs, and their dynamic expression was associated with cell commitment [95]. For example, *mir-181* was involved in the differentiation of hematopoietic cells to B lymphocytes. Its expression was detectable in undifferentiated progenitor cells, and upregulated in B lymphocytes. The ectopic expression of *mir-181* in progenitor cells increases the proportion of B-lineage cells both *in vitro* and *in vivo* [95]. The depletion of *Dicer* in the early stage of B cell development almost completely obstructs the transition from progenitor B (pro-B) to precursor B (pre-B) cells [96]. Gene expression analysis in *Dicer*-deficient and sufficient pro-B cells revealed that *Bim* and *Pten* are upregulated in *Dicer*-deficient pro-B cells and contain miRNA seed motifs in their 3' UTRs. Six miRNAs (*miR-17*, *mir-18a*, *mir-19a*, *mir-20a*, *mir-19b* and *mir-92*) encoded by *mir-17~92* were identified to modulate the expression of the proapoptotic molecule *Bim* and the tumor suppressor *Pten*. B cell development was also impaired in *mir-17~92* deficient mice, which showed increased pro-B cell death [97]. These discoveries

demonstrate that miRNAs are an important modulator in B lymphocyte development.

In addition to B cell development, recent studies have also elucidated that miRNAs were linked to T cell selection and differentiation [98]. MiRNA expression patterns were similar among naïve, effector and memory T cells while several miRNAs showed significant expression variations in different cell populations. Compared to the naïve cells, most of miRNAs were downregulated in the effector cells, and tended to be upregulated in the memory cells [99]. MiRNA *mir-181* plays important function in T cell function. The increasing *mir-181* expression augmented mature T cell sensitivity to peptide antigens and downregulated multiple phosphatases to reduce T cell receptor signaling threshold [100]. Two essential components in TCR signaling, *Lck* and *ZAP70*, were inactivated by protein tyrosine phosphatase PTPN22, whose expression was repressed by *mir-181*. Overexpression of *mir-181* increased ERK1/2 activity by inhibiting dual specific phosphatases DUSP5 and DUSP6. Thymocytes treated with the antagonist of *mir-181* decreased ERK1/2 activity and disrupted positive selection. T cell tolerance is mediated through Dicer-dependent miRNA pathway. In disease-free mice, the *Dicer*-deficiency repressed the regulatory T cells (T_{reg}) and homeostatic potential of T_{reg} was weakened. In mice with autoimmune disease, *Dicer*-deficiency lead to the complete loss of suppressive function of T_{reg} [101].

Cancer is a complex disease, associated with the aberrant expression of coding and non-coding RNAs, and it has become evident that miRNAs are involved in tumorigenesis [102]. To address the contribution of miRNAs to cancer, Volinia et al. (2006) compared miRnome in lung, breast, colon, stomach, prostate, and pancreatic

tumors [103]. Twenty one miRNAs showed commonly differential expression in at least 3 types of tumors. At the top of the list was *mir-21*, which was upregulated in all six types of cancers, and directly targeted tumor suppressor PTEN [104]. Moreover, the depletion of *mir-21* stimulated the activation of caspase dependent apoptosis and resulted in enhanced cell death, indicating the role of *mir-21* as an anti-apoptotic factor. Taken together, the evidence pertaining to abnormal expression of *mir-21* in tumor samples implies it may be involved in the malignant phenotype via diminishing apoptosis-related gene expression [105]. The miRNA *let-7* family is the first identified group of miRNAs that regulate oncogene expression [106]. Members of the *let-7* family also direct oncogene *RAS* expression in both *C. elegans* and humans [76, 107]. Recent studies showed that the reporter constructs that contained *RAS* 3'UTR were downregulated by *let-7*, and *let-7* inhibitors could reverse this suppression [76, 107]. In addition, it has been reported that *let-7* expression is low in lung tumor tissues compared to normal and adjacent tissues, and *Ras* oncoprotein is highly expressed in tumors, suggesting the potential mechanism of *let-7* in cancer [106]. The repression of *let-7* is a unique phenomenon observed in lung cancer development. MiRNA analysis in lung cancer revealed that *let-7* was dramatically reduced, and other 167 miRNAs were not remarkably changed. However, the function of miRNAs as tumor suppressors or oncogenes is not absolute. For example, the *mir-17~92* cluster was implicated as oncogenes in B cell lymphoma which coordinated with MYC to block the apoptosis [108]. The another study using human B cell line showed that *mir-17-5p* and *mir-20a*, from *miRNA-17~92* cluster, decreased the translation of *E2F1* and, sequentially inactivated MYC-mediated cell cycle progression, suggesting

their role as tumor suppressors [109, 110]. The expressions of both *mir-17~92* and *E2F1* were elevated by *MYC* at transcription level, forming a feedback loop, and allowing the accurate and robust control of cell proliferative signals.

The defensive role of miRNAs in viral infections was uncovered recently by several studies. In *Arabidopsis*, the *dicer* mutants sufficiently elicited the susceptibility to single strand RNA virus and the accumulation of viral miRNAs [111]. A similar phenomenon was observed in vertebrates. Mice with inactivated *Dicer* became hypersusceptible to vesicular stomatitis virus infection following the downregulation of two cellular miRNAs *mir-24* and *mir-93* [112]. In another study, cellular miRNAs were induced by interferon- β to repress hepatitis C virus (HCV) replication through targeting HCV genomes [113]. In humans, miRNA *hsa-mir-32* limited the proliferation of primate foamy virus type 1 (PFV-1) in human cells [114]. Several human miRNAs were upregulated after HIV infection which targeted the viral genome to inhibit HIV replication [115]. The discovery of antiviral functions of miRNAs adds new information to the host-virus interaction, however, it is far from complete. Further elucidation of miRNA functions during infection of particular viruses is required.

Chicken and MDV microRNAs

As mentioned above, miRNAs are conserved among many animal species, but miRNAs from viruses do not show sequence similarity between each other, even within in the same family [116]. The identification of miRNAs in the Epstein-Barr virus (EBV) initiated the discovery and functionality studies of viral encoded

miRNAs [117]. Presently, 20 viruses have been found to encode at least one miRNAs, and most of them are from herpesviruses [118]. By using the MDV transformed T cell line and MDV infected chicken embryo fibroblasts (CEF), 26 mature MDV-1 miRNA sequences and 14 pre-miRNA sequences have been identified [119, 120]. Most of MDV miRNAs are clustered together, at the terminal or internal repeat regions of U_L and U_S . Five of MDV miRNAs have been mapped to LAT region, and are antisense to viral immediate-early gene *ICP4*, suggesting that viral miRNAs may regulate the switch to latent stage in MDV infection [120]. *MDV1-miR-M4*, the ortholog of *gga-mir-155*, shares targets with *gga-mir-155*. The deletion of this viral miRNA or mutations in its seed sequence inhibits the induction of lymphoma [121, 122]. *MDV1-miR-M4* was found to inhibit the expression of host genes, such as c-Myb and C/EBP, as well as viral genes *U_L28* and *U_L32*. *MDV1-miR-M3* suppresses apoptosis by directly downregulating Smad, a key component in TGF β pathway [123, 124]. These results demonstrated that viral-encoded miRNAs plays a direct role in inducing tumors *in vivo*.

Recently, chicken miRNAs were profiled in different tissues and cells during development [119, 125, 126]. The current version of the miRNA database (miRbase version 18 <http://www.mirbase.org/>) contains 499 chicken miRNAs, including bioinformatically predicted and experimentally confirmed miRNAs. By using deep sequencing technique, Burnside *et al.* identified chicken miRNAs in CEF, and also compared miRNA expression between MDV infected CEF and uninfected CEF. MDV infection did not significantly disrupt miRNA biosynthesis, and the transcription of most of miRNAs was similar between MDV infected and uninfected

CEF. Several chicken miRNAs showed lower expression levels in the infected CEF than in MDV free CEF, including *let-7*, *mir-199a-1* and *mir-26a*, implying that miRNAs probably play regulatory roles after MDV infection [119]. Other studies have also reported dynamic expression patterns of chicken miRNAs in the development of the immune organs, such as embryonic spleen and bursa. These results indicate that miRNAs may be the key regulators in immune system development and maturation [126]. For example, *gga-mir-10a* was highly expressed during the development of spleen in embryonic chickens, and regulated the expression of genes in Ras signaling [127]. It also has been proven that *c-Myb*, a gene controlling hematopoiesis and tumorigenesis, was the target of *gga-mir-150* [128]. The function of miRNAs in MDV infection has been revealed. In MDV-transformed cell line MSB-1, *gga-mir-221* and *gga-mir-222* were significantly upregulated. This upregulation directly contributed to the repression of cell cycle regulator p27^{Kip1} through the interaction between miRNAs and the 3' UTR of the gene. Inhibition of these two miRNAs partially alleviated the miRNA mediated suppression. These data suggested that MDV is able to take advantage of the miRNA pathway for T cell lymphoma development and progression through controlling cell cycle regulators *in vitro* [129]. However, the relationship between miRNAs and MDV infection *in vivo* has not yet been established.

DNA Methylation

The regulation of DNA methylation

DNA methylation is an epigenetic process of transferring the methyl group from the methyl donor S-adenosylmethionine (SAM) to the 5 position of cytosine. This process is catalyzed by DNA methyltransferases (DNMTs), which include 3 major members, DNMT1, DNMT3a and DNMT3b. The task of DNMT1 is to maintain DNA methylation during cell division when DNA is duplicated. DNMT3a and DNMT3b establish *de novo* methylation, which introduce new 5'-methylcytosine (5mC) to the genomic positions that were not previously methylated. Methylation primarily occurs at CG dinucleotide (CpG) sites in mammals and other vertebrates. Non CG methylation is observed in plants, and recently it was discovered in human embryonic stem cells (ESCs) and induced pluripotent stem (iPS) cells, but the enzymes that catalyze the non CG methylation have not yet been identified in mammals [130].

Methylation is not equally distributed within the genome. In mammals, about 70% of all CpG sites are methylated, including repetitive DNA, intergenic non-repetitive DNA and exons of genes, while genome regions called CpG islands (CGIs) are one exception [131]. CGI is defined as a region at least 200 bp in length, containing a (C+G) content greater than 50%, and that has an observed-to-expected CpG ratio greater than 60% [132]. CGI is one of the markers for gene promoters, and about 60% of human genes have CGIs in the promoter regions. Two possible mechanisms may protect CGIs from being methylated. The first explanation is that

other DNA binding proteins are recruited to CGIs, which exclude the binding of DNMTs [133]. Second, DNA demethylation pathways may remove the methyl group from the methylated CGIs. It has been reported that both 5'-hydroxymethylcytosine (5hmC), the intermediate of demethylation, and TET1, the enzyme responsible for hydroxymethylation of 5mC, were enriched in the CG-rich promoters in the ESC, suggesting that the methylation free zone at CGIs was established from the early developmental stage [134].

Two mechanisms, active and passive processes, are involved in DNA demethylation at a genome-wide scale or at specific loci. Passive demethylation occurs through DNMTs. If the activities of DNMTs are inhibited, methylation is reduced after several rounds of cell divisions, due to the loss of methylation on the newly synthesized strand. Hydroxymethylation by TET family, glycosylation and DNA repair pathways, as well as other DNA binding proteins are involved in the active demethylation [135]. Methylcytosine is oxidized by Tet to 5hmC, which can be converted to T by deamination and then replaced by C via a base excision repair pathway. Hydroxymethylcytosine can be further converted to 5'formylcytosine (5fC) and 5'carboxylcytosine (5caC), and decarboxylase and DNA repair mechanisms can direct the substitution to C (Figure 1.4).

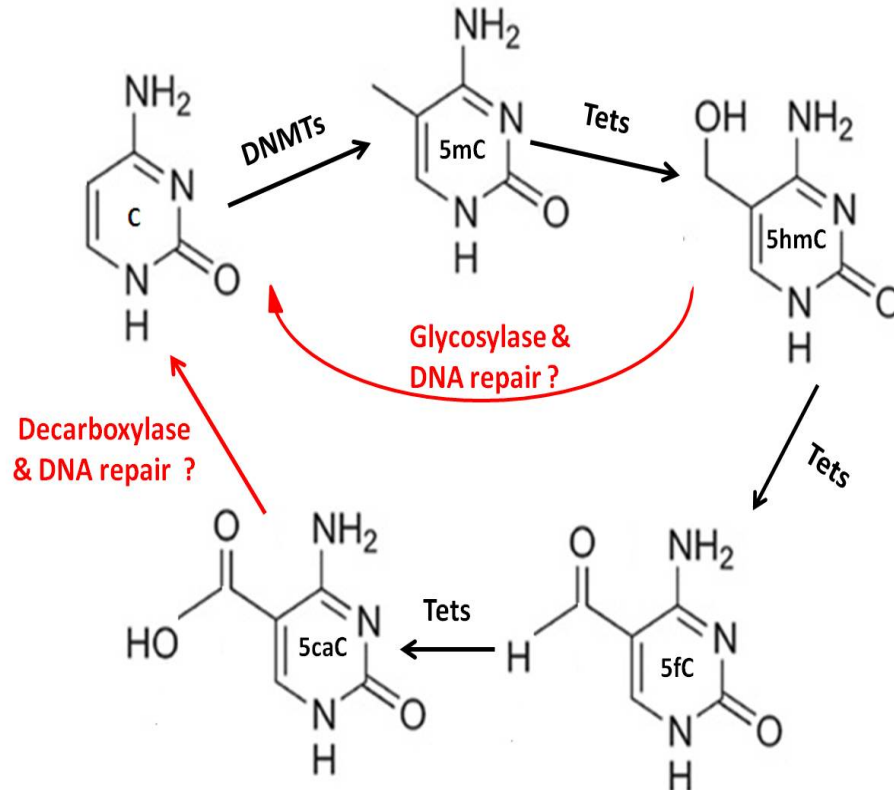


Figure 1.4. Proposed mechanisms for DNA demethylation. C is methylated to 5mC by DNMTs. Demethylation is achieved through the oxidation of 5mC by Tet, DNA glycosylase, decarboxylase and DNA repair pathways. 5hmC, 5fC and 5caC are all intermediates of demethylation.

DNA methylation can also be influenced by its chromatin structure. For example, the lack of methylation on histone 3 lysine 9 (H3K9) causes the loss of DNA methylation in the heterochromatic repeat region [136]. By applying a newly developed method, bisulfite sequencing of immunoprecipitated DNA (BisChIP-seq), the crosstalk between DNA methylation and histone modifications was directly studied. The results showed that DNA methylation and histone 3 lysine 27 trimethylation (H3K27me3) were compatible at most genome regions except at the CGIs, where they were mutually exclusive. The knockout of *DNMTs* altered the

global H3K27me3 pattern, and depletion of histone lysine methyltransferase (HKMT) also caused the loss of DNA methylation at specific loci [137, 138]. Plants and fungi exploit RNA interference (RNAi) pathway to direct DNA methylation at transposons and repetitive DNA regions. A similar phenomenon was observed in cultured mammalian cells, but the mechanism was not elucidated [139]. Environmental stimulation, such as nutrients, triggers DNA methylation alterations. The methyl supplement in the diet of female adult mice changed the DNA methylation patterns in their offsprings. Adult females fed with methyl donor tended to have offsprings with brown coats, which resulted from DNA methylation at the coat color gene, *agouti* [140, 141]. Prenatal exposure to the endocrine disrupters changed the DNA methylation pattern in the germ line, and had a transgenerational influence on the reproduction system in offsprings [142].

The biological functions of DNA methylation

DNA methylation at promoter regions is a repressive mark for gene expression. Methylated CpGs recruit methyl-binding proteins, which mediate the binding of repressor complex to promoters and inactivate gene transcription. Methyl binding protein MeCP2 interacts with methylated CpGs and attracts corepressors, polycomb group proteins, HKMT or histone deacetylase (HDAC). Some evidence has suggested that MeCP2 is able to directly block transcription by the contact with the transcription initiation complex [143]. Methylated CpGs also interfere with the interaction between transcription factors and gene promoters. In the imprinting gene *Igf2*, the maternal copy is not methylated at the CTCF binding site, which allows the

activation of *Igf2*. In the paternal copy, CTCF binding site is methylated, preventing the interaction between CTCF and the enhancer, which silences the paternal gene expression [144].

DNA methylation is involved in numerous biological processes, including genomic imprinting, X chromosome inactivation, germ cell reprogramming, immune responses and carcinogenesis [145]. Several studies have discovered that DNA methylation regulates cell differentiation and maintained the cell type identity. Differential methylation regions (DMRs) were found in mouse ESCs before and after differentiation as well as in sperm and somatic tissues, indicating that DNA methylation was altered in a specific way according to the cell lineage, tissue type and during cell differentiation [16]. Bibikova *et al.* compared genome-wide DNA methylation profiles between human ESCs and 24 other cell types, including cells derived from different cancers and normal human tissues [146]. The results demonstrate that the DNA methylation signatures clearly distinguish human ESCs from different cell types, and could be markers for the cell differentiation. They also suggest that DNA methylation contributes to maintenance of the pluripotency in the ESCs, and is engaged in the cell differentiation process. In another study, DNA methylation variations occur during the development of B cells. In B cell early development stage, *Pax5* was activated due to the hypomethylation at its promoters; and later on this region was remethylated and the transcription was turned off during B cell maturation [147].

It is also clear that DNA methylation plays a role in immune disorders, such as autoimmunity and inflammation. The loss of DNA methylation in mature T cells

causes T-cell autoreactivity *in vitro* and autoimmunity *in vivo* [148]. DNA methylation discordance between monozygotic twins is associated with systemic lupus erythematosus (SLE), with the loss of methylation in CD4⁺ T cells from SLE patients [149]. Hypomethylation reduced the specificity of antigen presentation and induced T cell proliferation and activation. From genome-wide analysis, about 49 genes were found to be differentially methylated between healthy and sick twins. These genes are enriched in gene ontology (GO) categories in relevant to defense response, cell activation and cytokine production.

DNA methylation is a dynamic process throughout life time [150]. After fertilization, methylation on the prenatal and maternal DNA in a zygote is eased, and then the pattern is rebuilt following implantation by *de novo* DNMTs, especially *DNMT3b* [151]. During remethylation, genes expressed in the germ line stage are switched off due to the hypermethylation, and promoters of lineage-specific genes are demethylated until terminal differentiation. The expression of pluripotency associated genes, such as *Oct4*, are controlled by DNA demethylation and remethylation during reprogramming. Global methylation alterations are also observed during the aging process. The DNA methylation levels are reduced in human aging-related diseases. From the 8-year observation of people from 55- to 92-years-old, a significantly declined DNA methylation level was observed in repetitive DNA, Alu elements [152]. The loss of DNA methylation in Alu elements was linear and time-dependent. DNA hypomethylation in another DNA repeat element, long interspersed nuclear element 1 (LINE-1), also demonstrated the weaker correlation with aging. Therefore, the progressive loss of DNA methylation in the repetitive sequence is one

characteristic of aging.

DNA methylation and miRNAs in diseases

Cancer is both an epigenetic and a genetic disease, and DNA methylation variations in cancer are recognized, including the hypomethylation at the promoters of oncogenes and the hypermethylation of the tumor repressor genes [12]. Tumor development is associated with the gain of DNA methylation at CGIs, and the loss of imprinting and DNA methylation fluctuations at repetitive genomic regions [153].

Infective agents belong to the environmental stimulus, and influence DNA methylation patterns in the hosts as well as in pathogens. The manipulation of host methylome by viruses is achieved by the interaction between viral proteins and DNA methylation modifiers. Several viral oncoproteins, such as E1A from Adenovirus, LMP1 from EBV, LANA from KSHV, and HBx from Hepatitis B virus as well as E7 from Papillomavirus, have been discovered to interact with DNMTs, which consequently induce oncogenic cell signaling [8]. Infection with bacteria *C. rectus* promoted the methylation level of *Igf2* in murine placenta and inhibited the gene expression [154]. Herpes simplex virus infection causes hypomethylation in the host cells although the mechanism is unclear. EBV infection in human B cells inhibits the expression of apoptotic Bcl-2 family member Bim, which is rescued by a methylation inhibitor. The promoter region of *Bim* is highly methylated in all EBV positive cells, and unmethylated in EBV negative cells [155]. DNA methylation causes chronic infection by silencing viral gene transcription to escape from the host immunity. In herpesviruses, latency is a critical period for viruses to build a long-lasting infection

in hosts, and is associated with the immunosuppression and tumors. DNA methylation controls the switch from latency to lytic phase in EBV infected human B cells. Viral gene *BZLF1*, a transactivator, preferentially binds to methylated CpGs, and induces the productive life cycle of EBV from latency. In the newly infected cells, the unmethylated viral DNA prevents the interaction from *BZLF1* and establishes the non-productive infection [156]. With the progresses of the infection, EBV genome becomes methylated, and *BZLF* interacts with the methylated promoters of EBV genes and reactivates the EBV. MDV infection also changes methylation patterns of several genes in the chicken spleens probably via regulating the expression of *DNMTs* [3]. Moreover, DNA methylation is present in some intergenic regions in MDV genome but reduced at the region containing LATs and some active genes [4].

Similar to coding genes, miRNA expression is directed by DNA methylation at promoter CpGs [157, 158]. Han et al. (2007) compared miRNA expression and miRNA gene methylation in colon cancer cell line HCT 116 and its derivative, *DNMT1* and *DNMT3b* double knockout cell lines (DKO) [159]. They found that the majority of CpG islands upstream of miRNA genes were hypermethylated in HCT 116 cell line, but unmethylated in the DKO cells. Out of 135 miRNAs, 13 miRNAs were upregulated in the DKO cells than in the HCT116 cells, and 7 of them had CpG sites in the close vicinity to the promoter regions. This result indicated that the transcription of some miRNAs was probably dependent on the methylation status in the promoters. Works done by Saito Y et al. (2006) demonstrated that DNA demethylation agent 5-aza-2'-deoxycytidine (5-aza-CdR) treatment increased miRNA

expression more than 3-fold in T24 human bladder cancer cells [160]. Among the upregulated miRNAs, *mir-127* expression was 49 times higher than in the untreated cells, which was embedded in a CpG island and highly methylated in the primary tumors. *Mir-127* target gene *BCL6* was repressed when the cancer cells were treated with 5-aza-CdR, which reactivate *mir-127* [161]. On the other hand, miRNA is another regulator for DNA methylation by targeting the *DNMTs*. Three members of *mir-29* family, *mir-29a/b/c*, interact with the coding regions of *DNMT3a/b* to negatively control protein yield [162]. This miRNA family is repressed in patients, and inversely correlates with elevated *DNMT3a/b* expression. Forced expression of *mir-29a/b/c* restores the normal DNA methylation patterns in the lung cancer cell lines, and reactivates the previously silenced tumor suppressor genes *FHIT* and *WWOX*. The anti-tumor effect of *mir-29* family is also observed *in vivo*, by limiting tumor growth. MiRNA transfection reduces cell growth and induces apoptosis in the cancer cell line A549.

DNA methylation and miRNA work together to control cancer metastasis [163, 164]. The regulation of miRNAs by DNA methylation is uncovered by the study that showing the deregulation of miRNA in the cancer line treated with DNA methylation inhibition agent 5-aza-CdR. Altogether, 57 miRNAs were upregulated at least 2-fold upon the treatment, including 27 of them residing in the CpG sites. After excluding the tissue-specific DNA methylation, *mir-34b/c*, *mir-148a*, and *mir-9-1/2/3* were identified as candidate metastasis suppressor miRNAs, which were unmethylated in normal tissues but highly methylated in tumors. Overexpression of *mir-34b/c* and *mir-148a* increased the cell mobility *in vitro* and facilitated the tumor

formation in mice.

Rationale and significance

Marek's disease outbreak is one of the major health problems causing large economic losses to the poultry industry due to the high mortality rate. The frequent unexpected outbreaks of MD reveal severe limitations in current MD control system. Therefore, it is necessary to develop new strategies in order to better protect chickens from the disease. Understanding the mechanisms of MD resistance/susceptibility is the essential step towards the development of effective defenses to MD. This goal could be achieved by identifying molecular basis of MDV-host interaction and the association between MD resistance/susceptibility and microRNAs as well as DNA methylation. Although some studies described the variations of miRNAs and DNA methylation induced by MDV infection, the global scenarios have not been characterized. The goals of the project were to identify viral-induced miRNA expression profiles and DNA methylation patterns at a genome-wide scale, as well as to determine how these virally-induced changes exert a physiological or pathological action during MD progression in MD resistant and susceptible chickens. The outcome of the research will improve our understanding of how genetic and epigenetic differences in chickens influence MDV infection and provide clues to develop new strategies to enhance immune response to MDV infection and to eliminate viruses through the host itself; moreover, the implications of this project will advance our knowledge of the roles of microRNAs and DNA methylation in virus induced lymphomagenesis. For this purpose, the research project had 3 major objectives:

1. To explore the miRNA expression signatures in MD resistant and susceptible chickens after virus infection;
2. To investigate the function of selected miRNAs on MDV infection;
3. To characterize the genome-wide DNA methylation profiles in MD resistant and susceptible chickens before and after MDV exposure.

Chapter 2: MiRNA Expression Signatures Induced by Marek's Disease Virus Infection in Chickens

Abstract

MiRNAs are small, non-coding RNAs that regulate gene expression at the post-transcriptional level. Emerging evidence suggests that differential miRNA expression is associated with viral infection and cancer. MDV infection induces lymphoma in chickens. However, the host defense response against MD progression remains poorly understood. Here, we utilized microarrays to screen miRNAs that were sensitive to MDV infection. QRT-PCR analysis confirmed the microarray data and revealed expression patterns of some miRNAs in tumor samples. Chicken miRNA *gga-miR-15b* and *gga-let-7i*, which was reduced in infected susceptible chickens and splenic tumors, controlled the expression of ATF2 (activating transcription factor 2) and DNMT3a (DNA methyltransferase 3a). The expressions of *ATF2* and *DNMT3a* were significantly increased in infected susceptible chickens. Our results indicated that differential expression of miRNA in resistant and susceptible chickens was caused by MDV infection, which effectively influenced protein expression of ATF2 and DNMT3a. This latter result might be related to Marek's disease resistance/susceptibility.

Introduction

MiRNA are a class of small single-stranded, non-coding RNAs (~22 nt in

length) that govern post-transcriptional repression of target genes by binding to 3' UTRs or gene bodies [76]. It has been shown that miRNAs are involved in a broad range of biological processes, including development, metabolism and cell differentiation [9, 76]. MiRNAs have been specifically implicated in tumorigenesis and pathogen infection [9, 165]. Functional evaluations of differentially expressed miRNAs have uncovered their abilities to elicit diverse immune responses, mainly through the regulation of immune cell differentiation and their association with immunity and inflammation [98, 165, 166].

MD is a chicken lymphoma caused by MDV1, which is an α -herpesvirus that is closely related to human herpesvirus 1 (herpes simplex virus type 1, HSV-1) and human herpesvirus 3 (varicella-zoster virus, VZV) [19]. MDV infection exhibits an early cytolitic phase between 3 to 7 days post infection (dpi) and then enters into the latent phase within 2 weeks. During this period, the MDV genome is maintained in host cells without the production of infectious progeny viruses [19]. Reactivation of MDV to the late cytolitic phase occurs between 14 to 21 dpi in MD susceptible chickens, which coincides with permanent immunosuppression [19, 167]. Here, we analyzed miRNA expression profiles in MD-resistant and MD-susceptible chickens to elucidate the function of miRNA in the regulation of Marek's disease (MD) resistance.

To date, 499 predicted and confirmed chicken miRNAs as well as 14 MDV-1 miRNAs have been released from miRBase (<http://miRNA.sanger.ac.uk/sequences/>). A portion of chicken miRNAs were repressed in MDV-infected chicken embryo fibroblast cells [119] and displayed dynamic expression patterns during the

development of chicken immune organs [126]. Several MDV-1 miRNAs, including MDV1-M2, MDV1-M3 and MDV1-M5 have been physically mapped to the regions flanking the MDV oncogene Meq [28]. However, the differences in miRNA expression between MD-resistant and MD-susceptible chickens, especially before and after MDV infection, are still unknown. These variations appear to be important for understanding host-virus interactions. In this study, we used two highly inbred chicken lines (line 6₃ and line 7₂) to evaluate the hypothesis that MDV infection induces distinct miRNA expression signatures in MD-resistant and MD-susceptible chickens that modulate target gene expression. MDV can enter target cells in line 6₃ and line 7₂ chickens, but line 6₃ chickens survive after infection and most of them do not develop tumors. In contrast, line 7₂ is susceptible to MD, which leads to the development of lymphoma. Using this model, we identified 64 candidate miRNAs that were differentially expressed in the spleens of MDV-infected and noninfected line 7₂ chickens. Among these miRNAs, *gga-miR-15b* deregulation in infected line 7₂ was shown to control the expression of activating transcription factor 2 (ATF2) and DNMT3a (DNA methyltransferase 3a), which were both increased in infected line 7₂ chickens. Collectively, our data demonstrated that MDV infection caused distinct miRNA expression patterns in MD resistant and MD susceptible chickens, which effectively influence the protein levels of target gene in the infected samples. Taken together, these results provide clues for future exploration of how miRNAs are regulated in viral-induced tumors *in vivo*.

Materials and Methods

Experimental animals and sample preparation

Line 6₃ and line 7₂ (USDA-ARS Avian Disease and Oncology Laboratory, East Lansing, Michigan, USA) are two highly inbred lines of specific-pathogen-free white leghorn chickens that are resistant and susceptible, respectively, to MD tumors. Chickens from each line were separated into two groups. One group was infected with a very virulent (vv+) strain of MDV (648A passage 40) at day 5 after hatching, while the other group did not receive MDV. Four chickens were selected from each group at 5, 10 and 21 days post infection (dpi), and none of them developed tumors during the experiment period. Besides the infected spleen samples from line 6₃ and line 7₂, we received 4 spleen tumor samples of MDV infected chickens and 4 spleen samples of uninfected control birds from Avian Disease and Oncology Laboratory (ADOL, USDA). The tumor diagnosis and tumor sample collection were done by the veterinary medical officer in ADOL. Fresh spleen samples were harvested individually and stored in RNAlater solution (QIAGEN) at -80°C for DNA or RNA extraction. The entire animal experiment was conducted following the procedures and guidelines described in the “Guidelines for Animal Care and Use” manual approved by the Animal Care and Use Committee, the USDA-ARS, and the Avian Disease and Oncology Laboratory (Approval ID 111-26).

Quantification of MDV genome DNA loads in spleen samples

As previously described [168], the MDV oncogene *Meq* was used to quantify

viral genomic DNA at 5, 10 and 21 dpi. Quantitative PCR of viral copy number was performed on genomic DNA (100 ng/μl) with the iCycler iQ PCR system (Bio-Rad, USA) and QuantiTect SYBR Green PCR Kit (Qiagen, USA). Relative MDV loads were determined after normalization to a single-copy gene *VIM* (vimentin) [169].

MiRNA array profiling and data Analysis

Total RNA was extracted from three spleen samples using the miRNeasy Mini Kit (QIAGEN). Total RNA quality was verified with Agilent 2100 Bioanalyzer chips (Agilent, Santa Clara, CA, USA). Three of the samples from each of the treatment groups from two chicken lines were processed for miRNA microarray analysis. Microarray analysis was done by Exiqon (Exiqon, Denmark). Briefly, total RNA (1 μg) from each of the samples and the common reference sample were labeled with Hy3™ and Hy5™ fluorescent label, respectively, using the miRCURY™ LNA Array power labeling kit (Exiqon, Denmark) following the manufacturer's specifications. The Hy3™-labeled samples and a Hy5™-labeled reference RNA sample were mixed pair-wise and hybridized to the miRCURY™ LNA array (Version 9.2; Exiqon, Denmark), which contained capture probes targeting all of the miRNAs for all the species registered in the miRBASE (Version 10.1) at the Sanger Institute. One hundred and sixty-two of these probes were chicken-related miRNAs. Hybridization was performed according to the miRCURY™ LNA array manual with a Tecan HS4800 hybridization station (Tecan, Austria). After hybridization, the microarray slides were scanned and stored in an ozone free environment (ozone level below 2.0 ppb) to prevent potential bleaching of the fluorescent dyes. The miRCURY™ LNA

array microarray slides were scanned using the Agilent G2565BA Microarray Scanner System (Agilent Technologies, Inc., USA) and image analysis was performed with ImaGene 8.0 software (BioDiscovery, Inc., USA). Microarray data were analyzed in R using the Limma package [170, 171]. Quantified signals within arrays were averaged and normalized using the global LOWESS (LOcally WEighted Scatterplot Smoothing) regression algorithm. Contrasts were made to compare noninfected and infected groups in both lines. Differentially expressed miRNAs were selected to perform cluster analysis with CLUSTER/TreeView software [172]. The target genes for miRNAs were predicted by RNA22 (<http://cbcsrv.watson.ibm.com/rna22.html>).

Quantification of miRNA and mRNA Levels using real-time PCR

MiRNAs and mRNAs were extracted from four chicken spleen samples per treatment group using the miRNeasy Mini Kit (QIAGEN) and RNeasy Mini Kit (QIAGEN) according to the standard protocol by manufacturer. The on column DNase digestion was done for miRNA and mRNA purification to remove DNA. MiRNA samples were reversely transcribed and quantified with a miScript Reverse Transcription Kit (QIAGEN), a miScript SYBR Green PCR Kit (QIAGEN), and 5 miScript Primer assays (QIAGEN). Reverse transcription and quantification of mRNA were performed with SuperScript™ III Reverse Transcriptase (Invitrogen) with oligo (dT)₁₂₋₁₈ primers (Invitrogen), and the QuantiTect SYBR Green PCR Kit. In the reverse transcription control, PCR water (Invitrogen) was used to replace miRNA or RNA samples.

The primers were designed using NCBI/Primer-BLAST tool from NCBI web site (<http://www.ncbi.nlm.nih.gov/tools/primer-blast/>). The melting temperatures were between 55-65 °C, and the length of the amplicons was between 100-200 bp. The primer pairs were designed to separate by one intron, and were specific to *Gallus gallus*. The forward and reverse primers for *ATF2*, *GAPDH* and *Meq* quantification are listed in Table 2.1.

Briefly, 1 µg of purified miRNA or total RNA was used for reverse transcription, respectively, and 2 µl of RT products (1:5 dilution) were used for real-time PCR quantification. Two types of controls were applied in real-time PCR, including reverse transcription control and blank using PCR water. No amplicon was observed in the controls. A final volume of 20 µl real-time PCR product was incubated in an iCycler iQ PCR System (Bio-Rad), and each was performed on four biological replicates from the treatment per line in each experiment. Four biological replicates were carried out for each gene and miRNA, and each biological replicates were technically repeated 3 times. *U6* or *GAPDH* (glyceraldehyde-3-phosphate dehydrogenase) were used as normalization controls for the data [120]. After normalization, ANOVA and Tukey test were used to compare the miRNAs or genes expression levels (SAS version 9.2).

Table 2.1 Real time-PCR

Gene ^A		Sequences
<i>ATF2</i> ^B	Forward	5'-CCTCCCCACAGCCAGTGCAG-3'
	Reverse	5'-TGAGCTGGTGATGCCGGTGT -3'
<i>DNMT3a</i> ^B	Forward	5'-ATGAACGAGAAGGAAGACATC-3'
	Reverse	5'-GCAAAGAGGTGGC GGATCAC-3'
<i>Meq</i> ^B	Forward	5'- AAGTCACGACATCCCCAACAGC-3'
	Reverse	5'-TACATAGTCCGTCTGCTTCCTGCG-3'
<i>GAPDH</i> ^B	Forward	5'- GAGGGTAGTGAAGGCTGCTG-3'
	Reverse	5'-ACCAGGAAACAAGCTTGACG-3'
<i>Vim</i> ^B	Forward	5'-CAGCCACAGAGTAGGGTAGTC-3'
	Reverse	5'-GAATAGGGAAGAACAGGAAAT-3'
<i>ATF2</i> ^C	Forward	5'- GTTTAAAC TCCAGGCCCGTTTCCTCTGCT -3'
	Reverse	5'-TCTAGA AGCTTCCGTGTGTGGGCTGC -3'
<i>DNMT3a_1</i> ^C	Forward	5'- GTTTAAAC CATGAAGCACGGCCCAAG-3'
	Reverse	5'-TCTAGA TGTGCCGCAGACACCTCT -3'
<i>DNMT3a_2</i> ^C	Forward	5'- GAGCTC AAGATTGGCCGTCGCGCCTC -3'
	Reverse	5'-TCTAGA AGGTCTGAAGGGGCCCCACT -3'

^A: Gene name. ^B: Primers for real time-PCR. ^C: Primers for amplifying *ATF2* and *DNMT3a* fragments that contain microRNA interacting sites and for plasmid construction

Western blot

Total protein was extracted by lysis of ~20 mg of tissues with RIPA buffer (150 mM sodium chloride, 1.0% NP-40, 0.5% sodium deoxycholate, 0.1% SDS and 50 mM Tris, pH 8.0) containing a protease inhibitor cocktail (Sigma). Approximately 20 mg of splenic tissue was homogenized in RIPA buffer, and the lysate was incubated at 4 °C for 2 hours with constant agitation and subsequently centrifuged at 4°C for 30 min. Protein concentration for each sample was determined by the BCA

assay (Thermo Scientific). For the western blotting, 30 µg of extracted protein was heated at 95-100°C for 5 min and loaded on 10% SDS-PAGE for electrophoresis. After separation, proteins were transferred onto polyvinylidene fluoride (PVDF) membrane and blocked with 5% nonfat milk in TBST containing 0.1% Tween 20. Primary antibodies against ATF2 (Santa Cruz), DNMT3a (Abcam) and *β-actin* (Abcam) were prepared at 1:500 and 1:1000 dilutions, respectively. Membranes were incubated with primary antibodies overnight at 4°C. Membranes were washed quickly 3 times (less than 1 min) and 3 more times for 5 min. Membranes were then incubated with anti-rabbit IgG and anti-mouse IgG secondary antibodies (Santa Cruz) diluted in TBST (1:5000 or 1:10,000) for 1 hr at room temperature. The membranes were quickly washed 3 times and then washed 3 more times for 5 min each. Membranes were developed with ECL (Amersham) and measured using ChemiDoc XRS (Bio-Rad). To quantitate the amount of protein, the signal volume was measured with Quantity One software using volume analysis. The band signals were measured, and background correction was applied. The background-adjusted volume signals of each band were export to excel. The relative protein expression was calculated as the ratio of the adjusted volume signals between protein of interest and *β-actin*. Four independent experiments were done for each antibody.

Cell culture, Plasmid constructs, Transfection and Luciferase Reporter

Assay

Hela cells were grown in Dulbecco's modified Eagle's medium supplemented with 10% fetal bovine serum, streptomycin (100 mg/ml) and penicillin (100 U/ml)

(Invitrogen). Cells were maintained at 37°C in humidified 5% CO₂ conditions. *ATF2* cDNA fragments containing miRNA target sequences were amplified by PCR (Table 2.1), and cloned into pmirGLO Dual- Luciferase miRNA target expression vector (Promega) to create plasmid constructs. For transfection, cells were plated in 24-well plates and were ~25% confluent 24 hrs before transfection. Before transfection, the medium was replaced with growth medium without antibiotics. Chicken miRNA mimics (QIAGEN) were diluted to working concentration (3 pmol/μl), and were co-transfected with plasmids (500 ng) harboring miRNA target sites using Lipofectamine 2000 transfection reagent (Invitrogen), and the medium was replaced with normal growth medium 4-6 hrs later. Cells were harvested after 24 hrs, and Renilla and firefly luciferase activities were measured using Dual-Luciferase Reporter Assay System (Promega).

Results

Validation of MDV infection in resistant and susceptible chickens

MDV successfully infected chickens from line 6₃ and line 7₂, but this infection had discordant behavior in the two lines. By measuring the copies of two important viral genes (*Meq* and *ICP4*), virus copy number was estimated and was similar between infected line 6₃ and infected line 7₂ chickens at 5 dpi, but was much higher in infected line 7₂ chickens than in infected line 6₃ chickens at 10 and 21 dpi (Figure 2.1 A).

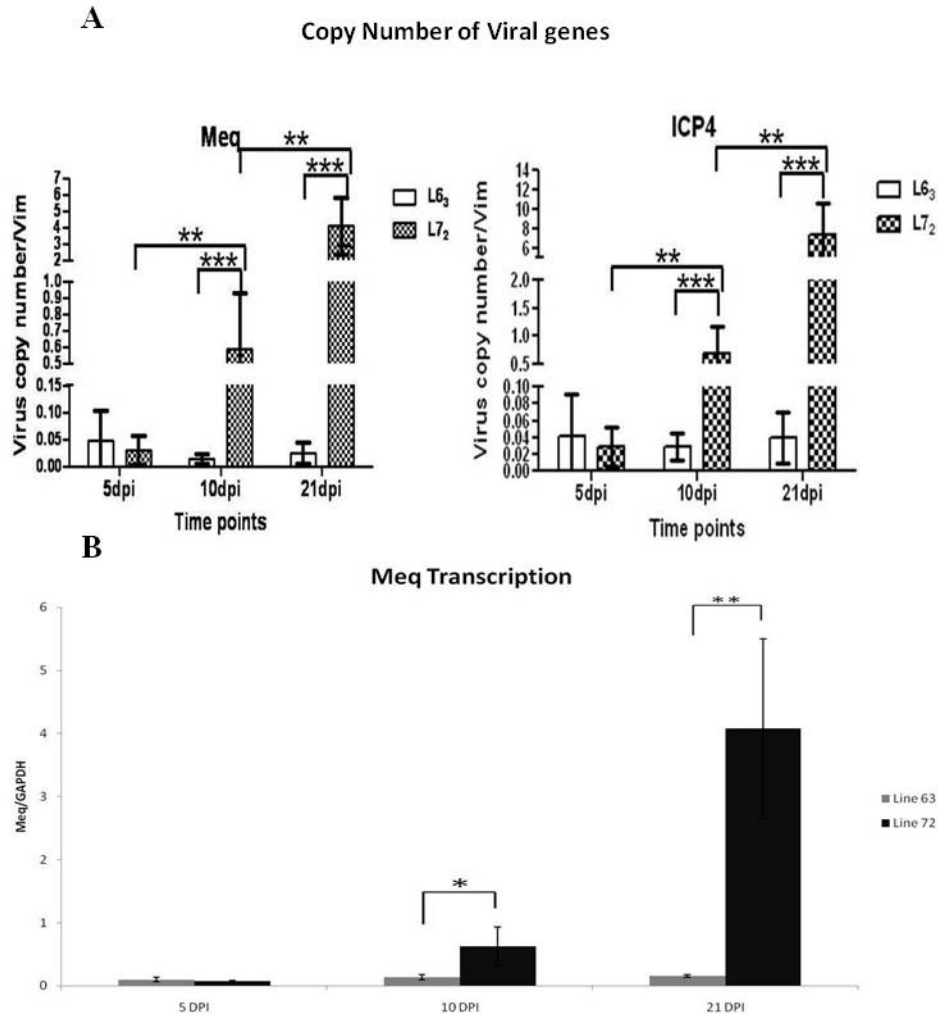


Figure 2.1 Quantification of viral gene copy number and viral gene expression. (A) Virus copy number, based on *Meq* and *ICP4*, in MDV-infected line 6₃ and line 7₂ chickens were measured (5, 10 and 21 dpi) and normalized to a single copy gene, *Vim*. (B) *Meq* transcription levels were measured in MDV-infected line 6₃ and line 7₂ chickens (5, 10 and 21 dpi) and normalized to *GAPDH*. Quantitative results are represented as Mean ± SEM (n=4). L6₃: infection line 6₃ and L7₂: infected line 7₂.

MiRNA expression profiles

Based on our criterion (p-value less than 0.05 and false discovery rate (FDR) smaller than 0.1) using in microarray analysis, 64 out of the 162 miRNAs had significant differential expression between infected and noninfected line 7₂ chicken

spleen at 21 dpi, including the downregulation of 58 miRNAs and the upregulation of 6 miRNAs in the infected line 7₂ group (Table 2.2 and Appendix I.). Notably, using the same criteria, none of the miRNAs were expressed differently between the infected and noninfected line 6₃ chickens (Table 2.2). Sixty-two miRNAs were expressed differently when infected line 6₃ and line 7₂ chickens were compared, including 50 downregulated and 12 upregulated miRNAs in the infected line 7₂ group (Appendix II.). In total, 73 miRNAs showed differential expression. By using the cluster analysis that included all of the significantly expressed miRNAs, we found that the experimental birds were categorized into two groups (Figure 2.1). The infected line 7₂ birds were in one subgroup. In the other subgroup, noninfected line 7₂ chickens were associated with line 6₃ chickens that were both infected and noninfected, indicating that their microRNA profiles were less varied (Figure 2.1). Additionally, we also found that the abundance of 10 MDV1 miRNAs dramatically increased in infected line 7₂ chickens but not in infected line 6₃ birds (Appendix III.).

Table 2.2 Numbers of chicken microRNAs differentially expressed between chicken lines and MDV treatment groups

	<i>L6₃.non vs L6₃.inf</i>	<i>L7₂.non vs L7₂.inf</i>	<i>L6₃.non vs L7₂.non</i>	<i>L6₃.inf vs L7₂.inf</i>
Downregulated	0	58 ^A	0	50 ^C
Upregulated	0	6 ^B	0	12 ^D
Total	0	64	0	62

^A and ^C: MicroRNA levels were downregulated in the infected line 7₂ chickens compared to noninfected line 7₂ or infected line 6₃ chickens, respectively, based on p<0.05 and FDR<0.1.

^B and ^D: MicroRNA levels were upregulated in the infected Line 7₂ chickens compared to noninfected line 7₂ or infected line 6₃ chickens, respectively, based on p<0.05 and FDR<0.1

clustering analysis classified the samples based on significantly differentially expressed miRNA in the normalized data. Green or red bars denote that the level of specific miRNA was decreased or increased in samples. Black bars indicate that the levels of miRNA were similar between samples and the common reference sample. Gray indicates data that are not available. The scale of the color bar represents fold changes of miRNA expression relative to the common reference. L7₂.inf.1-3: 3 samples from infected line 7₂; L7₂.non.inf.1-3: 3 samples from noninfected Lines 7₂; L6₃.non.inf.1-3: 3 samples from noninfected line 6₃; L6₃.inf.1-3: 3 samples from infected line 6₃.

Based on the results from the microarray analysis, 3 *gga-miR-15b*, *gga-miR-456* and *gga-let-7i* miRNAs, which potentially regulate *ATF2* and *DNMT3a*, were chose to verify the results from the microarray analysis. The expression of *gga-miR-15b*, *gga-miR-456* and *gga-let-7i* were all significantly downregulated in infected line 7₂ samples compared to MDV-free chickens ($p < 0.05$) (Figure 2.3 A). Significantly reduced expression of *gga-miR-456* and *gga-let-7i* were observed in infected line 7₂ chickens compared to infected line 6₃ chickens ($p < 0.01$ and $p < 0.05$ respectively). Transcription of *gga-miR-15b* was decreased in infected line 7₂ samples relative to infected line 6₃ samples, although this difference was not statistically significant (Figure 2.3 A). These 3 miRNAs did not show significant variance between infected and noninfected in line 6₃ samples. Additionally, these 3 miRNAs were also repressed in splenic MD tumors compared to healthy spleen ($p < 0.05$), which was consistent with the microarray results (Figure 2.2 B). Besides chicken miRNAs, the expression levels of *MDV-miR-M2* and *MDV-miR-M5* were significantly higher in the infected line 7₂ birds than in infected line 6₃ chickens ($p < 0.01$) (Figure 2.3 C).

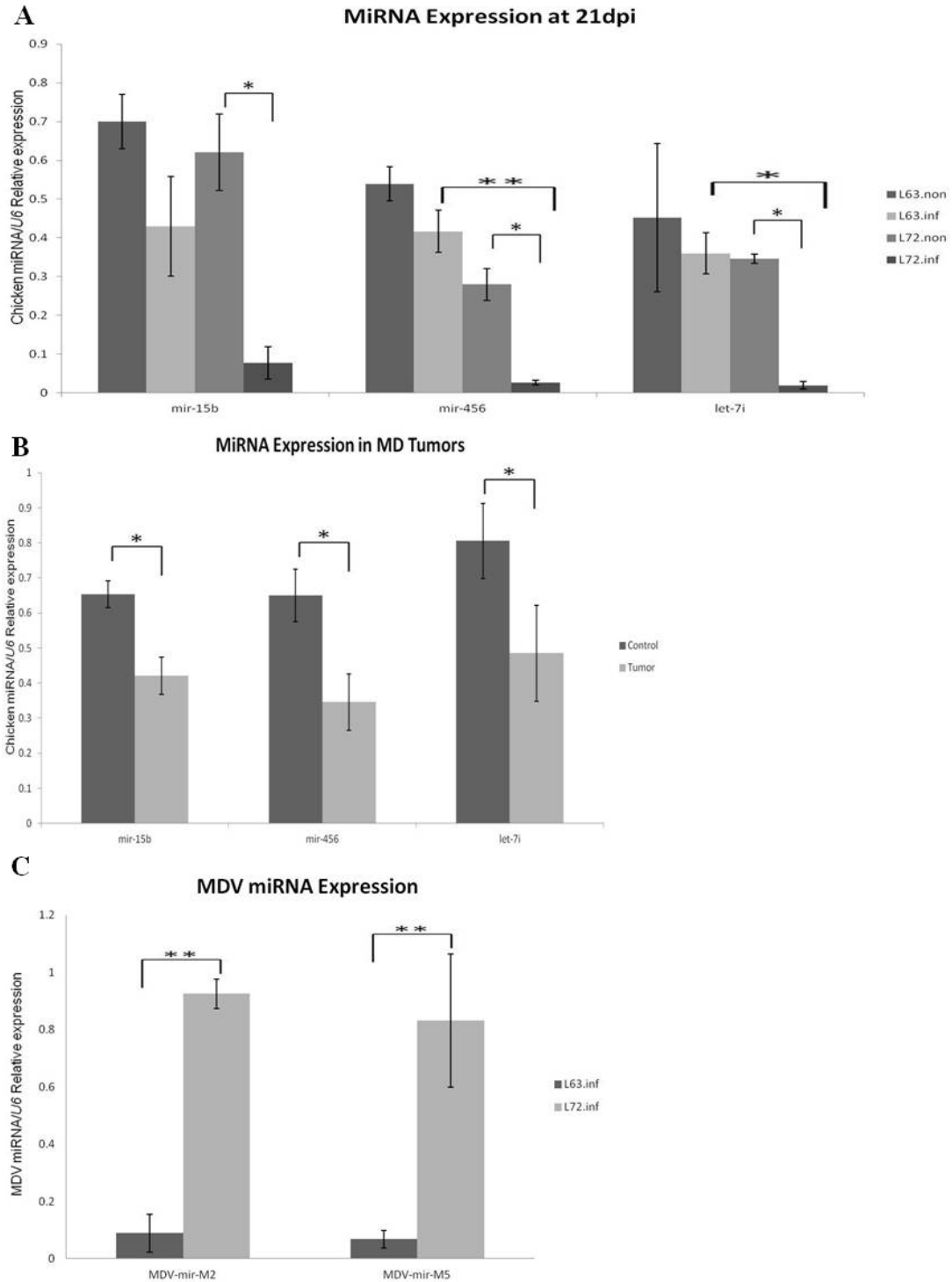


Figure 2.3 Expression of chicken and MDV miRNAs in MDV. Expression of *gga-miR-15b*, *gga-miR-456* and *gga-let-7i* was measured by qRT-PCR in spleen samples from noninfected and infected line 6₃ and line 7₂ chickens as well as in the normal (A) and tumor spleen (B), and the expression was normalized to *U6*. (C) Expression

levels of *MDV1-miR-M2* and *MDV1-miR-M5* in infected line 6₃ and line 7₂ chickens were detected using qRT-PCR and normalized to *U6*. The quantitative results are represented as mean ± SEM (n=4). A single asterisk (p-values <0.05) and double asterisks (p-values < 0.01) indicate the transcription level in the specific group was significantly different when compared to the adjoined group. L7₂.inf: infected line 7₂; L7₂.non.inf: noninfected line 7₂; L6₃.non.inf: noninfected line 6₃; L6₃.inf: infected line 6₃.

MiRNA Target Identification

To further understand the potential functions of miRNAs in MDV resistance and susceptibility, we examined the protein and mRNA levels of several genes that were reported to interact with MDV oncogene *Meq*. The protein level of activating transcription factor 2 (*ATF2*) was significantly increased in infected line 7₂ chickens compared to MDV-free chickens, whereas its expression was stable in line 6₃ birds before and after MDV challenge (Figure 2.4 A). Comparably, qRT-PCR revealed that the mRNA levels of *ATF2* were slightly decreased upon MDV infection in the two lines but were not significantly different (Figure 2.4 B), indicating that miRNAs might be regulating *ATF2* expression. By using a bioinformatic tool (RNAhybrid), 3 chicken miRNAs (*gga-miR-15b*, *gga-miR-456* and *gga-let-7i*) were found to be among those differentially expressed and predicted to interact with *ATF2* mRNA in its coding regions (Figure 2.5 A). The speculation that *ATF2* translational regulation requires chicken miRNAs was verified by the observation that induction of *gga-miR-15b* inhibited luciferase activity by ~20% compared to negative control (p<0.05) (Figure 2.5 B). However, the presence of *gga-let-7i* silenced firefly luciferase activity by ~15% although this difference was not statistically significant. We also found that *gga-miR-456* did not influence the translation activity of the *ATF2* (Figure 2.5 B).

Since MDV infection was reported to induce DNA methylation alterations, the same bioinformatic tool was applied to investigate if miRNAs were involved in the regulation of *DNMTs*. The protein expression was significantly upregulated in line 7₂ infected chickens, and no transcriptional changes were observed among the 4 samples (Figure 2.6). *DNMT3a* was predicted to contain binding sites for *gga-let-7i* and *gga-miR-15b* at the gene body regions (Figure 2.7 A). The reporter assay showed that *gga-let-7i* and *gga-miR-15b* significantly repressed the luciferase activities by miRNA mimics about 20% ($p < 0.05$) (Figure 2.8 B and C).

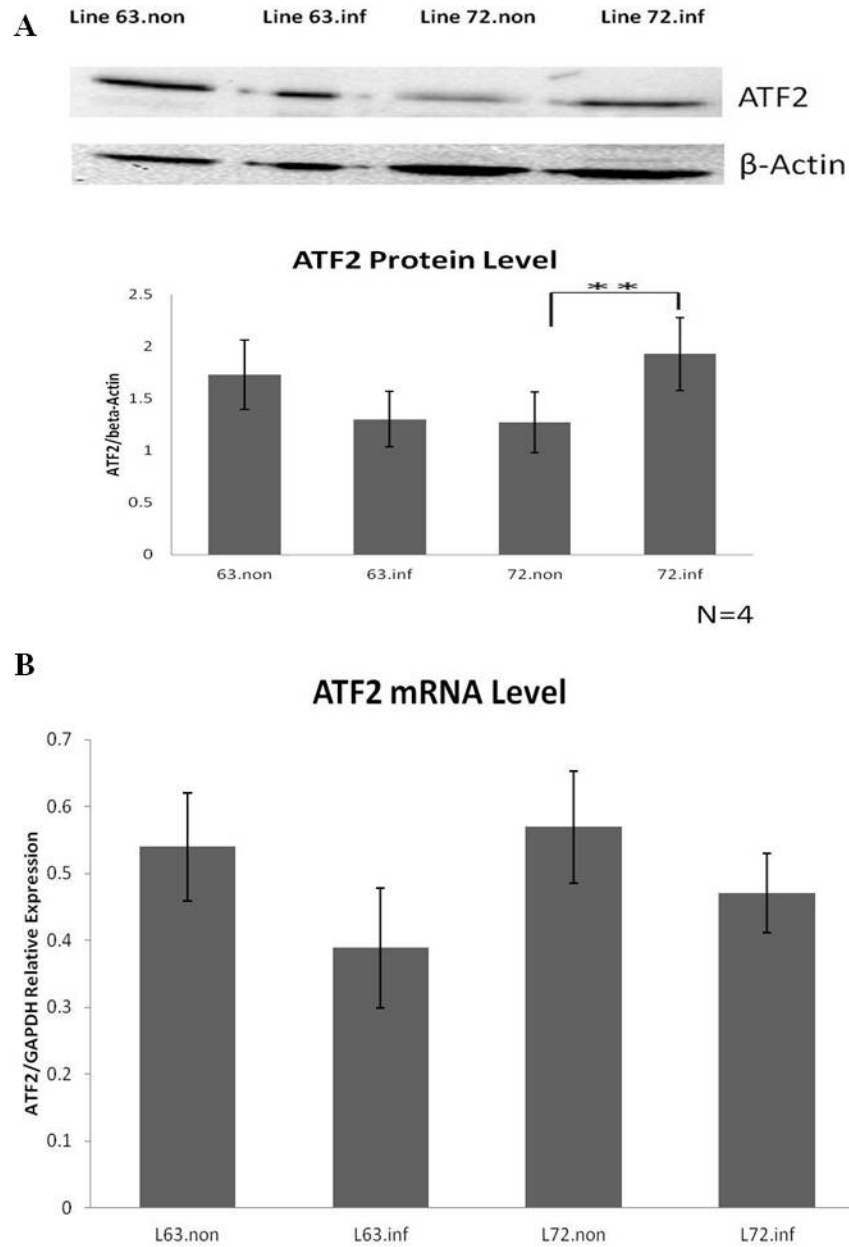


Figure 2.4 Protein and mRNA quantification of *ATF2*. Western blot (A) and qRT-PCR (B) of *ATF2* were measured in the spleen samples from the two lines before and after MDV infection at 21 dpi. The quantitative results are represented as mean \pm SEM. A single asterisk (p-values <0.05) and double asterisks (p-values <0.01) indicate the expression level in the specific group was significantly different when compared to the adjoined group. L63.inf: infection line 6₃ and L72.inf: infected line 7₂.

A Schematic of miRNA Binding Sites in Chicken *ATF2* mRNA

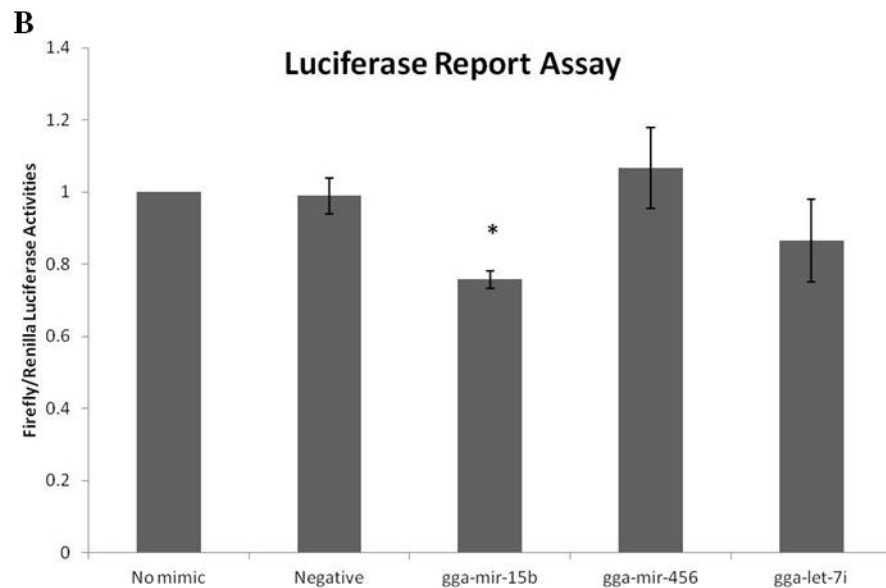
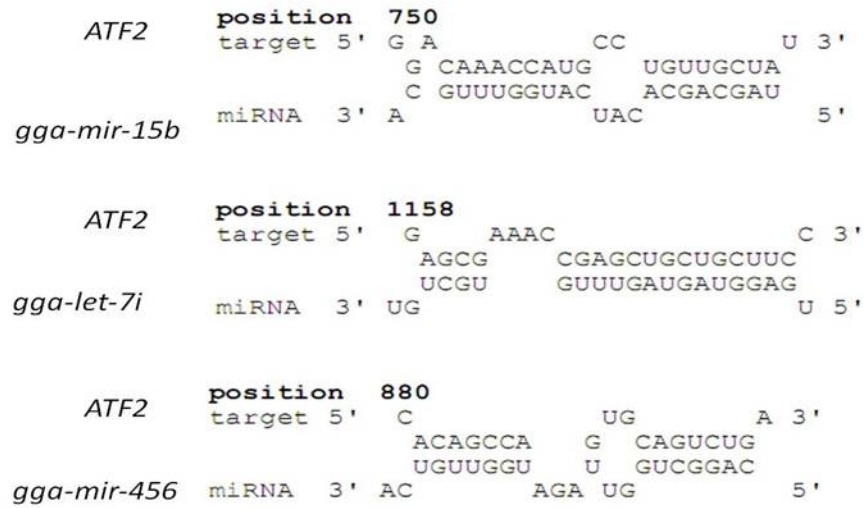


Figure 2.5 The validation of miRNA-*ATF2* interaction. (A) Schematic of *gga-mir-15b*, *gga-let-7i* and *gga-mir-456* binding sites in chicken *ATF2* mRNA. (B) Luciferase reporter assay was used to measure the interaction between microRNAs and the plasmid construct containing microRNA target sites. Firefly luciferase activity was normalized to Renilla luciferase activity for each treatment. A single asterisk indicates a significant difference ($p < 0.05$) between microRNA-mimicked treatments and negative controls.

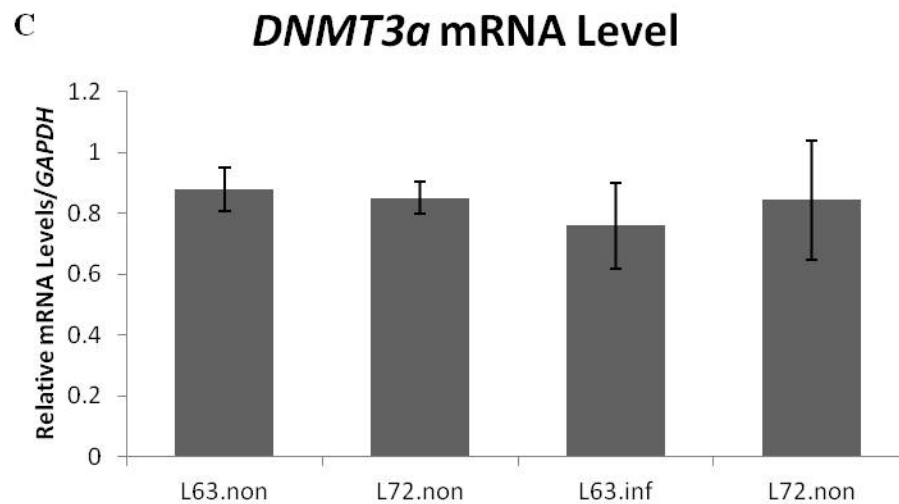
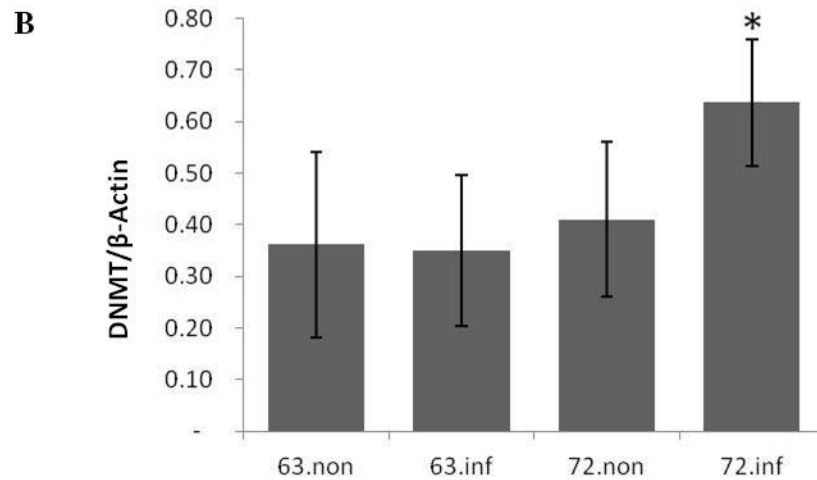
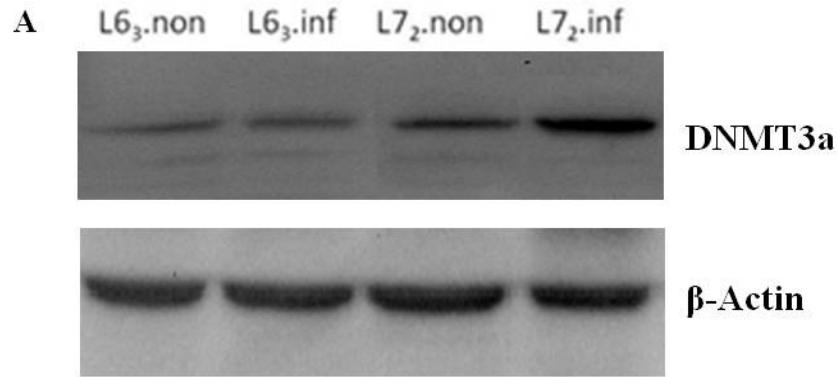


Figure 2.6 Protein and mRNA quantification of *DNMT3a*. Western blot (A) and qRT-PCR (B) of *DNMT3a* were measured in the spleen samples from the two lines before and after MDV infection at 21 dpi. The quantitative results are represented as mean \pm SEM. A single asterisk (p-values <0.05) and double asterisks (p-values <0.01) indicate the expression level in the specific group was significantly different when compared to the adjoined group. L63.inf: infection line 6₃ and L72.inf: infected

line 7₂.

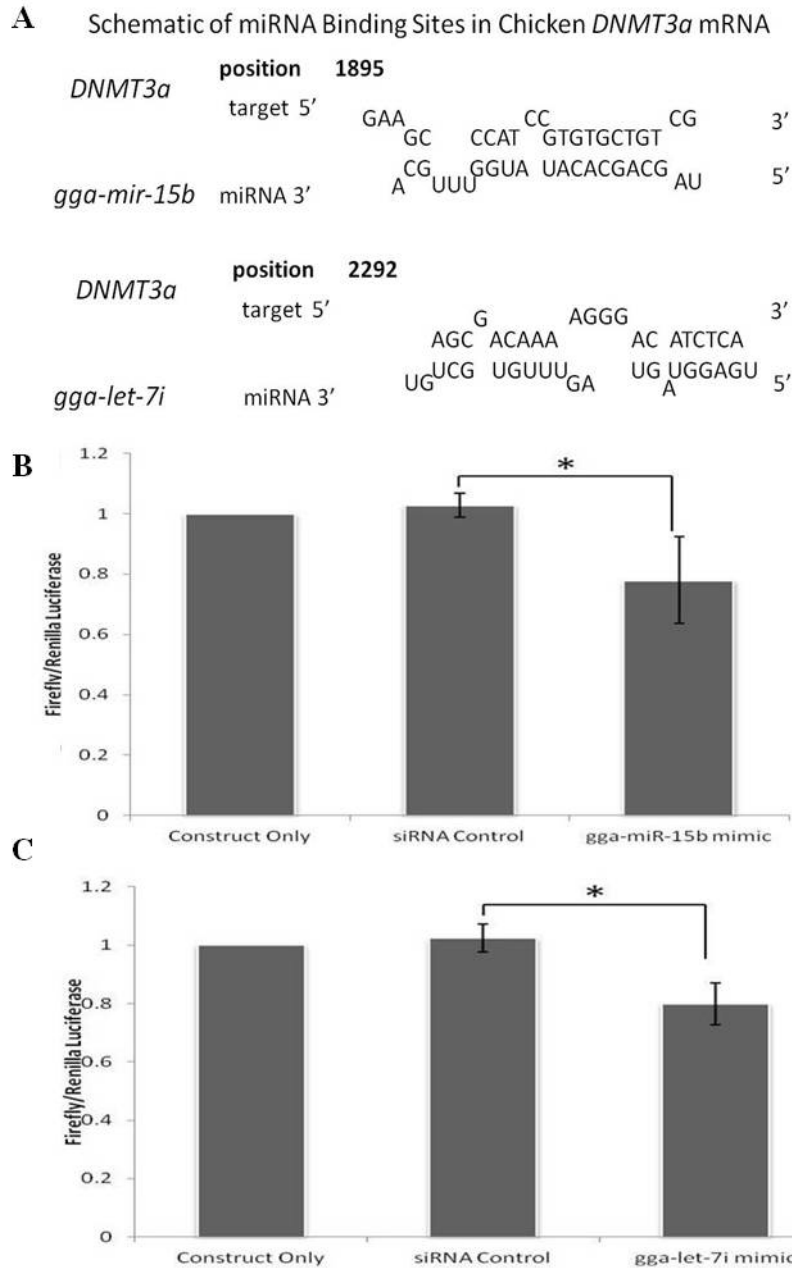


Figure 2.7 The validation of miRNA-*DNMT3a* interaction. (A) Schematic of *gga-mir-15b* and *gga-let-7i* binding sites in chicken *DNMT3a* mRNA. (B) Luciferase reporter assay was used to measure the interaction between *gga-mir-15b* and the plasmid construct containing microRNA target sites. (C) Luciferase reporter assay was used to measure the interaction between *gga-let-7i* and the plasmid construct containing microRNA target sites. Firefly luciferase activity was normalized to Renilla luciferase activity for each treatment. A single asterisk indicates a significant difference ($p < 0.05$) between microRNA-mimicked treatments and negative controls.

Discussion

MDV has been reported to be replicated relatively faster in line 7₂ than in line 6₃ [58, 173]. This phenomenon may be caused by the differential expression of microRNAs or may lead to the distinct microRNA expression in these two lines; however, this requires further investigation. The highest virus copy number was found at 21 dpi in both lines, and virus induced or repressed microRNAs could be detected at this time point for microarray analysis. Compared to high-throughput sequencing, microarray relies on the prior sequence information for probe designs, and focuses only on the well-studied miRNAs which were printed on the array, therefore, was inadequate to identify novel miRNAs. Despite of these limitations, array-based approach is a feasible and cost-efficient method to identify differentially expressed miRNAs. Therefore, to generate a global view of differentially expressed microRNAs, microarray analysis was conducted on samples from 21 dpi.

The spleen is an important immune organ that provides a niche for MDV to reach its primary targets (B cells and CD4⁺T cells) during infection [19]. Because of the absence of classical transforming genes in MDV, the environment provided by the spleen is critical for viral replication [174]. Therefore, all the experiments were carried out using splenic samples. To gain insights into MDV-induced microRNA expression variations in the immune system, this study profiled microRNA expression in resistant and susceptible chickens *in vivo*, which will improve our knowledge of the MDV-chicken interaction.

Variation in miRNA expression induced by MDV infection has been

identified in chicken embryo fibroblast (CEF), including some miRNAs that also showed differential expression in our study [119]. Based on the current microarray cutoff for differential expression ($p < 0.05$ and $FDR < 0.1$) in the microarray, miRNA expression was only significantly different between infected and noninfected line 7₂ groups, and between the infected line 6₃ and line 7₂ groups. This finding suggested that potential functions of these miRNAs were related to MD resistance and susceptibility. However, we did observe significant miRNAs between line 6₃ infected and uninfected chickens or between line 6₃ and line 7₂ if with $p < 0.05$ only, but none of these miRNAs were confirmed by qRT-PCR. Because microRNA expression signature following MDV infection in line 6₃ and line 7₂ has not been studied, we compared our results with cDNA microarray analysis in the two lines. Previous studies [36] examined gene expression in peripheral blood lymphocytes (PBLs) in two chicken lines and revealed that the expression of some genes show at least two fold changes between infected line 6₃ and line 7₂ chickens, while the transcriptional profiles of uninfected birds were similar, which was consistent with our findings. Collectively, our results demonstrated that differential expression of miRNAs was driven by MDV infection in line 6₃ and line 7₂. Results from qRT-PCR were consistent with the microarray analysis for both cellular and viral miRNAs. These data demonstrated significant inactivation of cellular miRNA production and the increased MDV miRNA transcription in infected line 7₂ at 21 dpi. Moreover, we found a set of miRNAs (*gga-miR-15*, *gga-miR-456* and *gga-let-7i*) that were deregulated in MD tumors, similar to infected line 7₂, which implied their potential roles as tumor suppressors and early indicators of MD progression. However, other

miRNAs had different transcriptional levels between tumor samples and infected line 7₂ (data not shown), suggesting different functions in viral infection and tumorigenesis. In contrast to cellular miRNAs, all of the MDV miRNAs were significantly upregulated. For example, *MDV1-miR-M2* and *MDV1-miR-M5*, located at the 5' upstream of *Meq* [28], were overexpressed in the infected line 7₂ at 21 dpi compared to the infected line 6₃. This result is consistent with the higher DNA copy number and activated transcription of *Meq*, and highlighted increased viral replication in infected line 7₂.

The candidate target genes that may be regulated by differentially expressed miRNAs were predicted using bioinformatic tools miRDB and MDV MicroRNA Target Prediction. The pathway analysis was done using IPA (Ingenuity systems pathway analysis) to further clarify the molecular functions that miRNAs may be involved in (Appendix IV.). Several immune related pathways, such as *NF-κB* signaling and T cell and B cell receptor signaling were included, implying that miRNAs may influence MD resistance or susceptibility through controlling the immune responses.

The discovery of the miRNA *gga-miR-15b* target, *ATF2*, is valuable for understanding the etiology of MD. *ATF2* is a sequence-based DNA binding protein that belongs to the cAMP-response element (CRE)-binding protein (CREB) family, which regulates proliferation and apoptosis by altering downstream gene expression [175]. The mRNA level of *ATF2* was only slightly reduced (20 % and 10 %, respectively) after MDV infection in line 6₃ and line 7₂, suggesting MDV infection did not modulate *ATF2* transcription. In line 7₂ chickens, after MDV infection, *ATF2*

protein increased significantly compared to non-infected birds. Interestingly, in the same line, the increase of ATF2 was coincident with the decrease of *gga-miR-15b* level. Bioinformatics analysis predicted that *ATF2* was one of direct targets for *gga-miR-15b*. The luciferase reporter assay showed that *gga-miR-15b* indeed depressed ATF2. This information suggested that MDV infection resulted in the downregulation of *gga-miR-15b* thus released its inhibition on ATF2 translation in line 7₂. The coexpression of ATF2 and *gga-miR-15b* was observed in line 6₃. Traditionally, it is believed that because of its inhibition effect, miRNA and its target show mutually exclusive pattern. However, this classic view has been disputed by recent publications that show miRNA and its target can be coexistent to maintain the balance of translational network [176-179]. It appeared that the abundance of ATF2 protein was similar in line 6₃ chickens regardless of MDV infection; however, this observation was not surprising because it was well possible that in this resistant line, some unknown mechanisms prevent MDV from reducing *gga-miR-15b* expression to increase *ATF2* translation. The mechanisms that inhibit MDV-mediated reduction of *gga-miR-15b* in line 6₃ remained unclear. The distinct genetic backgrounds, such as SNPs and gene expression variations between two lines may contribute to the different regulatory mechanisms. The unique expression pattern and distinctive regulatory mechanism may suggest that ATF2 plays different roles in line 7₂ and line 6₃. As far as the biological function of ATF2 is concerned, several lines of evidence suggest that ATF2 may work as an oncogene or tumor suppressor dependent on the cellular systems. For example, it has been reported that ATF2 elicited tumor suppressor or oncogene activities in different cancers by in cooperation with other

tumor suppressors or oncogenes [34, 180, 181]. Chicken ATF2 was documented to form a heterodimer with c-Jun, MDV oncogene Meq and other b-ZIP proteins [19, 34, 35]. In line 7₂, we found ATF2 protein level was higher in MDV infected birds than uninfected ones. Since MDV oncogene Meq was highly expressed in line 7₂ after MDV infection, ATF2 probably formed a heterodimer with Meq and favor MD development. In the line 6₃, due to the absence of *Meq* after MDV exposure, ATF2 may be in cooperation with c-Jun and perform distinct functions as in line 7₂. Considering the dramatic difference in Meq expression between infected line 7₂ and infected line 6₃, it is likely that ATF2 may have different partners and play distinct roles in two chicken lines after MDV infection even though the expression was similar between infected line 7₂ and infected line 6₃. The other chicken miRNA *gga-let-7i*, which was also deregulated in line 7₂ after MDV challenge, may have negative effects on ATF2 translation since it slightly suppressed luciferase activities, but might not control ATF2 translation alone. In general, miRNA regulation of gene expression is largely dependent on binding at the 3' UTR. However, miRNA target sites in the coding regions of genes have recently been reported in humans [92]. The validation that *gga-miR-15b* reduced *ATF2* expression provided further evidence that the miRNA regulation of gene expression could depend on the binding at the coding region.

DNA methylation variations were induced by MDV infection in chicken [3], therefore, it was reasonable to speculate the expression of DNMTs was changed after MDV exposure. In chickens, there are 3 different DNMTs, including DNMT1, DNMT3a and DNMT3b. Among these 3 DNMTs, only DNMT3a showed increased

protein expression without the mRNA alterations, suggesting its expression may be regulated by miRNAs. The manipulation of DNMTs by miRNAs was discovered, such as *DNMT3a* and *DNMT3b* directly targeted by *has-mir-29b* as well as the regulation of DNMT1 by *has-mir-148a* and *has-mir-152* in human [182, 183]. The interaction between chicken *DNMT3a* and miRNAs was confirmed by luciferase report assay. Before MDV infection, DNMT3a expression was similar between line 6₃ and line 7₂, and the MDV infection activated DNMT3a expression in line 7₂, which was controlled by the downregulation of *gga-mir-15b* and *gga-let-7i*.

In summary, MDV challenge in resistant and susceptible chicken lines resulted in differential miRNA expression signatures in the spleens of infected chickens. The expression of most cellular miRNAs was dramatically decreased, but viral miRNAs were overexpressed in the MDV-infected susceptible line. In contrast, chicken miRNA transcription was relatively stable while MDV miRNA expression was suppressed in infected resistant lines. The repression of miRNA results in distinct target gene expression in the two lines after MDV infection. *ATF2* and *DNMT3a* were identified as direct targets for *gga-miR-15* and *bgg-let-7i*, and the biological consequences of activation of ATF2 and DNMT3a and on MD resistance and susceptibility *in vivo* should be further elucidated.

Chapter 3: The Functional Analysis of Selected Chicken MicroRNAs on Marek's Disease Virus Infection

Abstract

MicroRNAs (miRNAs) are a class of short, noncoding RNA, which are emerging as major regulators for the antiviral mechanism. Marek's disease (MD) is an aggressive T-cell lymphoma in chickens induced by the infection of MD virus (MDV). Host resistance and susceptibility to MD are tightly determined by different molecular mechanisms. The distinct chicken miRNA transcriptional signatures were identified in MD-resistant and -susceptible chickens. In this study, the function of some cellular miRNAs on MDV infection was further revealed. The selected miRNAs, *gga-mir-15b* and *gga-let-7i*, were overexpressed in chicken fibroblast (CEF) cell line DF-1. MDV infection of the cells demonstrated that the miRNA expression levels were inversely correlated with MDV replication in the infected cells. This result highlighted the important function of the chicken miRNAs against MDV replication in cultured cells.

Introduction

Marek's disease virus (MDV), an α -herpesvirus, is the causative agent for Marek's disease (MD). MDV infection results in a lymphoproliferative disorder in susceptible chickens, which is one of major health threats for poultry industry. The non-oncogenic herpesvirus of turkey (HVT) and attenuated MDV were used as

vaccines to control MD since 1970s [1]. However, with the evolution of MDV towards higher virulence in chickens, virus appeared to be escaping the vaccine control, as new and acute symptoms were identified [19]. Therefore, understanding the molecular mechanism on MD resistance will help to improve the current disease control strategy.

MicroRNAs (miRNAs) are a class of small single-stranded non-coding RNA molecules, approximately 22 bp in length. MiRNAs mediate gene repression at post-transcriptional level by imperfect complementarity to the 3'UTR or coding regions of transcripts [76]. MiRNAs were identified in multicellular eukaryotes and viruses, and are involved in diverse biological processes. It has been demonstrated that miRNAs play intricate roles in the cross-talk between host and pathogen [113, 184]. The cellular miRNAs have dual functions in virus-host interactions through the regulation of host and viral gene expression. Some miRNAs promoted the viral gene translation while some repressed virus propagation [113, 185, 186]. Therefore, regulation of cellular miRNAs through RNA interference (RNAi) could be a promising approach for MD control.

In vivo and *in vitro* studies have revealed that MDV infection provokes the downregulation of miRNAs in MDV-transformed T cell lines and susceptible chickens, but does not affect miRNA expression in MD resistant chickens [5, 119, 187]. All these findings suggest that miRNAs are essential to the functional immune response against MDV infection. Our previous work showed that the expression of chicken miRNAs was significantly decreased in MD susceptible inbred chicken line 7₂ [5]. Two chicken genes, activation transcription factor (*ATF2*) and DNA

methyltransferase 3a (*DNMT3a*), were identified as the target of miRNAs *gga-mir-15b* and *gga-let-7i*, which were both downregulated in the infected MD susceptible chickens. However, the impacts of *gga-mir-15b* and *gga-let-7i* on MDV infection were not known yet.

To explore the effects of miRNAs on MDV infection, in the current study two chicken miRNAs, *gga-mir-15b* and *gga-let-7i*, were overexpressed in the chicken embryonic fibroblast cell line DF-1 using the avian leukosis virus (ALV) construct-based retroviral vectors (RCAS system) [125, 126]. The overexpression of the two cellular miRNAs repressed MDV replication in the MDV-infected DF-1 cells, and the expression of MDV oncoprotein Meq was reduced as well. Collectively, the results demonstrated the antiviral function of the cellular miRNAs against MDV infection.

Materials and Methods

Vector construction and cell transfection

The miRNAs were cloned into a retroviral vector based on the replication-competent avian leukosis virus construct (provided by Dr. H.C. Liu at North Carolina State University) [188]. The sequences of two pre-mature miRNAs (*gga-miR-15b* and *gga-let-7i*) and scrambled control were synthesized (Eurofins) and the SphI and NgoMIV restriction enzyme sites were added to the 5' end of the sense and anti-sense oligonucleotides, respectively (Table 3.1). The sense and antisense oligo stocks of 50 μ M were mixed and incubated at 95°C for 5 min, and then transferred to 70°C water bath for 10 min. The water bath was turned off and the oligo mixture was

left in the water bath overnight to allow complete annealing. The pENTR3C entry vector was digested with SphI and NgoMIV restriction enzymes at 37°C for 4-6 hrs with 1× NEB buffer 4 (NEB). The annealed pre-miRNA duplex was ligated to the entry vector with T4 DNA ligase by incubation at 4°C overnight (Progema). The ligation products were transformed to the DH5α competent cells (ZYMO research) and the positive insertion was selected by Kanamycin after incubation at 37°C overnight. The selected colonies were cultured at 37°C with shaking. The plasmid DNA was isolated using QIAprep® Miniprep Kit (QIAGEN), and the correct insertions were confirmed by restriction enzyme digestion and DNA sequencing.

To transfer the inserts to the destination vector, 150 ng of each of miRNA pENTR3C entry vectors with correct insertion were mixed with 150 ng of pRCASBP (A)-YDV (provided by Dr. H.C. Liu at North Carolina State University), and incubated with Gateway® LR clonase mixture (Invitrogen) according to the manufacture's recommendations. The products were transformed to the competent DH5α competent cells (ZYMO research) and selected by ampicillin after incubation at 37°C overnight. The selected colonies were cultured at 37°C with shaking. The plasmid DNA was isolated using QIAprep® Miniprep Kit (QIAGEN), and the correct insertions were confirmed by restriction enzyme digestion and DNA sequencing.

The miRNA overexpression vector was delivered into DF-1 cells by transfection using Fugene® transfection reagent (Promega) based on the manufacturer's instructions. The overexpression was confirmed 3 days post-infection by miScript system (QIAGEN) and immunofluorescence staining of viral *gag* protein with mouse monoclonal antibody 3C2 (Developmental Studies Hybridoma Bank at

University of Iowa) and FITC-conjugated donkey anti-mouse IgG (Santa Cruz).

Table 3.1 Pre-miRNA sequences

	Sequence
mir-7i_F	5'-C CTGGCTGAGGTAGTAGTTTGTGCTGTTGGTCGGGTTTGACA TTGCCCGCTGTGGAGATAAAGTGGCAAGCTACTGCCCTTGCTA G-3'
mir-7i_R	5'- CCGGC TAGCAAGGCAGTAGCTTGGCAGTTATCTC CACAGCGGG C AATGTCACAA CCCGACCAAC AGCACAAACT ACTACCTCAG CCAG GCAIG -3'
mir-15b_F	5'-C TGAGGCCTTAAAGTACTCTAGCAGCACATCATGGTTGCAATGCT GTAGTGAAGATGCCGATCATTTATTGCTGCTTTAGAAATTTAAGGAA G-3'
mir-15b_R	5'-CCGGC TTCCTTAAATTTCTAAAGCAGCAATAATGATTCGCATCTT CACTACAGCATGCAAAACCATGATGTGCTGCTAGAGTACTTTAAGGCCITCA GCAIG -3'
SC_F	5'- C GACTTACAGCCAGTTCCTAGTATAGTGAAGCAGCAGATGGTATA CTAGGAAGCTGGCTGTAAGCT G-3'
SC_R	5'-CCGGC AGCTTACAGCCAGTTCCTAGTATACCATCTGCTGCTTCACTATACT AGGAACTGGCTGTAAGTC GCAIG-3'

Cell culture and MDV infection

Chicken embryo fibroblast DF-1 cells were grown in Dulbecco's modified Eagle's medium supplemented with 10% fetal bovine serum, streptomycin (100 mg/ml) and penicillin (100 U/ml) (Invitrogen). Cells were maintained at 37°C in humidified 5% CO₂ conditions. The very virulent + (vv+) strain of MDV (648A passage 40) was obtained from USDA-ARS Avian Disease and Oncology Laboratory. The DF-1 cells were inoculated with the MDV at multiplicity of infection (M.O.I) of 0.1 and incubated for 3 days.

Quantification of MDV genomic DNA loads

Genomic DNA from DF-1 cells was extracted by using Wizard Genomic DNA purification kit (Promega). RNase treatment was performed to remove RNA from DNA samples. DNA concentration was measured using Nanodrop. As previously described [168], the MDV genes *Meq* and *ICP4* were amplified to quantify viral genomic DNA. Quantitative PCR was performed on genomic DNA (10 ng/μl) with the iCycler iQ PCR system (Bio-Rad, USA) and QuantiTect SYBR Green PCR Kit (Qiagen, USA). Relative MDV loads were determined after normalization to a single-copy gene *VIM* (vimentin) [169]. Primers used in the PCR were listed in Table 2.1.

Quantification of miRNA and mRNA levels using real-time PCR

MiRNAs and mRNAs were extracted from the DF-1 cells using the miRNeasy Mini Kit (QIAGEN) and RNeasy Mini Kit (QIAGEN) according to the

manufacturer's instructions. The on-column DNase digestion was done for miRNA and mRNA purification to remove DNA. MiRNA were reverse transcribed and quantified with a miScript Reverse Transcription Kit (QIAGEN), a miScript SYBR Green PCR Kit (QIAGEN), and 5 miScript Primer assays (QIAGEN). Reverse transcription and quantification of mRNA were performed with SuperScript™ III Reverse Transcriptase (Invitrogen) with oligo (dT)₁₂₋₁₈ primers (Invitrogen), and the QuantiTect SYBR Green PCR Kit. In the reverse transcription control, PCR water (Invitrogen) was used to replace miRNA or RNA samples.

Western blot

Total protein was extracted from DF-1 cells with RIPA buffer (150 mM sodium chloride, 1.0% NP-40, 0.5% sodium deoxycholate, 0.1% SDS and 50 mM Tris, pH 8.0) containing a protease inhibitor cocktail (Sigma). Briefly, the cell lysates were incubated at 4 °C for 2 hours with constant agitation and subsequently centrifuged at 4°C for 30 min. Protein concentration for each sample was determined by the BCA assay (Thermo Scientific). For Western blotting, 30 µg of proteins were heated at 95-100°C for 5 min and separated by 10% SDS-PAGE. After separation, proteins were transferred onto polyvinylidene fluoride (PVDF) membrane. The membrane was blocked with 5% nonfat milk in TBST containing 0.1% Tween 20. Primary antibodies against Meq, ATF2 (Santa Cruz), DNMT3a and β-actin (Abcam) were prepared at 1:500 to 1:1000 dilutions in TBST, respectively. Membranes were incubated with primary antibodies overnight at 4°C followed by washing quickly for 3 times (less than 1 min) and 3 times of 5-minute washing. The membranes were then

incubated with anti-rabbit IgG or anti-mouse IgG secondary antibodies (Santa Cruz) diluted in TBST (1:5000) for 1 hr at room temperature. The membranes were quickly washed 3 times and then washed 3 more times for 5 min each. Specific reactions were revealed with ECL (Amersham) and luminescence signals were recorded using ChemiDoc XRS (Bio-Rad). To quantitate the amount of protein, the signal volume was measured with Quantity One software using volume analysis. The band signals were measured, and background correction was applied. The background-adjusted volume signals of each band were export to excel. The relative protein expression was calculated as the ratio of the adjusted volume signals between protein of interest and β -actin. Three independent experiments were performed.

Results

Validation of miRNA overexpression

To confirm the transfection of ALV-based retroviral vector in DF-1 cells, immunostaining of the ALV gag protein was conducted (Figure 3.1). Green fluorescence was observed in the cytoplasm of the transfected cells, indicating gag protein expression. The qRT-PCR was done to confirm the overexpression of the specific miRNA. The result showed that *gga-mir-15b* was only highly expressed in cells transfected with the vector containing pre-*gga-mir-15b* sequence (RCAS-*gga-mir-15b*) ($p < 0.05$), while its expression level was lower in the cells transfected with scramble control vector (RCAS-sc) or *gga-let-7i* overexpression vector (RCAS-*gga-let-7i*) (Figure 3.2). Similarly, the transcripts of *gga-let-7i* increased about 9 folds in

cells transfected with RCAS-*gga-let-7i* than the cells transfected with RCAS-sc or RCAS-*gga-mir-15b* (Figure 3.2). These results confirmed the overexpression of miRNAs using the retroviral constructs.

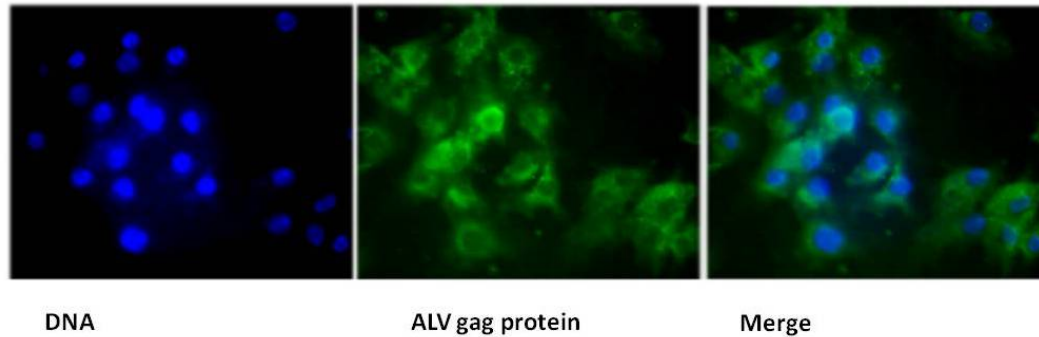


Figure 3.1 The expression ALV gag protein. The left panel showed the location of nuclei using DAPI to stain DNA (blue). The middle panel was the location and expression ALV gag protein (green). The right panel indicated gag was expressed in the cytoplasm of the transfected DF-1 cells.

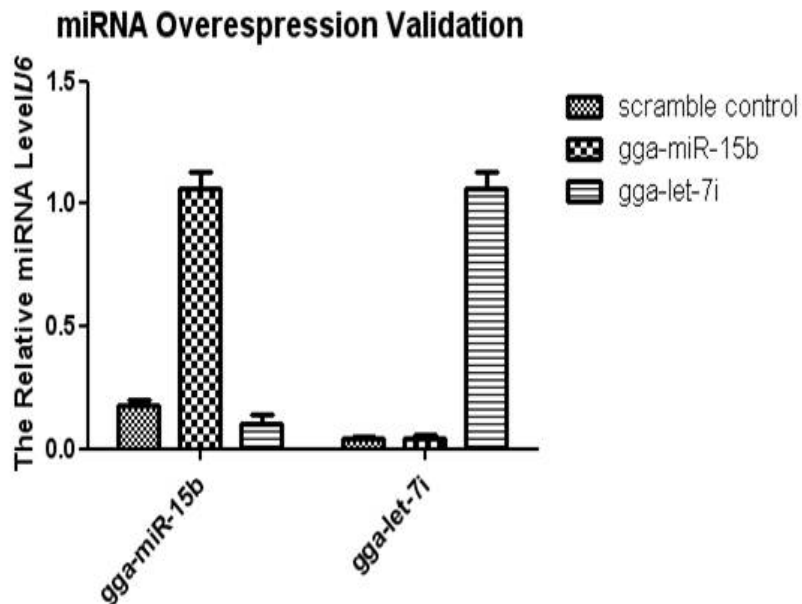


Figure 3.2 The validation of miRNA expression by qRT-PCR. The x-axis included two miRNAs detected by qRT-PCR. The y-axis was the miRNA relative expression normalized using U6. Scramble control, *gga-mir-15b* and *gga-let-7i* represented DF-1 cells transfected with RCAS-sc, RCAS- *gga-mir-15b* and RCAS- *gga-let-7i*. The relative expression value was denoted as mean \pm STD.

The expression of target genes in miRNA overexpressed cells

Two chicken genes, activation transcription factor (*ATF2*) and DNA methyltransferase 3a (*DNMT3a*), are the known targets of *gga-mir-15b* and *gga-let-7i* [5]. The expression of DNMT3a was downregulated by about 72% in *gga-let-7i* overexpressed cells ($p < 0.05$). The overexpression of *gga-mir-15b* repressed DNMT3a by about 37%, but not statistically significant (Figure 3.3). ATF2 expression was suppressed by approximately 73% by overexpression of *gga-mir-15b* ($p < 0.05$), and was influenced by *gga-let-7i* upregulation (Figure 3.3).

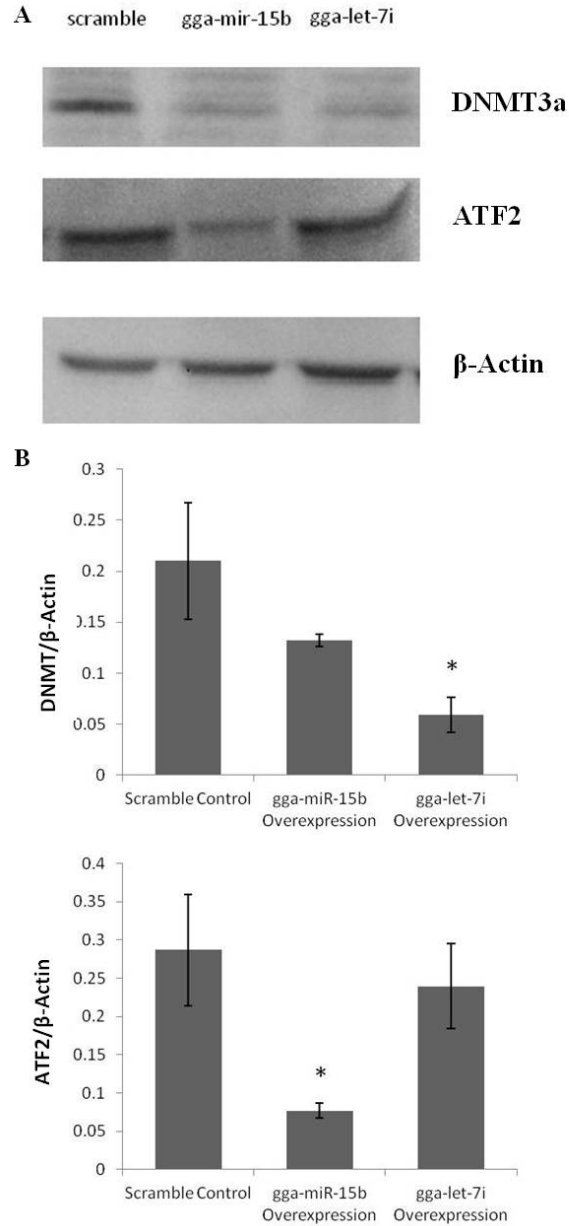


Figure 3.3 Detection of DNMT3a and ATF2 by Western blotting. The DNMT3a and ATF2 were detected in the DF-1 cells transfected with RCAS-sc, RCAS-*gga-mir-15b* and RCAS-*gga-let-7i* by the western blot (A). The result was quantitated using the densitometry analysis (B). The results are represented as mean \pm STD. A single asterisk ($P < 0.05$) indicates the expression level in the test group was significantly different from the control.

The virus loads in MDV-infected DF-1 cells with miRNA overexpression

In order to assess the impacts of miRNAs on MDV infection, two important

viral genes (*Meq* and *ICP4*) were used to estimate the virus copy numbers in the MDV-infected DF-1 cells with miRNA overexpression. Real time PCR of *Meq* showed that the virus genome copies were about 61% in cells with *gga-mir-15b* overexpression and 39% in cells with *gga-let-7i* ($p < 0.01$) compared to the RCAS-sc control cells (Figure 3.4). Similarly, relative to the RCAS-sc transfection control cells, *ICP4* was declined about 40% in RCAS-*gga-mir-15b* transfected cells and 64% in RCAS-*gga-let-7i* transfected cells. The expression of MDV oncoprotein *Meq* was decreased about 34% in the DF-1 cells with *gga-mir-15b* overexpression cells ($p < 0.05$) and 65% in cells with *gga-let-7i* compared to the transfection control cells ($p < 0.05$) (Figure 3.5).

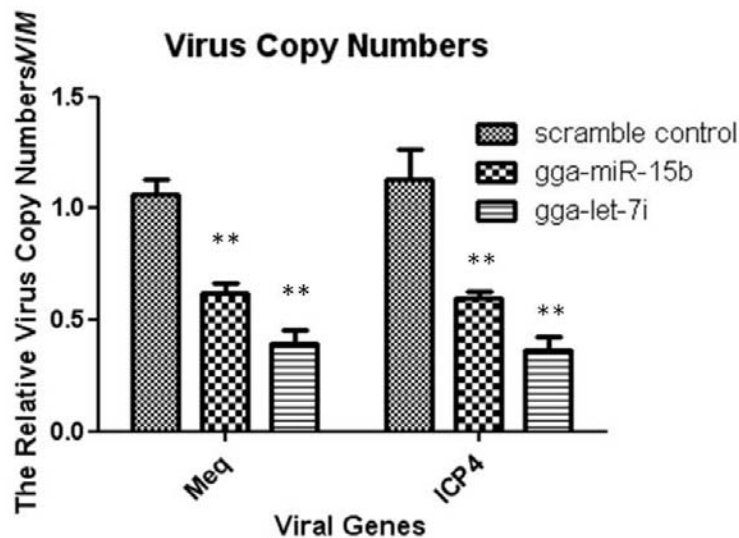


Figure 3.4 Quantification of viral genome copy numbers. The virus genomic copy numbers were estimated by real time PCR amplification of viral gene *Meq* and *ICP4* in DF-1 cells with miRNA overexpression, and normalized to a single copy gene, *Vim*. Quantitative results are represented as Mean \pm STD ($n=3$).

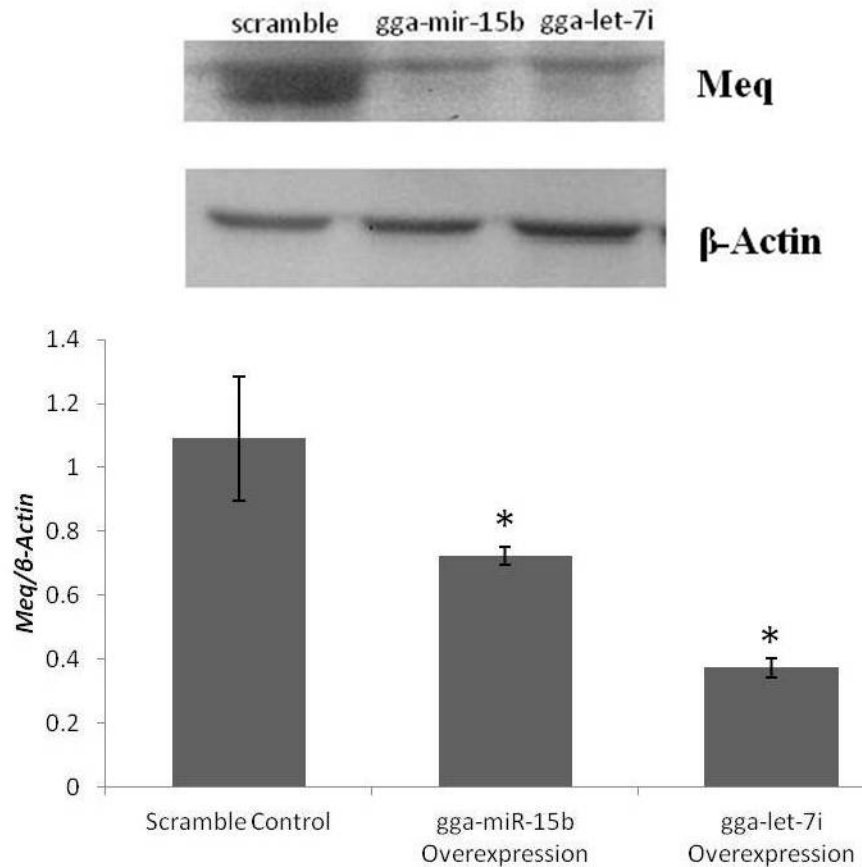


Figure 3.5 Detection of oncoprotein *Meq* in MDV-infected DF-1 cells by Western blotting. The band intensity was analyzed by densitometry and shown as relative folds in comparison with control after normalization with actin. Scramble control, gga-mir-15b overexpression and gga-let-7i overexpression indicate DF-1 cells transfected with RCAS-sc, RCAS-gga-15b and RCAS-gga-let-7i vectors. The error bars indicate standard deviation (n=3).

Discussion

Among the antiviral strategies, RNAi has drawn much attention due to its high efficiency and specificity [189]. Delivery of small interfering RNAs (siRNAs) by the transient transfection generated obvious effects against a variety of viruses [190, 191], however, the constant expression of siRNAs is essential to inhibit the chronic infection caused by virus. The retroviral vector-based method, such as the lentiviral

vector system, was widely used in RNAi-based gene therapy [191]. The replication-competent retroviral vector, ALV construct, was used to express short hairpin RNAs (shRNAs) and miRNAs in both chicken and mammalian systems [125, 188]. In the current study, chicken miRNAs, *gga-mir-15b* and *gga-let-7i*, were successfully delivered into DF-1 cells using ALV vector construct, which was confirmed by the expression of ALV gag protein in the transfected cells. The expression of either *gga-mir-15b* or *gga-let-7i* did not change the transcription of the other miRNA, suggesting that the regulation of these two miRNAs was independent. The downregulation of *ATF2* and *DNMT3a*, the known targets for the two miRNAs, is consistent with previous findings [5].

Cellular miRNAs mediated antiviral effect through targeting the virus genomes in infected mammalian cells [113]. Several miRNAs were induced by the interferon- β to repress hepatitis C virus (HCV) replication through targeting HCV genomes [113]. Human miRNA *has-mir-32* limited the proliferation of primate foamy virus type 1 (PFV-1) in human cells [114]. The current study demonstrated that chicken cellular miRNAs, *gga-mir-15b* or *gga-let-7i*, effectively inhibited MDV propagation *in vitro*. The quantitation of MDV genomic copy numbers using two viral genes, *Meq* and *ICP4*, showed similar reduction in the DF-1 cells with miRNA overexpression, ~40% in RCAS-*gga-mir-15b* cells and ~60% in RCAS-*gga-let-7i* cells. The result indicated that both the miRNAs had antiviral function. The miRNA *gga-let-7i* offered better protection to the cells than *gga-mir-15b*, however, neither of them could completely remove the virus. The downregulation of MDV oncoprotein *Meq* indicated that the miRNAs may regulate MDV infection through the repression

of *Meq* or the reduction of total virus replication. Searching of miRNA binding sites on *Meq* mRNA did not find any possible *gga-mir-15b* and *gga-let-7i* interacting sites. Thus, presumably, the *Meq* was indirectly modulated by these two cellular miRNAs.

Taken together, the current study suggested that the cellular miRNAs might participate in the host defense against the viral infection by regulating the viral replication or viral gene expression. Further work is required to uncover the involvement of miRNA targets in the antiviral responses. Moreover, different host miRNAs could be combined to improve the inhibitory effect against the viral infection.

Chapter 4: MDV Infection Induced Expression Changes of *DNMT* Genes Resulting in DNA Methylation Alternations in Marek's Disease Resistant and Susceptible Chickens

Abstract

Cytosine methylation, an epigenetic modification to DNA, has been reported to be involved in host-virus interaction. Marek's disease (MD) is characterized as a T cell lymphoma induced by a cell-associated alpha-herpesvirus, Marek's disease virus type 1 (MDV1). As with many viral infectious diseases, DNA methylation variations were observed in the progression of MD. Three major DNA methyltransferases were differentially expressed in MD resistant line 6₃ and MD susceptible line 7₂ at 21 days after MDV infection. Therefore, the genome-wide DNA methylation was conducted to explore the methylation variations induced by MDV infection in both chicken lines using Methyl-MAPS (methylation mapping analysis by paired-end sequencing). Overall, the methylation levels were reduced in resistant line 6₃ chickens after MDV infection, and infection induced differential methylation regions (iDMRs) were identified. The number of iDMRs was larger line 7₂ chickens than in line 6₃ chickens, and most of iDMRs found in line 6₃ were overlapped with the iDMRs found in line 7₂. The methylation variations in genes may control gene transcription, which may sequentially turn on or off specific pathways in the two lines. Collectively, the findings in the study provided more comprehensive information of the chicken

methylome. The results suggested that the host DNA methylation may be associated with disease resistance or susceptibility. The methylation variations induced by the viral infection may consequentially change the host transcriptome and result in the diverse disease outcomes.

Introduction

In mammalian cells, DNA methylation usually occurs at CG dinucleotides (CpG sites), and is catalyzed by the three DNA methyltransferases, including DNMT1 for maintaining methylation and the *de novo* methyltransferases DNMT3a and DNMT3b. The inhibition of DNMTs contributed to DNA demethylation through the passive mechanism [135]. Methylation is associated with the repression of transcription and essential for key biological processes, including development, X-chromosome inactivation, imprinting and tissue specific gene expression [15]. Tissue-specific variation in DNA methylation patterns have been observed; and abnormal DNA methylation contributes to disease, including cancer and some infectious diseases [8, 135, 192]. Methylome analysis has been conducted in different types of cancers. In a normal mammalian genome, the genome is primarily heavily methylated except for CpG dense promoters. In cancer cells, DNA methylation levels decrease at genome-wide, including hypomethylation in repetitive regions, while some tumor suppressor genes are observed to become hypermethylated [193]. DNA methylation alterations have also been identified in Epstein-Barr virus (EBV) transformed lymphoblastoid cell lines [2]. Likely, proper maintenance of DNA methylation patterns plays a vital role to prevent tumorigenesis and disease progression.

Marek's disease virus (MDV) is the causative agent for Marek's disease (MD), the T cell lymphoma in chickens and other birds. Although vaccines against MD have been developed, vaccination efforts have driven the virus to greater virulence. MDV infection is divided into four different phases. The entry of virus to target cells initiates early cytolitic infection from 3-7 days post infection (DPI). Latent infection starts at 7-8 DPI and primarily occurs at activated CD4⁺ T cells. Late lytic infection is reactivated from latency around 2-3 weeks post infection in susceptible chickens, and then switches to transformation stage and lymphoid tumors are observed in chickens [1]. Thus, late cytolitic stage is a critical step for MD progression and disease outcome. As many viruses, MDV infection induces changes in DNA methylation patterns in the hosts and virus itself which contribute to MD progression by activating or silencing genes crucial for MD immunity [3, 8, 194].

To explore the role of DNA methylation in MD immunology, two inbred chicken lines, were used. Most birds in line 7₂ develop tumors after MDV infection, and line 6₃ is resistant to the disease. These two chicken lines have the same major histocompatibility complex (MHC) haplotype but show significantly different MD incidences after MDV infection, which allows us to determine which genes affect MD resistance. *DNMTs* were found to be differentially regulated in line 6₃ and 7₂ after MDV infection, which may explain the promoter methylation alterations triggered by the infection [3]. DNA methylation was lost at active promoters in MDV carrying T cell lines and MD tumors, and was present in some CpG regions in MDV genome [3]. However, conclusions from these studies are limited since they focused on methylation variations at specific loci. Genome-wide alterations have not yet been

probed.

The emergence of next generation sequencing (NGS) provides a unique opportunity to explore global methylation variation following MDV infection in MD resistant and susceptible chickens. Since DNA methylation cannot be reliably directly detected, several approaches are available for genome-wide methylation analysis, including antibody affinity enrichment of methylated DNA, sodium bisulfite conversion and enzymatic digestion [195]. A newly developed method, called Methyl-MAPS (methylation mapping analysis by paired-end sequencing) [196], was adopted to study MDV induced methylation fluctuation in MD resistant and susceptible chickens. This method yields high resolution information with no bias towards the CpG rich regions; both single-copy and repetitive regions are directly probed. The current study revealed that *DNMTs* were differentially expressed in thymus of line 6₃ and line 7₂ chickens 21 days post infection (DPI) when the virus was reactivated from the latent stage. Global methylation levels were found to differ between non-infected 6₃ and 7₂ lines, and were reduced after MDV infection in line 6₃. The identified infection induced differential methylation regions (iDMRs) suggested that DNA methylation likely regulates distinct pathways in resistant and susceptible chickens. *In vitro* experiment demonstrated that methylation inhibition repressed spread of MDV. Collectively, DNA methylation is an important regulator of MD resistance and susceptibility, and the findings may improve our understanding of the role of DNA methylation in other infectious diseases and viral-infection induced tumors.

Materials and Methods

Experimental Animals and Sample Preparation

Line 6₃ and line 7₂ (USDA-ARS Avian Disease and Oncology Laboratory, East Lansing, Michigan, USA) are two highly inbred lines of specific-pathogen-free white leghorn chickens that are resistant and susceptible, respectively, to MD tumors. Chickens from each line were separated into two groups. One group was infected with a very virulent (vv+) strain of MDV (648A passage 40) at day 5 after hatching, while the other group did not receive MDV. Four chickens were selected from each group at 21 DPI, and none of them developed tumors during the experiment period. Fresh thymus samples were harvested individually and stored in RNAlater solution (QIAGEN) at -80°C for DNA or RNA extraction. The entire animal experiment was conducted following the procedures and guidelines described in the “Guidelines for Animal Care and Use” manual approved by the Animal Care and Use Committee, the USDA-ARS, and the Avian Disease and Oncology Laboratory (Approval ID 111-26).

DNA preparation and endonuclease digestion

Genomic DNA from four samples of each group was extracted using the Wizard Genomic DNA purification kit (Promega). The RNase treatment was performed to remove RNA from DNA samples. DNA concentration was measured by the Qubit dsDNA Broad-Range Assay (Invitrogen).

Four DNA samples from each group were pooled together with equal amounts. The pooled samples were separated into two parts, and were digested by

methyl-dependent (McrBC) or 5 methyl-sensitive restriction enzymes (HpaII, HpyCH4VI, AciI, HhaI and BstUI), respectively (New England Biolabs, referred to as RE). The amount of starting DNA was 15 ug for both RE and McrBC digestions. Three rounds of McrBC digestion were performed to assure complete digestion of methylated DNA. The digestion reaction included 1×NEB buffer 2, 2×GTP, 1×BSA, and 10 Units of McrBC per microgram of DNA and performed at 37°C for 4-6 hrs. For the first two rounds, DNA was extracted using phenol-chloroform extraction and ethanol precipitation. Briefly, 2 volumes of phenol and chloroform were added, shaken for 5 min and then centrifuged at 14,000 rpm for 10min. The upper layer was transferred to a new tube, and 6 volumes of 100% ice-cold ethanol were added with 0.1 volume of 3M Sodium Acetate pH 5.5 and 5 µl of 20 mg/ml glycogen. Tubes were mixed well, incubated at -20 °C for 30 min, and then spun at 4 °C at 14,000 rpm for 15min. The supernatant was decanted, and the pellet washed with 6 volumes of 70% cold ethanol. This was followed by a spin at 4°C at 14,000 rpm for 5 min. The supernatant was discarded, and pellet was dried and resuspended in 50 µl TE. After the last round of digestion, DNA was purified using QIAquick spin columns (QIAGEN) to remove the GTPs. Four rounds of RE digestion were conducted and followed by phenol-chloroform extraction and ethanol precipitation. The first round of RE was set up with 1×NEB buffer 2, 10 Units of HpaII and 10 Units of HpyCH4IV per microgram of DNA, and digested at 37°C for 4-6 hrs. The second round included 1×NEB buffer 3, 1×BSA, and 10 Units of AciI and 5 Units of HhaI per microgram of DNA and conducted at 37°C for 4-6 hrs. The third round was performed with 1×NEB buffer 2, 10 Units BstUI per microgram of DNA at 60°C for

2-3 hrs. The last round repeated the HpaII and HpyCH4IV digestion for 2-4 hrs at 37 °C.

SOLiD mate-pair library construction

Mate-pair libraries were prepared with slight variation to the SOLiD library preparation guide. Fractionated DNA was repaired using End-It DNA End-repair kit (Epicentre), and incubated at room temperature for 45 min. DNA was purified using QIAquick spin columns (QIAGEN) to remove the ATPs and dNTPs, and quantified by Qubit dsDNA Broad-Range Assay (Invitrogen). Endogenous EcoP15I sites were then methylated using EcoP15I enzyme with 1×NEB buffer 3, 1×BSA, 360 μM SAM. The methylation reaction was performed at 37°C for 2-3 hrs, and then boosted with additional EcoP15I, NEB buffer 3, BSA, and SAM for another 2-3 hrs at 37°C. The DNA was purified using QIAquick spin columns (QIAGEN) and quantified by Qubit dsDNA Broad-Range Assay (Invitrogen). The EcoP15I cap adapter (50 pmol/μl) was ligated to the end-repaired and EcoP15I methylated DNA using Quick Ligation Kit (NEB). The reaction was incubated at room temperature for 10 min, and purified using MinElute (QIAGEN) to remove excess adapters.

DNA samples were run on 1% agarose gel at 50 V for 1.5-2 hrs. DNA was selected based on 7 fragment sizes: 0.8-1.1 kb, 1.1-1.5kb, 1.5-2 kb, 2-3kb, 3-5 kb, 5-8kb and >8kb. Each fraction was purified using QIAquick Gel Extraction kit (QIAGEN), and the concentration was measured using Qubit dsDNA High-Sensitivity assay kit (Invitrogen). DNA from each fraction was circularized with the biotin labeled T30 sticky linker using the Quick Ligation Kit (NEB). The circularized

DNA was purified using QIAquick spin columns (QIAGEN). Fractions were then combined into two tubes, one for <2 Kb and the other for >2 kb. Circularized DNA was isolated using ATP-dependent Plasmid-safe DNase (Epicentre) to degrade the linear DNA. The purified DNA samples were digested with EcoP15I, 1×NEB buffer 3, 1×BSA, 2mM ATP and 0.1 M Sinefungin overnight at 37°C on PCR machine. The reaction was boosted the next morning with fresh EcoP15I, ATP, BSA and Sinefungin for 1 hr, and terminated by denaturing at 65°C for 20 min. The digested DNA was repaired by 5 Units of Klenow (NEB) in the presence of 10 mM dNTPs for 30 min at 25°C, and then heat inactivated at 65°C for 20 min. P1 and P2 adapters were added to the end repaired DNA using Quick Ligation Kit (NEB). The ligation reaction was terminated by heat inactivation. P2 adapters contained distinct barcodes for each library so libraries can be later pooled for sequencing. The <2 kb and >2kb fractions were combined together for library purification.

M280 streptavidin beads (Invitrogen) were washed with 1× bead wash buffer (2% Triton X-100, 2% Tween 20, and 10mM EDTA) and 1×BSA, and resuspended in 1× binding buffer (40mM Tris-HCl, 4M NaCl, and 4mM EDTA). DNA samples were added to the beads, and incubated by rotation at room temperature for 15 min. The library DNA was bound to the beads through the biotin on the T30 internal adapter. The DNA-bead complex was washed with bead washing buffer and 1×NEB buffer 2. Finally, the complex was collected by quick spin and placing on a magnet. Washed library-bound beads were resuspended in 1×NEB buffer 2. Nick translation was performed on DNA-beads using DNA Polymerase I (NEB) in the presence of dNTPs. The beads were again collected with a magnet, and resuspended in Tris

buffer. Trial PCR was performed by serial dilution of beads to ensure the existence of 156-bp products and to determine the sufficient cycles to obtain enough products. Final libraries were amplified using all the beads and Pushion High Fidelity DNA Polymerase (NEB) with 19-23 cycles. Each 50 μ l reaction included 1 μ l bead template, 1 μ l of 50 μ M L-PCR-P1 primer, 1 μ l of 50 μ M L-PCR-P2 primer, 1 \times Phusion HF buffer, dNTPs, and 0.02 Units of Pushion Hot Start DNA Polymerase. The PCR products were combined together for ethanol precipitation.

A 6% DNA PAGE gel (Lonza) was used to purify the 156-bp library DNA. The gel was pre-run for 5 min, and PCR products as well as a 25 bp DNA ladder (Invitrogen) were loaded on the gel and run at 115 V for 55 min. The gel was stained in 1:6,000 ethidium bromide (10 mg/ml) in TBE for 10 min, destained in water for 10 min twice, and the 156-bp library band excised. The gel fragment was shredded, the library eluted in PAGE elution buffer, and gel fragments removed using a Nanosep MF Centrifugal Devices 0.45 micron filter column (Pall). The eluted DNA was purified with MinElute kit (QIAGEN). The final library DNA concentration was measured using the Qubit HS assay kit (Invitrogen), and the quality and quantity was assessed by Bioanalyzer DNA 1000 LabChip (Agilent).

DNA sequencing

The DNA libraries were sequenced by EdgeBio (EdgeBio). Biscally, each sequencing library was amplified on 1 μ m beads using emulsion PCR according to the SOLiD emulsion PCR protocol (Applied Biosystem). The DNA libraries were sequenced on SOLiD sequencing machine. Twenty-five base-pair DNA fragment was

obtained by sequencing from forward and reverse on each bead. Eight libraries from 4 samples were pooled and sequenced on a single chip using the standard SOLiD protocol.

Tag mapping and data analysis

Sequence tags were mapped using SOLiD system software analysis package Corona-lite (Applied Biosystem). Two mismatches in each 25 bp read to the chicken genome (<http://genome.ucsc.edu>) were allowed. Reads were filtered to remove fragments without at least one enzyme cut site on the fragment end. Read counts were normalized as in Edwards et al [196]. The methylation level for each CpG site was calculated as the number of reads from methylation (RE) library divided by the number of reads from both RE and McrBC libraries. Each CpG site was annotated according to its genomic location (promoter, gene body, intergenic, repetitive regions and CpG islands). The differential methylation regions (DMRs) were discovered by merging adjacent sliding windows with at least 3 differentially methylated CpGs in a 2 kb window. DMRs were reported only if their length was greater than 3 kb. Fisher's Exact test was used to identify the differential methylation CpG site controlling for an FDR greater than 0.01. The annotation information, including Refseq, repeatMask, CpG islands were obtained from the UCSC genome browser (galGal3).

Bisulfite conversion, pyrosequencing and bisulfite sequencing

Sodium bisulfite conversion reagents were used to treat 500 ng of DNA (EZ

DNA Methylation Golden Kit) using the standard protocol provided by the manufacturer. PCR primers for methylation validation were listed in Table 4.1. For pyrosequencing, we used biotin labeled universal primer in the PCR reaction. The bisulfite PCR included 1 µl of 1:5 diluted bisulfite converted DNA, primers and PCR reagents from Hotstar Taq polymerase kit (QIAGEN) with four biological replicates. The methylation level was detected individually by Pyro Q-CpG system (PyroMark ID, Biotage, Sweden) using 20 µl of PCR products. For bisulfite sequencing, an equal amount of DNA from four samples of treated or control groups from each chicken line were pooled together, serving as a template for the bisulfite conversion and the bisulfite PCR, and then PCR products were purified (QIAquick Gel Extraction Kit, QIAGEN). The purified PCR products were ligated to pCR® 2.1 Vector (The Original TA cloning® Kit, Invitrogen), transformed to DH5α competent cells (ZYMO Research), and screened for successful insertions (blue-white selection) after incubation at 37°C overnight. Ten white colonies from each group were cultured in a 37°C shaker overnight. Plasmid DNA was isolated using the QIAprep® Miniprep Kit (QIAGEN), and M13 reverse primer was used for sequencing.

Purification and quantification of mRNA levels

RNA was extracted from four samples per group using the RNeasy Mini Kit (QIAGEN) and the standard method described by the manufacturer. An on-column DNase digestion was performed to remove any contaminant DNA. RNA concentration was measured by Nanodrop. Reverse transcription was performed on 1 µg of purified total RNA using SuperScript™ III Reverse Transcriptase (Invitrogen)

with oligo (dT) 12-18 primers (Invitrogen); mRNA levels were quantified using SYRB Green PCR Kit (QIAGEN) with four biological replicates from each group.

PCR primers for mRNA quantification are listed in Table 4.1.

Table 4.1 PCR Primers

Gene		Sequences
<i>GATA2</i> ^A	Forward	5'-GATGAAGGGTAATATAGGAGGAGT-3'
	Reverse	5'-CACCTACTATACCTTTTCCTCCC-3'
<i>CDC42</i> ^A	Forward	5'-GAGGAGGGTAGTGTGTGGTT-3'
	Reverse	5'-AACCCCATATCTTTCAATCCC-3'
<i>CRI-B</i> ^A	Forward	5'-AGGGGATAGTTGTGATTAGGAT-3'
	Reverse	5'-CCCCACCAACCATATCATT-3'
<i>FAR1_CGI</i> ^A	Forward	5'-GGTGGTTATAAGGTGGTGGTGTGG-3'
	Reverse	5'-AAACCCAAATACCCCTCACTTCA-3'
<i>HDAC9_CGI</i> ^A	Forward	5'-TTGGGATATGGGTTGTCGAAAT-3'
	Reverse	5'-GGACACC GCTGATCGTTA GCTAATACTCTCGTTCGCAACA-3'
	Sequencing	5'-TGGGTTGTCGAAATAGTT-3'
<i>FABP3</i> ^A	Forward	5'-AGAGGGGGAAATTGAGGTA-3'
	Reverse	5'-GGGACACCGCTGATCGTTT AAACACACACACACGATCC-3'
	Sequencing	5'-GGGGGAAATTGAGGTA-3'
<i>GAPDH</i> ^B	Forward	5'-GAGGGTAGTGAAGGCTGCTG-3'
	Reverse	5'-ACCAGGAAACAAGCTTGACG-3'
<i>DNMT1</i> ^B	Forward	5'-CCACCAAAGGAAATCAGAG-3'
	Reverse	5'-TAATCCTCTTCTCATCTTGCT-3'
<i>DNMT3a</i> ^B	Forward	5'-ATGAACGAGAAGGAAGACATC-3'
	Reverse	5'-GCAAAGAGGTGGCGGATCAC-3'
<i>DNMT3b</i> ^B	Forward	5'-CGTACTTCTGGGGCAACCTC-3'
	Reverse	5'-ATGACAGGGATGCTCCAGGAC-3'
<i>CDC42</i> ^B	Forward	5'-CGCTTACGCAGAAAGGCCTAAA-3'
	Reverse	5'-GGAGGGACGTTTCATAGCAGC-3'

^A: PCR primers for bisulfite sequencing and pyrosequencing. ^B: Primers for real time-PCR.

DNA dot blot

DNA samples were mixed with 0.1 volume of 1M NaOH, denatured at 99°C

for 5 min, and snap cooled on ice. The denatured DNA was neutralized with 0.1 volume of 6.6 M Ammonium acetate. DNA samples were then loaded on a nitrocellulose membrane (Bio-rad), and UV cross-linked. Blocking was performed using 10% non-fat milk. The membrane was incubated with primary antibodies against 5'-methylcytosine (5mC, Active Motif) and 5'-hydroxymethylcytosine (5hmC, Diagenode), and diluted in blocking solution (1:5,000) at 4 °C overnight. After 3 washes, the membrane was incubated with anti-rabbit IgG and anti-mouse IgG secondary antibodies (Santa Cruz) and diluted in TBST (1:5000) for 1 hr at room temperature. Membranes were developed with ECL (Amersham) and measured using ChemiDoc XRS (Bio-Rad). Each dot was circled, and the average volume in the circle was exported to Excel to estimate 5mC and 5hmC contents using Quantity One software (Bio-rad). 5mC and 5hmC positive controls were synthesized by PCR using 5mCTPs and 5hmCTPs (ZMYO research).

Cell culture and MDV infection

The chicken embryo fibroblast cell line DF-1 was grown in Dulbecco's modified Eagle's medium supplemented with 10%, fetal bovine serum, streptomycin (100 mg/ml) and penicillin (100 U/ml) (Invitrogen). Cells were maintained at 37°C in humidified 5% CO₂ conditions. The very virulent + (vv+) strain of MDV (648A passage 40) was obtained from USDA-ARS Avian Disease and Oncology Laboratory. The DF-1 cells were inoculated with the virus at multiplicity of infection (M.O.I) of 0.1 for 3 days. The DNA methylation inhibitor 5-azacytidine (Fisher) was used to treat the infected cells at concentration of 5µM.

Immunofluorescence

The DF-1 cells were fixed with 4% of paraformaldehyde for 15 min, and permeabilized using 0.5% Triton-X 100 in PBS for 15 min. Primary antibodies were prepared at 1:500 and 1:1000 dilutions in PBS, and incubated with cells for 1 hr. After washing the cells 3 times, FITC-labeled donkey anti-mouse or donkey anti-rabbit IgG secondary antibodies were diluted 1:1,000 in PBS, and incubated with cells for 30 min. The nuclei were labeled with 4', 6-diamidino-2-phenylindole (DAPI) (Invitrogen). The immunoreactive complexes were visualized with a Zeiss LSM 510 confocal fluorescence microscope, and the images were processed using LSM Image Examiner software (Zeiss).

Results

The expressions of *DNMTs* in MDV infected chickens

To test the influence of MDV infection on *DNMT* expression, the mRNA levels of each of three DNA methyltransferases were examined by qPCR in the thymus of lines 6₃ and 7₂ at 21 DPI (Figure 4.1). Transcriptional levels of *DNMT1* were ~ 20% higher in line 7₂ compared to line 6₃ ($p>0.05$), and did not significantly altered in either line after MDV exposure. *DNMT3a* mRNA was similar in non-infected line 6₃ and line 7₂. However, its expression was repressed 30% in infected line 6₃ and line 7₂. The expression of *DNMT3b* was 2 fold higher in line 7₂ than in line 6₃ before MDV infection ($p>0.05$), and its transcription was further activated in line 7₂, with ~50% increase mRNA amount, after MDV infection

($p < 0.01$).

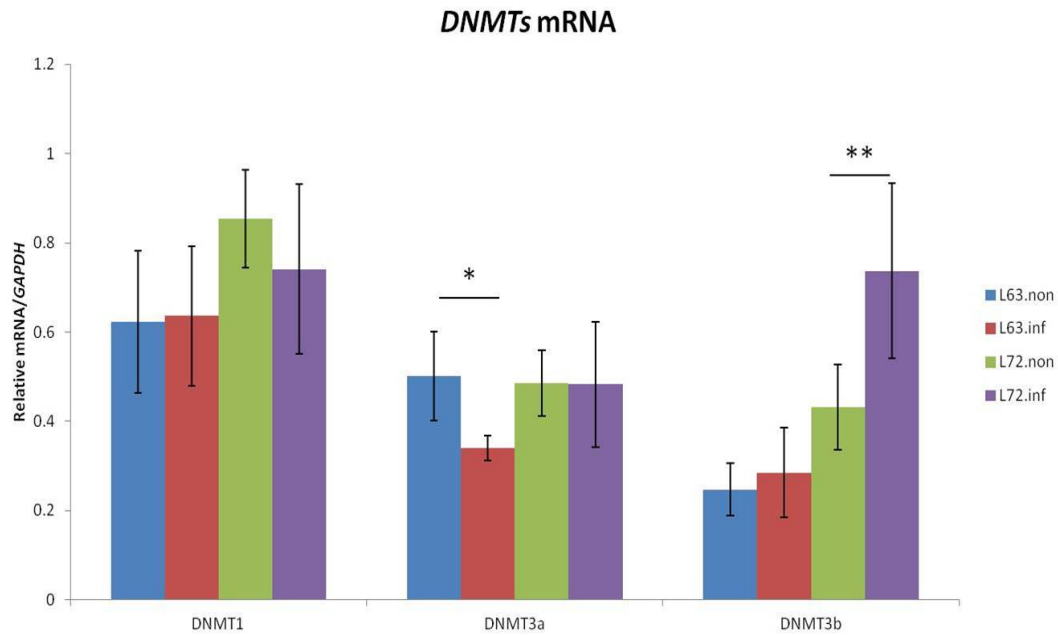


Figure 4.1 The mRNA Quantification of chicken *DNMTs*. Expression of *DNMT1*, *DNMT3a* and *DNMT3b* was measured by qRT-PCR in thymus samples from noninfected and infected line 6₃ and line 7₂ chickens, and normalized to GAPDH. The quantitative results are represented as mean \pm SEM (n=4). A single asterisk (p-values < 0.05) and double asterisks (p-values < 0.01) indicate the transcription level in the specific group was significantly different when compared to the adjoined group. L72.inf: infected line 7₂; L72.non.inf: noninfected line 7₂; L63.non.inf: noninfected line 6₃; L63.inf: infected line 6₃.

Global mapping of DNA methylation in chickens

To explore the consequences of differential expression of *DNMT3a* and *DNMT3b* in the two chicken lines, genome-wide DNA methylation analysis was carried out using Methyl-MAPS. The methylated compartment in the chicken was detected by the digestion with five methyl-sensitive restriction enzymes, and the unmethylated part was investigated by the methyl-dependent enzyme McrBC. From each sequencing library, ~26-90 million reads were obtained, with ~50 % of them

mapping to chicken genome. For each sample, 2.7 to 3.1 million CpG sites were detected, and 66-76% of them had coverage greater than 10 reads/site, which were used for the further analysis (Table 4.2).

Table 4.2 The Global mapping statistics.

Sample	Library	Raw Reads	F %	R %	No. CpGs	No. of CpGs (>=10)
L6₃. non	McrBC	38,941,424	51.27	57.99	3,002,069	1,991,421
	RE	47,622,587	54.48	58.32		
L7₂. non	McrBC	26,072,658	45.03	50.13	2,751,367	1,918,821
	RE	51,831,801	50.77	55.74		
L6₃. inf	McrBC	50,833,633	50.43	54.99	3,103,734	2,322,557
	RE	42,467,075	53.35	59.03		
L7₂. inf	McrBC	71,914,437	58.70	63.53	3,096,603	2,392,480
	RE	89,731,607	57.28	61.17		

Eight DNA libraries from 4 samples were sequenced. McrBC and RE represented the libraries from methyl-dependent and five methyl-sensitive enzyme digested DNA. Raw reads indicated the number of reads obtained from sequencing before data filter. F% and R% indicated the percentage of mapped reads from the forward and reverse primer sequencing. Number of CpG sites and number of CpG sites with coverage greater than 10 reads/site were listed. L7₂.inf: infected line 7₂; L7₂.non: noninfected line 7₂; L6₃.non: noninfected line 6₃; L6₃.inf: infected line 6₃.

In silico analysis of chicken genome showed that this method theoretically, covered 3,317,773 CpGs, which can be recognized by both methyl-dependent and methyl-sensitive restriction endonucleases (MR sites), counting for ~32% of CpGs in the chicken genome. Most of the CpGs were covered by 20-200 reads, and some had the coverage greater than 200 (Figure 4.2). The MR site coverage and CpG sites coverage were similar among 4 samples. With the cutoff of minimum 10 reads/site, 61.97-78.16% of MR sites were detected which included 19.97-25.18% of chicken CpG sites (Table 4.3).

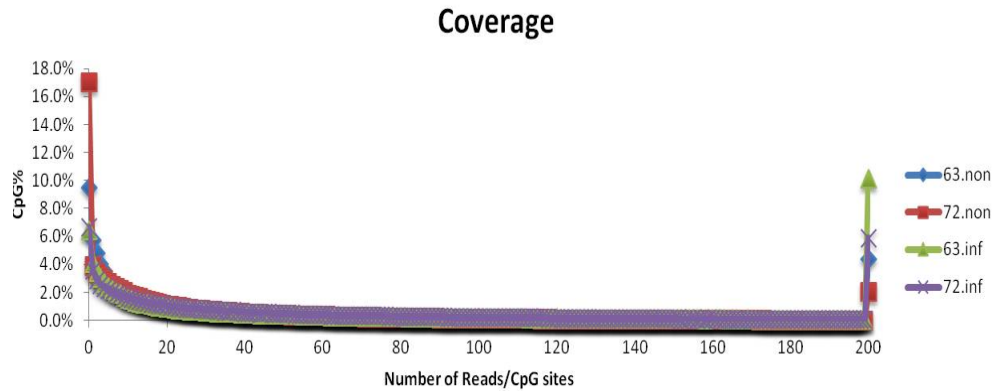


Figure 4.2 The CpG coverage distributions. The y-axis was the fraction of CpG sites, and the x-axis was the number of reads/CpG sites. 200 indicates the number of sites with 200 or greater reads. Sequencing libraries: 72.inf: infected line 72; 72.non: noninfected line 72; 63.non: noninfected line 63; 63.inf: infected line 63.

Table 4.3 The CpG coverage.

	L6 ₃ .non	L7 ₂ .non	L6 ₃ .inf	L7 ₂ .inf
MR site Coverage	72.99%	78.16%	61.97%	64.19%
CpG Coverage	23.52%	25.18%	19.97%	20.68%

MR sites indicated the CpGs which were able to be recognized by methyl-dependent (McrBC) and methyl-sensitive enzymes.

Totally, 2,575,854 CpGs were detected by Methyl-MAPS. Among these CpGs, 1,073,930 were annotated (CpGs in total) and distributed into 5 categories: exon, repetitive DNA, promoter absent of CGI, CGI overlapped promoter (CGI_promoter) and CGI_others (CGIs not in the other 4 categories) (Figure 4.3). An additional 1,501,924 CpGs (~58.31% of all detected CpGs) were unannotated. Nearly one third of annotated CpGs were found in CpG islands. About 42% of CpGs were in the annotated promoter regions, including 27.9% of them in the promoters within CGIs and 14.44% in the promoters lack of CGIs. There were 10.56% of CpG sites located in the exon regions and 15.02% of them in the repetitive DNA regions,

including the simple repeats (~2.16%) and satellite (0.16%), retrotransposons (11.51%) and DNA transposons (1.17%). The variations among four samples were demonstrated in Table 4.4. More CpGs on repetitive DNA, exons and promoter were detected in non-infected line 7₂, whereas the distribution of CpG in infected lines 6₃ and 7₂ was similar after MDV infection.

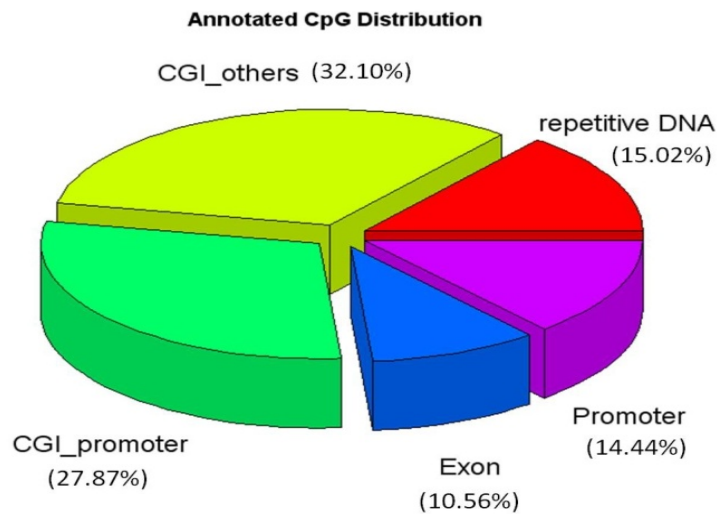


Figure 4.3 The distributions of annotated CpGs. The annotation of CpGs includes 5 categories: exon, repetitive DNA, promoter absent of CGI, CGI overlapped promoter (CGI_promoter) and CGI_others (CGIs not in the other 4 categories).

Table 4.4 The distributions of annotated CpGs among 4 samples.

	L6 ₃ .non	L7 ₂ .non	L6 ₃ .inf	L7 ₂ .inf
Repetitive DNA	15.34%	19.48%	13.21%	13.88%
CGI_other	31.84%	28.78%	33.57%	32.86%
CGI_promoter	27.12%	19.93%	30.48%	30.66%
Exon	10.84%	14.62%	9.23%	9.24%
Promoter	14.87%	17.20%	13.52%	13.37%

L7₂.inf: infected line 7₂; L7₂.non: noninfected line 7₂; L6₃.non: noninfected line 6₃; L6₃.inf: infected line 6₃.

DNA methylation variations induced by MDV infection

Generally speaking, the average methylation level was not significantly higher

in line 7₂ (0.44) than in line 6₃ (0.39) regardless of infection (Figure 4.4 and Figure 4.5). While methylation levels in line 7₂ stayed relatively constant after MDV infection, the global methylation level decreased to 0.17 in line 6₃ (Figure 4.4). The 5mC content in each individual was measured using anti-5mC dot blot (Figure 4.5). The quantitative result was in a good agreement with the sequencing results, which the methylation levels were decreased about 38% in infected line 6₃ ($p < 0.05$), and were increased about 6% in the infected line 7₂ chickens ($p > 0.05$). Between noninfected chickens, the methylation was about ~17% less in line 6₃ than line 7₂. To figure out how the methylation altered among 4 samples, we categorized the CpG sites as methylation (methylation level greater than 75%), intermediate methylation (25-75%), and unmethylation (<25%) groups. The methylated sites were dramatically decreased in line 6₃, while the methylated sites were increased slightly in line 7₂. In line 6₃, about two thirds of methylated CpGs became unmethylated, and the proportion of unmethylated CpGs was increased 1.5 times after MDV infection (Figure 4.6). In line 7₂, the proportion of CpGs in each class was similar after MDV infection, despite of 6% of increase in methylation category and the 2% of decrease in the unmethylation class. Before MDV infection, the number of methylated CpGs was less in line 6₃ than in line 7₂, and the number of CpG with the intermediate methylation was greater in line 6₃ than in line 7₂.

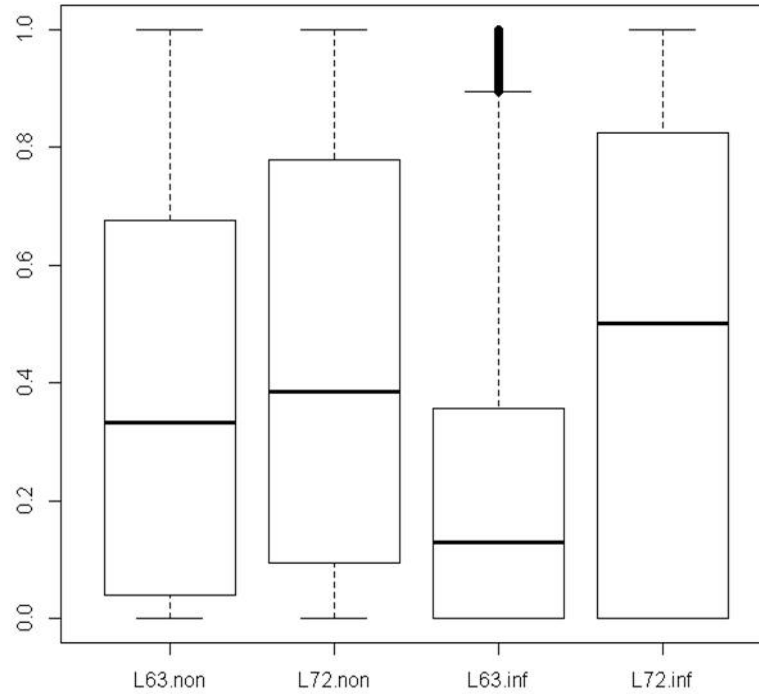
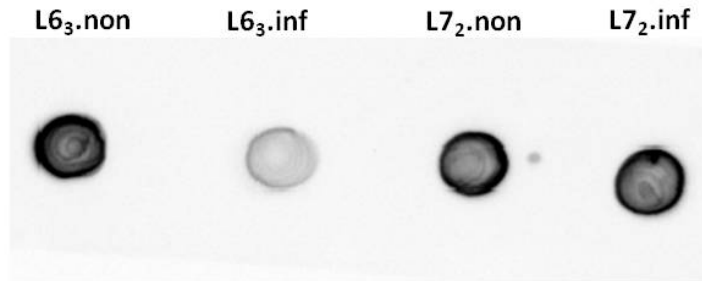
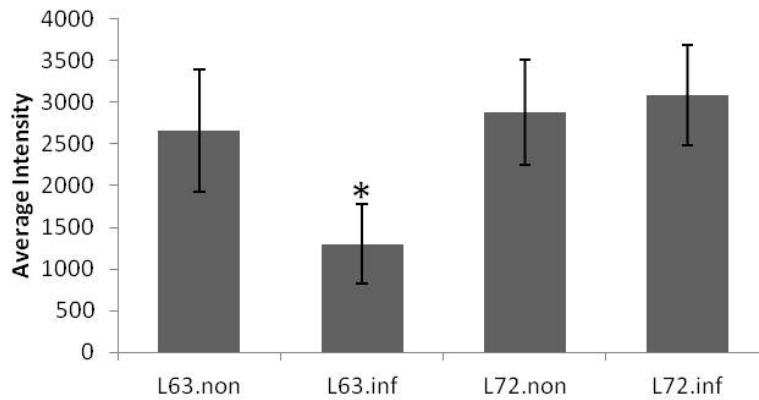


Figure 4.4 The boxplot of methylation levels for the detected CpGs. The y-axis was the methylation levels for all CpG sites calculated as the number of reads from methylated (RE) library divided by the number of reads from both methylated and unmethylated (McrBC) libraries. L7₂.inf: infected line 7₂; L7₂.non: noninfected line 7₂; L6₃.non: noninfected line 6₃; L6₃.inf: infected line 6₃.



5mC Dot Blot



N=4

Figure 4.5 Quantification of 5mC content by anti-5mC dot blot. The 5mC content was measured in DNA from thymus using dot blot, showing as (mean \pm STD, n=4). A single asterisk (p-values <0.05) indicated the 5mC contents in the specific group was significantly different when compared to other groups. L7₂.inf: infected line 7₂; L7₂.non: noninfected line 7₂; L6₃.non: noninfected line 6₃; L6₃.inf: infected line 6₃.

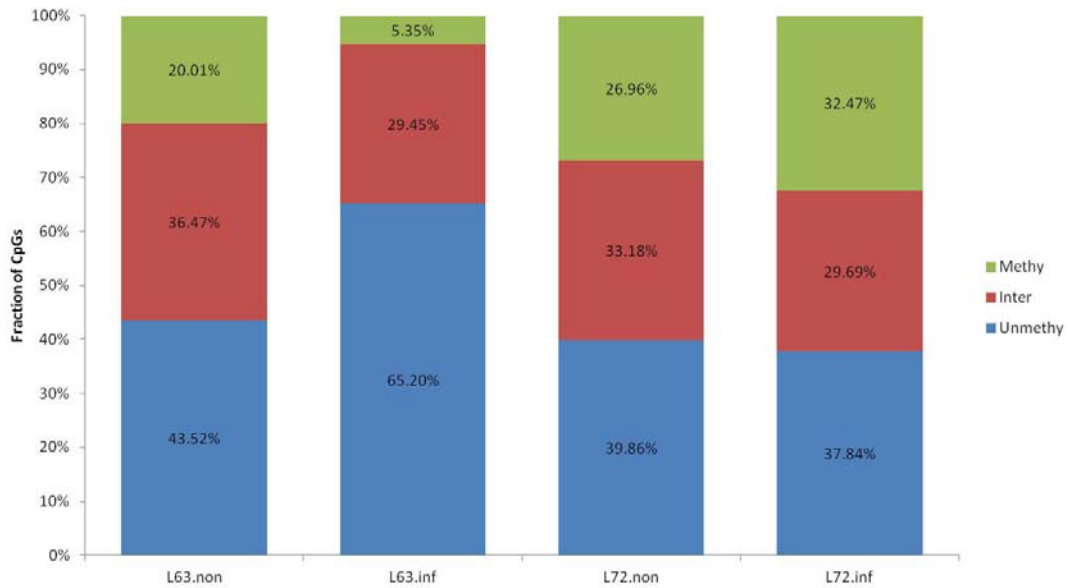
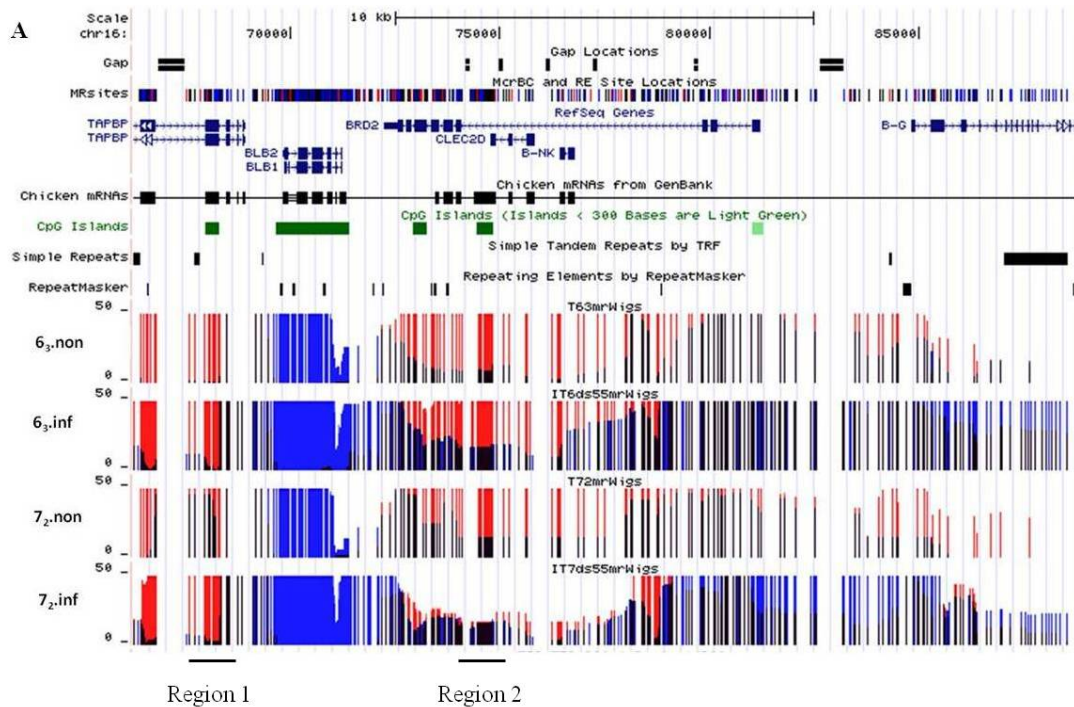


Figure 4.6 The classification of CpG based on the methylation levels. The CpGs were divided into 3 categories based on the methylation levels greater than 75% (Methy), 25-75% (inter) and unmethy (<25%). The number on the top of each bar represented the number of analyzed CpGs, and the percentage of CpGs in each category was labeled in the bar. L7₂.inf: infected line 7₂; L7₂.non: noninfected line 7₂; L6₃.non: noninfected line 6₃; L6₃.inf: infected line 6₃.

Many detected CpGs with different methylation levels were located in gene regions. *MHCII* (*major histocompatibility complex II*) region was taken as an example since it is one of the determinants for MD resistance, and its haplotype is the same between line 6₃ and line 7₂. The methylation status of *MHCII* region in non-infected and infected chickens is shown in Figure 4.7A. Methylation patterns are similar between non-infected line 6₃ and line 7₂. After infection, the methylation levels were increased in line 7₂ in region 1, and reduced in region 2. These two regions did not show methylation variations in line 6₃ after infection. Besides CpG methylation in genes, the methylation of CpGs on the repetitive DNA sequences was directly detected. The majority of them belonged to chicken repeat 1 (CR1), the long

interspersed nuclear elements (LINE) in chicken, counting for ~8.7%, and long-terminal repeats (LTRs) and DNA transposons both counting for 1.1%. An example of differential methylation at repeat elements after infection is shown in Figure 4.7B. The CGIs embedded in the repetitive regions (region 3) were highly methylated in uninfected line 7₂, and showed moderate methylation level in uninfected line 6₃. The methylation levels at this CGI were decreased after MDV infection in two lines, and line 7₂ chickens showed higher methylation than line 6₃. It was clear that the LTR repeat (region 4) upstream of chicken transcript was less methylated in line 7₂ than line 6₃ before MDV infection, whereas its methylation was raised in line 7₂ after the virus challenge (Figure 4.7B).



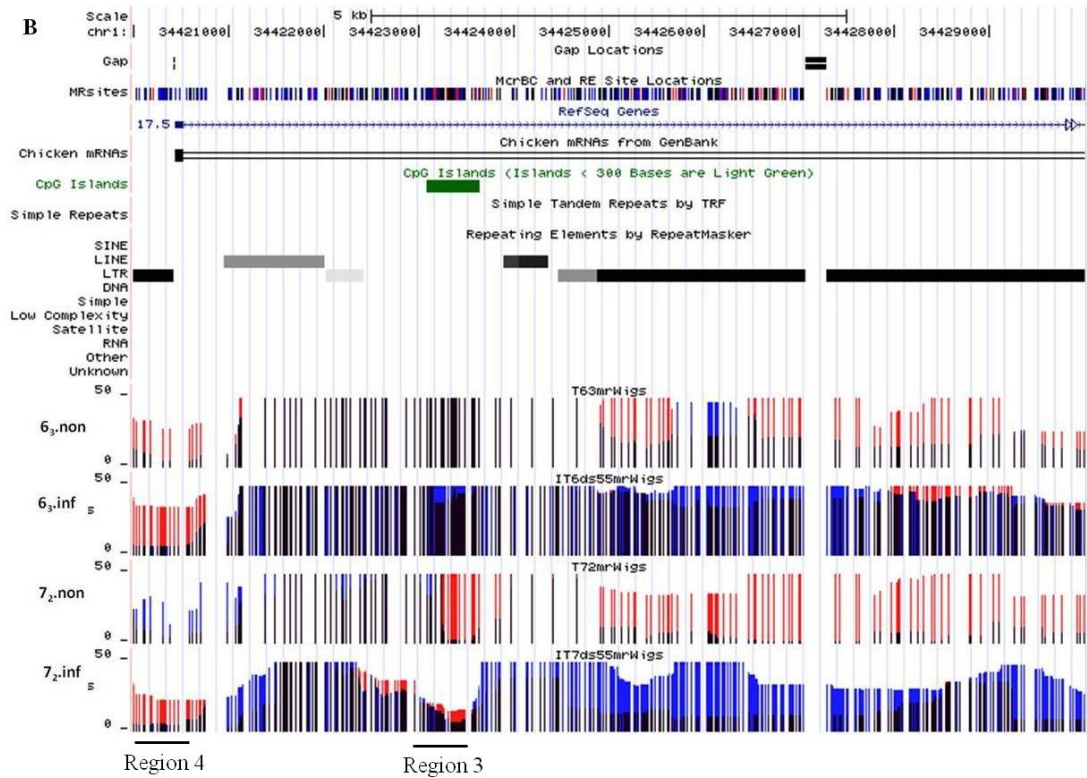


Figure 4.7 The genome-wide DNA methylation profiling. The top includes the genomic location and annotation information. MR site track indicated potential MCrBC and RE cut sites. The bars mean the absolute read counts mapped to the CpG site. The red bars represent CpGs cleaved by MCrBC and thus methylated, while the blue indicates CpGs cleaved by RE and thus unmethylated. The black denotes CpGs cleaved by both methyl-dependent and methyl-sensitive enzymes that have moderate methylation levels. (A) The genome browser view of the methylation status of the MHCII locus in lines 6₃ and 7₂ before and after MDV treatment. Region 1 and 2 showed methylation variations in two lines after infection. (B) The methylation status of a region of repetitive DNA sequences on chromosome 1. Region 3 and 4 are two examples showing methylation variations induced by MDV infection.

Methylation variation in CGIs and repetitive regions

A total number of 1,622,778 CpGs were located among the 22,806 CGIs in the chicken genome, and one thirds of these CpGs (540,390) were directly probed, including 16,927, about 74% of CGIs. CGIs had low average levels of methylation (0.09-0.20). In uninfected chickens, CGI methylation levels were similar between line

6₃ and line 7₂. The average methylation was reduced in line 6₃ from 0.16 to 0.09 after MDV infection, and was slightly increased in the infected line 7₂ from 0.16 to 0.20 (Figure 4.8). The methylation levels of the promoter CGIs were reduced in both lines after MDV infection, from 0.29 to 0.27 in line 6₃ and from 0.30 to 0.28 in line 7₂. To validate the genome-wide methylation results, 5 CpG sites in a CGI on chromosome 2 (29,264-29,264,968), upstream of *HDAC9* (histone deacetylase 9), were analyzed by pyrosequencing (Figure 4.9A and Appendix V). The average methylation difference was about 0.08 between line 6₃ and line 7₂ before virus infection, and the differences were greater than 0.1 in CpG site 1,2 and 5 ($p < 0.05$ and $p < 0.01$). The methylation was reduced about 5% and 10% after MDV infection, making the methylation levels similar between infected line 6₃ and line 7₂ ($p > 0.05$). The methylation of the other CGI on chromosome 5 (8,429,672-8,430,025), at the promoter of *FARI*, containing 33 CpGs was measured using bisulfite sequencing, showing the methylation levels were reduced after infection by 8% and 18% in lines 6₃ and line 7₂ respectively (Figure 4.9B).

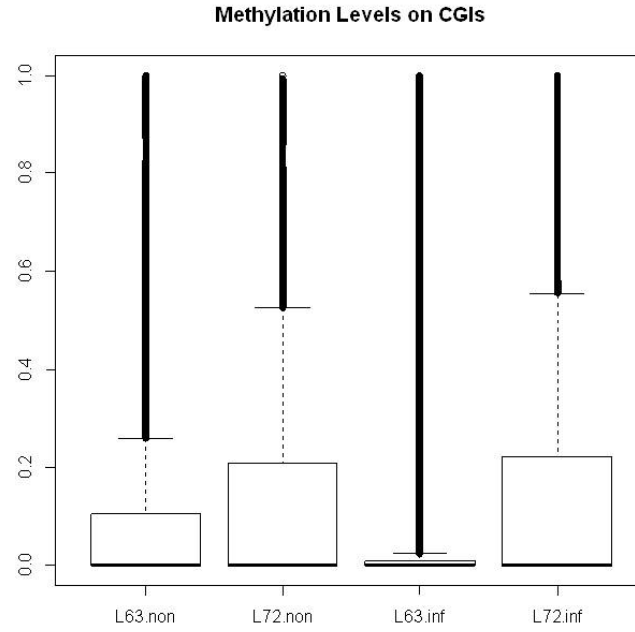


Figure 4.8 The CGI methylation status. The y-axis was the methylation levels of CpGs within repetitive regions. The x-axis indicated 4 groups. L7₂.inf: infected line 7₂; L7₂.non: noninfected line 7₂; L6₃.non: noninfected line 6₃; L6₃.inf: infected line 6₃.

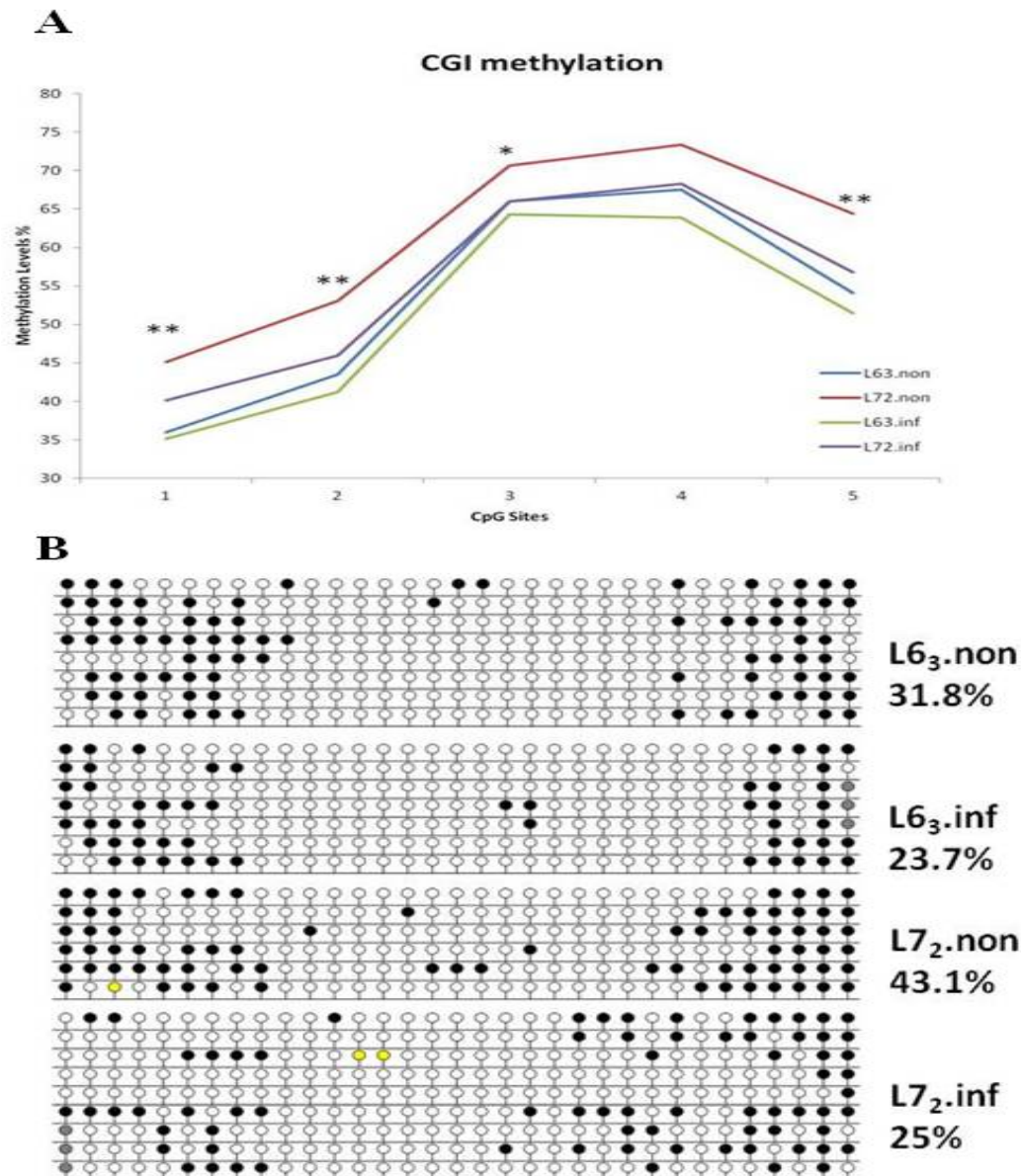


Figure 4.9 Pyrosequencing and bisulfite sequencing confirmation of promoter CGI methylation. **(A)** The pyrosequencing from CGI upstream of *HDAC9*. The y-axis is the absolute DNA methylation level of each CpG site. A single asterisk means p-values <0.05 and double asterisks p-values < 0.01. Each group includes 4 biological replicates. **(B)** The validation of CGI methylation on *FAR1* promoter by bisulfite sequencing. Each line represents a sequence of a plasmid, and each dot indicates a CpG site. The open dot indicated the unmethylated CpGs, and black dot was the methylated CpGs. The grey one denoted the CpG was undetected, and yellow one was the mutation. The methylation level was calculated as the number of methylated CpG sites divided by the total detected CpGs (yellow and grey were excluded). L7₂.inf: infected line 7₂; L7₂.non: noninfected line 7₂; L6₃.non: noninfected line 6₃; L6₃.inf: infected line 6₃.

Repetitive DNA regions contain 950,055 CpGs, about 27.05% of annotated chicken CpGs. The overall methylation levels of the repeat associated CpGs are plotted in Figure 4.10. The average methylation levels were similar between line 6₃ (0.31) and line 7₂ (0.35). These CpGs on the repetitive regions were hypomethylated in line 6₃ (0.16) but not in line 7₂ (0.37) after MDV infection.

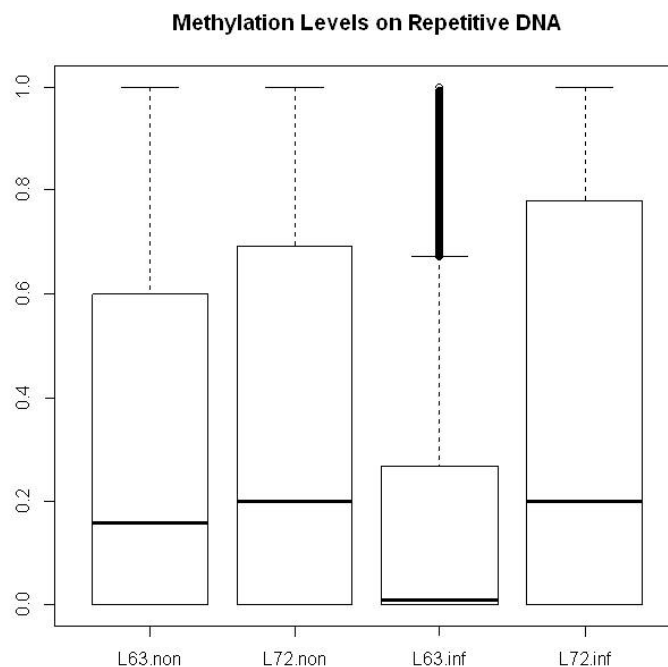


Figure 4.10 The CpG methylation in repetitive DNA regions. The y-axis was the methylation levels of CpGs within CGIs. L7₂.inf: infected line 7₂; L7₂.non: noninfected line 7₂; L6₃.non: noninfected line 6₃; L6₃.inf: infected line 6₃.

Methylation variations across genes

To ascertain the viral-induced methylation changes associated with genes, the CpG distribution and DNA methylation levels across gene body were plotted in Figure 4.11. The CpG density gradually increased towards the transcriptional start site. Methylation shows negative association with CpG density in this region. With

the increased CpG density towards the TSS, the methylation was declined. The CpG density reached the highest level at the 5' and 3' of splice site of the first exons, and these promoter-associated CGIs were unmethylated. For example, a CGI located upstream of *FABP3* (Fatty acid binding protein 3) were hypomethylated, with the methylation levels less than 0.1 among 4 groups (Figure 4.12 and Appendix VI). Within the coding region, compared to the low CpG density and methylation in introns, the internal exons and the last exon were enriched of the methylated CpGs, and both of the CpG density and methylation reached the maximum at the 5' and 3' ends. The CpGs were poor in the regions coding for 3'UTR and Poly (A) tail, and methylation in these regions was similar to the gene body.

The methylation across genes was similar among noninfected chickens of line 6₃ and line 7₂ as well as infected line 7₂, and was reduced in the line 6₃ infected chickens (Figure 4.12). The CpGs in the gene body showed higher methylation levels in infected line 7₂ than other groups. At the promoter region upstream of TSS, the difference between infected and noninfected line 6₃ was about 0.2. For example, the methylation of 19 CpGs ~200 bp upstream of *GATA2* (GATA binding protein 2) were decreased from 53.1% to 34.6% in line 6₃ after MDV infection, and only reduced 2% in line 7₂ (Figure 4.13 and Appendix VII).

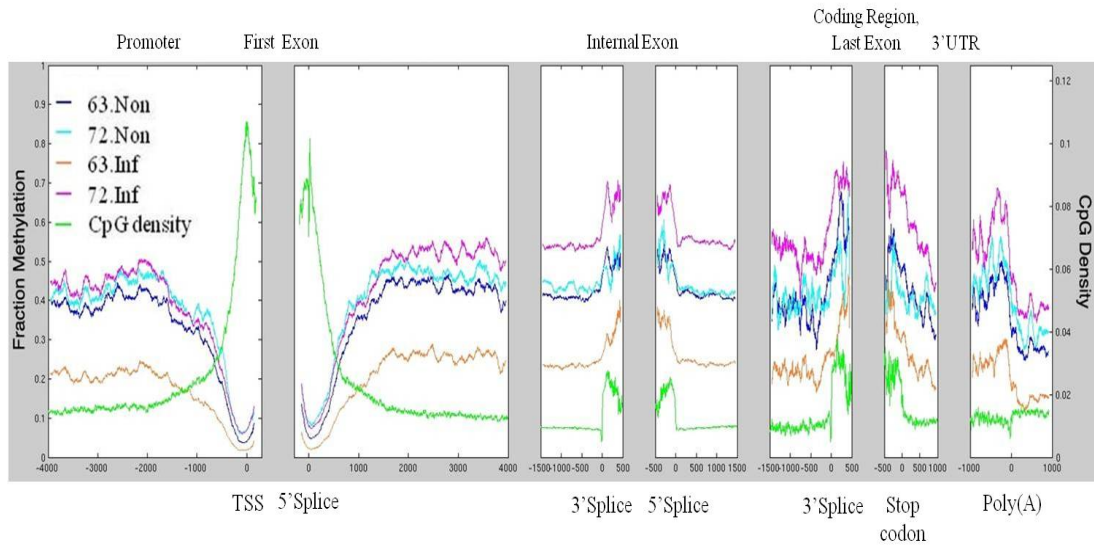


Figure 4.11 CpG distribution and DNA methylation pattern in chicken genes. CpG density and methylated CpG were plotted across gene from the promoter to the transcription terminal site.

Pyrosequencing of *FABP3* Promoter

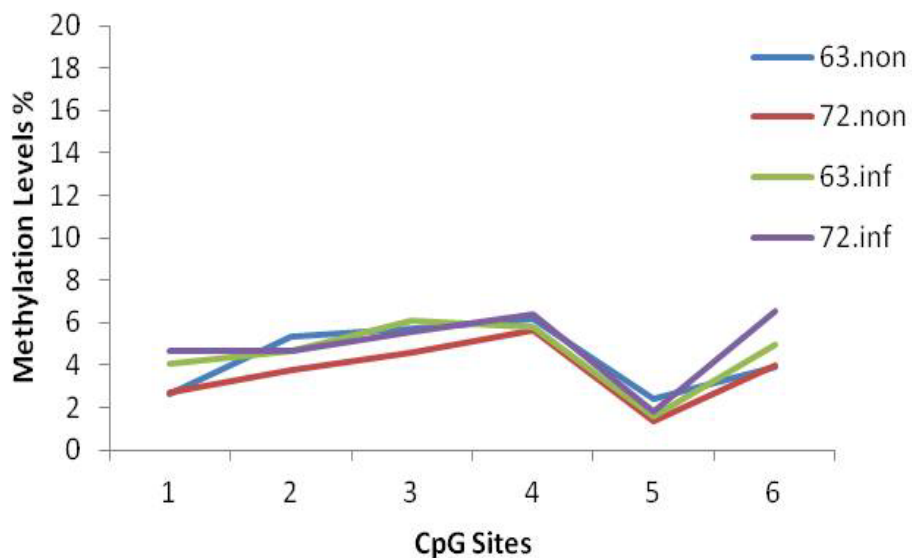


Figure 4.12 The methylation of CGI upstream of *FABP3*. The methylation was detected using pyrosequencing. Y-axis was the methylation level for each CpG site.

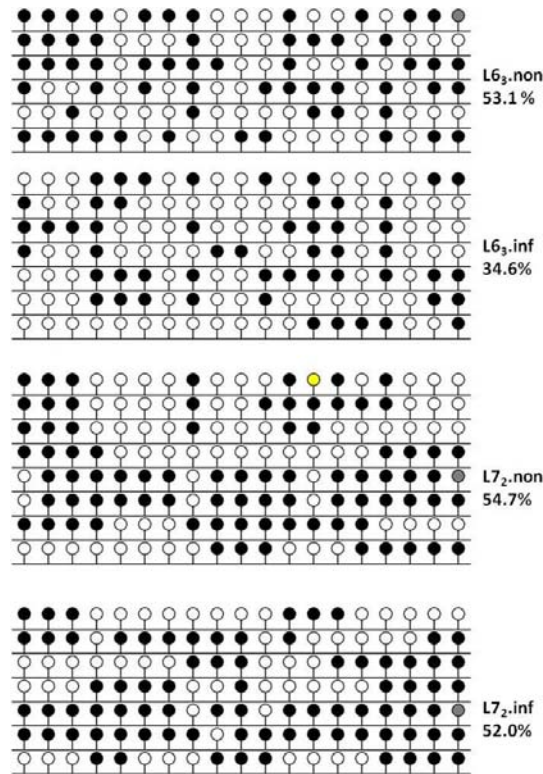


Figure 4.13 The bisulfite sequencing of CpGs upstream of *GATA2*. Each line represents a sequence of a plasmid, and each dot indicates a CpG site. The open dot indicated the unmethylated CpGs, and black dot was the methylated CpGs. The grey one denoted the CpG was undetected, and yellow one was the mutation. The methylation level was calculated as the number of methylated CpG sites divided by the total detected CpGs (yellow and grey were excluded). L7₂.inf: infected line 7₂; L7₂.non: noninfected line 7₂; L6₃.non: noninfected line 6₃; L6₃.inf: infected line 6₃.

Identification of infection induced differential methylation regions

(iDMRs)

The differential methylation site was defined as the absolute methylation level difference for each CpG between infected and noninfected sample greater than 30%. Based on the cutoff, 307,354 and 755,196 CpGs were identified as differential methylation sites between infected and noninfected chickens in line 6₃ and line 7₂, respectively. The adjacent differential methylation CpG sites were merged to get the infection induced differential methylation regions (iDMRs). In line 6₃, there were

7,952 iDMRs, which overlapped with 1,247 refseq genes and 1,603 repetitive regions. In line 7₂, 19,976 iDMRs were identified, which covered 3,079 genes and 4,683 repeats. For example, the CpG sites of CR1-B on chromosome 3: 110,191,142-110,191,684, were identified as the iDMRs in line 7₂, but not in line 6₃ due to the smaller methylation alterations induced by MDV infection (Figure 4.14 and appendix VIII). Before MDV infection, the DNA methylation was about 15% higher in line 7₂ than in line 6₃, and decreased about 5% in line 6₃ and 25% in line 7₂, respectively, after MDV infection. Among iDMRs, 94.6% of iDMRs in lines 6₃ were overlapped with iDMRs in line 7₂, which contains 884 genes and 1,496 repeated sequences. The iDMR was identified in the promoter of *GH* (growth hormone), the previously identified candidate gene of MD resistance, with the large reduction of methylation in line 7₂ and small decreases in line 6₃ after MDV infection (Appendix IX).

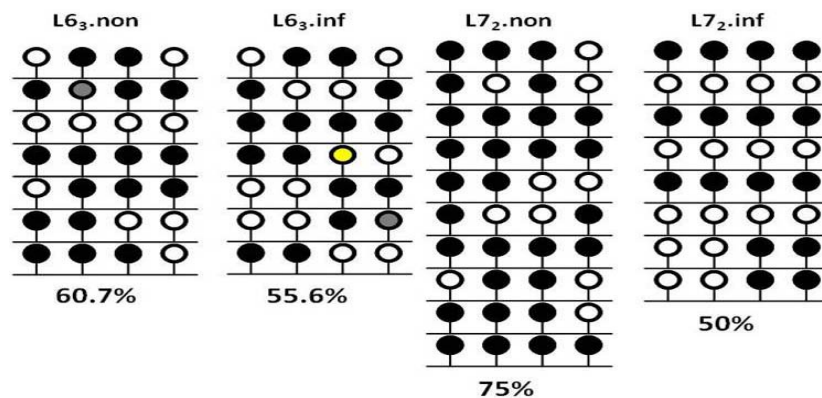


Figure 4.14 The validation of CR1-B methylation. Each line represents a sequence of a plasmid, and each dot indicates a CpG site. The open dot indicated the unmethylated CpGs, and black dot was the methylated CpGs. The grey one denoted the undetected CpG, and yellow one was the mutation. The methylation level was calculated as the number of methylated CpG sites divided by the total detected CpGs (yellow and grey were excluded). L7₂.inf: infected line 7₂; L7₂.non: noninfected line 7₂; L6₃.non: noninfected line 6₃; L6₃.inf: infected line 6₃.

The iDMRs at the promoters regulated gene transcription. The iDMR was

identified ~600 bp upstream of *CDC42* (cell division cycle 42) in line 7₂, with the reduced methylation level of 0.04 in line 6₃ and 0.33 in line 7₂ after MDV infection, respectively (Figure 4.15 and Appendix X). Correspondingly, the mRNA level of *CDC42* was upregulated about 24% in line 7₂ after MDV infection ($p < 0.05$), and were similar in line 6₃ (Figure 4.16).

These iDMR-related genes were enriched in the different pathways in line 6₃ and 7₂, such as the VEGF signaling and *IL-6* signaling in line 6₃ and *NF- κ B* related pathways in line 7₂ (Table 4.5). The iDMRs were separated into increased_iDMRs and decreased_iDMRs based on the directional methylation variation after MDV infection in two lines. The IPA annotation provided the link between biological functions and decrease_ or increased_iDMRs in two lines (Table 4.6). In line 6₃, genes associated with decreased iDMRs were enriched in the functions of infection diseases and inflammatory response. And in line 7₂, the MDV suppressed iDMRs were overlapped with genes involving in cancer and genetic disorder. The methylation of cancer related genes was increased in line 6₃ and decreased in line 7₂ after MDV infection.

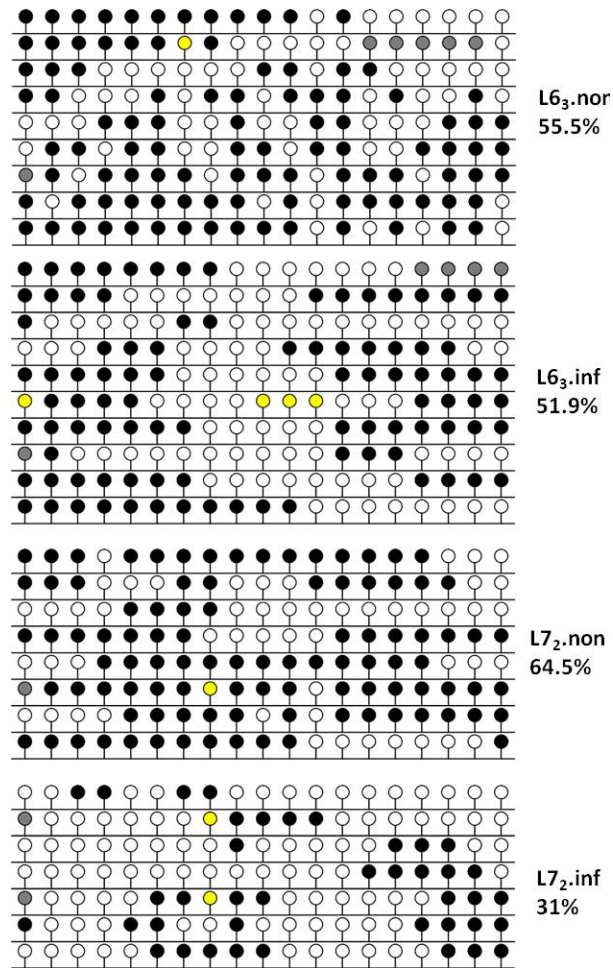


Figure 4.15 The bisulfite sequencing of iDMR upstream of *CDC42*. Each line represents a sequence of a plasmid, and each dot indicates a CpG site. The open dot indicated the unmethylated CpGs, and black dot was the methylated CpGs. The grey one denoted the CpG was undetected, and yellow one was the mutation. The methylation level was calculated as the number of methylated CpG sites divided by the total detected CpGs (yellow and grey were excluded). L7₂.inf: infected line 7₂; L7₂.non: noninfected line 7₂; L6₃.non: noninfected line 6₃; L6₃.inf: infected line 6₃.

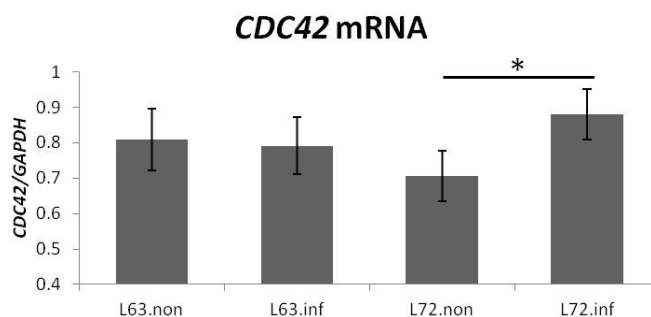


Figure 4.16 The quantification of CDC42 mRNA level. The transcription of *CDC42* was measured and normalized using *GAPDH* in the thymus samples from the two lines before and after MDV infection at 21 dpi. The quantitative results are represented as mean \pm STD. A single asterisk indicated p-values < 0.05 . For each group, n=4.

Table 4.5 Top Canonical Pathways

T63_IT63	T72-IT72
Glucocorticoid Receptor Signaling	Hepatic Fibrosis / Hepatic Stellate Cell Activation
Glioblastoma Multiforme Signaling	Glucocorticoid Receptor Signaling
VEGF Signaling	NF- κ B Activation by Viruses
Clathrin-mediated Endocytosis Signaling	NF- κ B Signaling
IL-6 Signaling	PTEN Signaling

Table 4.6 Top Networks

T63_IT63		T72-IT72	
Increase	Decrease	Increase	Decrease
Connective tissue disorder	Connective tissue development	Lipid metabolism	Genetic disorder
Cell morphology	Infectious disease	Cell death	Cell death
Cellular Development	Cellular development	DNA replication	Cancer
Cell-to-cell signaling and interaction	Inflammatory response	Energy production	Cellular movement
Cancer	Cardiovascular system function	Animo acid metabolism	Lipid metabolism

Increase and decrease indicated that the methylation level was up- or down-regulated after MDV infection.

DNA demethylation

To explore the reason behind the reduced methylation level in line 63 after

MDV infection, the contents of 5hmC, the intermediate in the active demethylation pathway, were detected among 4 samples using anti-5hmC dot blot (Figure 4.17). The quantitative results showed that 5hmC content in 10 μ g DNA sample was less than the 10 ng of 5hmC positive control.

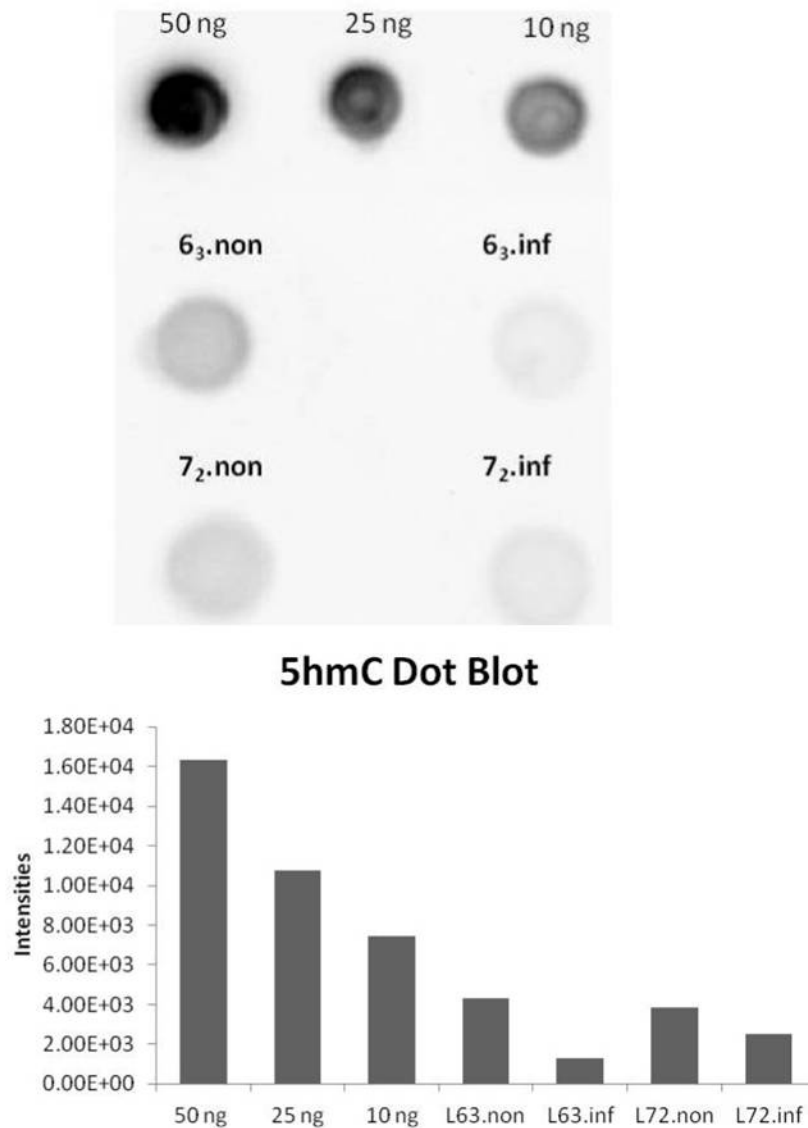


Figure 4.17 Quantification of 5hmC content by anti-5hmC dot blot. The top panel was the dot blot of 10 μ g of DNA from thymus with 5hmC positive controls of 50ng, 25ng and 10 ng DNA. The bottom panel was the quantitative measurement using densitometry.

Methylation inhibition and MDV infection *in vitro*

Because of the decreased DNA methylation on MD resistant line 6₃, it is reasonable to speculate that methylation was involved in the MD resistance. To study the role of DNA methylation on MDV infection, the methylation inhibitor 5'-azacytidine (5'AZA) was used to treat the MDV infected DF-1 cells. The virus genome contents were declined 40-57% in infected cells in the presence of 5'AZA relative to the untreated control cells ($p < 0.05$) (Figure 4.18). The MDV oncoprotein *Meq* expressed in most cells in the control group, and was absent in some drug treated cells (Figure 4.19).

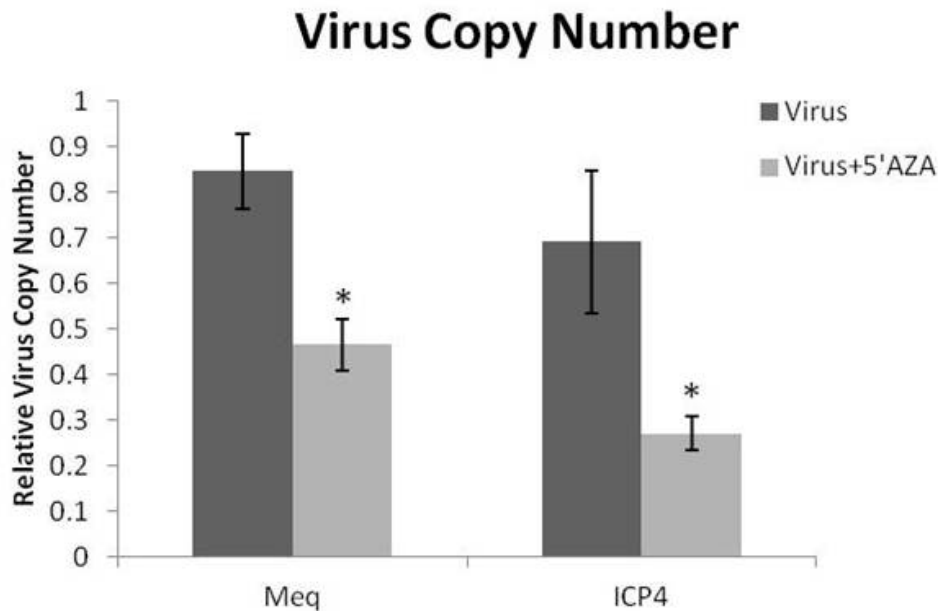


Figure 4.18 Quantification of viral genome copy numbers. The virus copy numbers were evaluated based on viral gene *Meq* and *ICP4* in MDV infected DF-1 cells with or without 5'AZA treatment, and normalized to a single copy gene, *Vim*. Quantitative results are represented as Mean \pm STD ($n=3$).

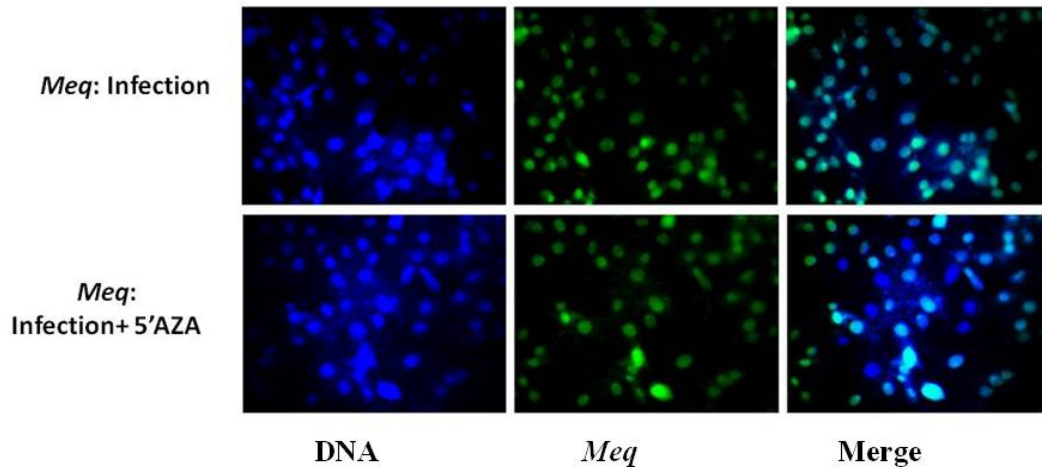


Figure 4.19 The expression of MDV oncogene Meq. The left panel showed the location of nuclei using DAPI to stain DNA (blue). The middle panel was the location and expression MDV oncoprotein Meq (green). The right panel indicated Meq expression in the MDV infected DF-1 cells with or without 5'AZA.

Discussion

Virus infection and tumorigenesis change *DNMTs* transcriptional patterns. Compared to the adjacent normal tissues, tumor tissues showed abnormal *DNMTs* mRNA levels [197-199]. EBV infection upregulated *DNMT3a* expression, and decreased *DNMT1* and *DNMT3b* [200]. Additionally, our lab found that *DNMT1* was activated in the spleen of susceptible chickens and *DNMT3b* was silenced in the resistant chicken after MDV infection during MD development [3]. These results suggest that the expression variations of *DNMTs* depended on the disease progression, tissues and cell types as well as the genetics of the host. *DNMT3a* and *DNMT3b* were two methyltransferases for *de novo* methylation, they interacted with *DNMT1*, the methyltransferase for maintaining methylation, to establish and spread methylation [201]. Changes in *DNMTs* can influence DNA methylation levels [202], therefore it is reasonable to speculate that decreases in *DNMT3a* in infected line 6₃

may result in the reduction of DNA methylation. The results demonstrate that DNA methylation variations at a genome-wide scale are coordinated with the transcriptional differences in *DNMTs* induced by MDV infection in MD resistant line 6₃ and susceptible line 7₂. The higher methylation in uninfected line 7₂ indicated that the inherited, pre-established DNA methylome may contribute to the MD resistance/susceptibility.

Previously the chicken methylome was characterized using MeDIP-seq, an antibody binding affinity based method [203]. However, this method is biased to the highly methylated CpG-rich regions with lower resolution and coverage [195, 203, 204]. In the current study we applied Methyl-MAPS, which allowed quantification of methylation at single copy and repetitive regions and avoided the bias due to the differences in methylation level or CpG density [196]. The MeDIP method only identified about 9-13% methylated CGIs in chicken genome, and was unable to detect CGIs with low methylation level [203]. The coverage of CGIs was improved to 74% by the current study, including CGIs at the promoters, intragenic and intergenic regions with high, low and intermediate methylation. Through intensive analysis, we found that there was a negative correlation between CpG density and DNA methylation at the TSS region and a positive association at other regions in chicken. The methylation pattern across genes was also detected in human and chicken [196, 203]. DNA methylation was depleted at the CGI associated promoter regions, which has been shown in other vertebrates to allow transcription factors and polymerase II to initiate transcription [205].

Intricate differences in DNA methylation exist between MD resistant and

susceptible chickens. In this study, we found that the global methylation level was higher in line 7₂ than in line 6₃ before infection, and average methylation level was dramatically reduced in line 6₃ but increased a little in line 7₂ after infection. The results were also confirmed by the 5mC dot blot. The slight upregulation of methylation in infected line 7₂ was because the number of unmethylated and moderately methylated CpGs declined and the number of CpGs with methylation status increased. More CpGs fell into the unmethylated group and fewer were in the methylation and intermediate methylation classes in uninfected line 6₃ than in line 7₂, leading to the lower methylation in line 6₃ before MDV infection. The decreases in methylation across entire gene in infected line 6₃ suggested that gene transcription may be triggered by the infection. The overall hypomethylation in MDV infected line 6₃ was caused by the methylation decreases in CGIs, repetitive regions and genes. Considering methylation as a key factor of transcriptional regulation, less methylation in line 6₃ may cause more active transcription in the resistant chickens than in susceptible chickens before MDV infection. The infection may further activate transcription in line 6₃ and silence expression in line 7₂. We found differential methylation at the *MHCII* locus between line 6₃ and line 7₂ before viral infection. Since the *MHC* locus contains several immune-related genes, we believe that the pre-established methylation pattern in lines 6₃ and 7₂ may influence their immunity to MDV infection, and also contribute to the infection induced methylation alterations in two chicken lines.

MDV infection changed methylation status of repetitive DNA sequences. A large reduction of methylation was observed on repetitive DNA in line 6₃, indicating

the methylation of these elements may be sensitive to the viral infection. Repeat DNA can exert regulatory functions on gene activities, and some *cis*-elements are originated from transposable elements (TEs) in humans, including LINEs and LTRs [206, 207]. DNA methylation of TEs was a determinant for their mobility, and can affect nucleosome binding and a variety of regulatory influences on nearby gene expression [208, 209]. Moreover, repetitive regions are often hypomethylated in cancer cells, resulting in the genomic instability [210]. In the chicken genome, less than 9% of the genome is comprised of interspersed elements. This is markedly lower than in the mammalian genome, which contains 40-50% [211]. The lower number of TEs is probably due to the lack of active elements in the chicken genome [212]. Therefore, it is reasonable to speculate that methylation variation at chicken TEs had potential influences on gene transcription, but not their retrotransposition [212]. It has been shown that CR1 elements upstream of *STAT1* (signal transducer and activator of transcription 1) and *IL12A* (interleukin 12A), contain potential binding sites for *GATA1* (GATA binding protein 1). The methylation levels on these two elements were downregulated after MDV infection, which were coordinated with the upregulation of mRNA levels. Since methylation inhibits transcription factor binding, the decreased methylation at repetitive regions may up- or down-regulate gene expression through the interaction between transcriptional activators or repressors after MDV exposure in both chicken lines. Our results also suggest that MDV infection changed the methylation levels at repetitive DNA, such as CR1 and LTR, which might have regulatory functions in response to infection.

The identification of genes in iDMRs implicated the potential functions of

DNA methylation in the responses to MDV infection. For example, we discovered an iDMR at the promoter of the MD resistance candidate *GH* [36, 213]. In addition, the enhanced transcription level of *CDC42* was coordinated with an observed decline in DNA methylation in nearby iDMR, consistent with the fact that methylation silenced the gene transcription [210]. *CDC42*, a small GTPase protein, works with other proteins to modulate cell cycle and adhesion [214]. The less methylation and higher transcription level of *CDC42* in infected line 7₂ implicated that it may contribute to MD susceptibility by the deregulation of cell cycle and proliferation. The biofunctional analysis demonstrated that different pathways may be provoked after the infection in each line via changes in methylation status. NF- κ B is known to regulate the immune response to infection, and is associated with human cancer and tumor development. [215]. NF- κ B related pathways were only found in line 7₂, suggesting line-specific DNA methylation variation might affect the disease susceptibility via target immune related pathways. Given the fact that methylation inhibits gene expression, the decreased methylation in iDMRs may activate genes controlling infectious disease and inflammatory responses in line 6₃, which will clean the virus from the host. Genes and pathways with functions related to the lipid metabolism and energy production may be suppressed by hypermethylation on iDMRs of infected line 7₂. The repression of lipid metabolism and abnormal cellular energy production have been characterized as the consequence of infection and nearly all of cancer [216, 217], suggesting that MDV infection may impair host metabolism via DNA methylation. It is worth noting that the relationship between atherosclerotic lesions and MDV infection has been found in MDV infected chickens [218, 219], and

the involvement of DNA methylation in this process needs to be further elucidated.

From our results, it seems the disturbance of DNA methylation after MDV infection did not involve active DNA demethylation through the conversion to 5hmC. Together with the downregulated *DNMT3a* expression, the decreased methylation in line 6₃ is likely controlled by passive demethylation. Since the methylation levels were lower in line 6₃ than line 7₂, the DNA methylation inhibition presumably improves MD resistance. Methylation inhibitor treatment limited MDV replication *in vitro*, which was confirmed by the independent estimation of virus copy numbers using *ICP4* and *Meq*. Lower expression of *Meq* in the drug treated infected cell suggested that 5'AZA either limited viral replication and spread or inactivated *Meq* transcription. However, there is a debate about the function of 5'AZA on MDV infection. *Meq* expression was elevated in the MDV infected B lymphocytes transformed by the avian leukosis virus (ALV) [220]. This disagreement may be explained by the differences between ALV transformed B cells and the chicken model used. The line 6₃ chickens are resistant to MD but susceptible to ALV, whereas line 7₂ chickens are resistant to ALV and susceptible to MD [56]. Resistance to ALV and MDV may be mediated by different mechanisms. Methylation inhibition may enhance ALV propagation, which may further assist MDV infection. In addition, the promoter of *Meq* was absent of DNA methylation in the MDV infected cells [3], and the methylation inhibitor was unable to directly regulate *Meq* expression, increasing the possibility that ALV infection favors secondary infection with MDV.

In summary, genome-wide and quantitative DNA methylation analysis in the current study provides better DNA methylation maps for chicken and global

methylation changes related to MDV infection. The comparison of methylation between MD resistant chicken line 6₃ and MD susceptible chicken line 7₂ suggested that less methylation in the host may be related to MD resistance by activating genes with anti-viral and anti-tumor functions. Higher methylation in the MD susceptible chickens might favor viral replication and spread by the disruption of the normal growth and immune responses. These results suggest a mechanism of disease resistance determined by DNA methylation patterns, and support the notion that methylation variations could be both the cause and the consequence of viral infection. Further work is required to functionally link observed gene expression and DNA methylation changes, together with histone modification analysis. Such analysis will provide a foundation to understand the role of the epigenetics in the crosstalk between virus and host through regulating gene expression. Additionally, the comprehensive integration of both genetic and epigenetic information will help to identify candidate genes implicated in disease resistance or susceptibility, and improve our understanding the epigenetic predisposition to viral infection and give clues for potential epigenetic therapy.

Chapter 5: Conclusions and Future Directions

Summary

The long term goal of our lab is to understand mechanisms involved in host-virus interaction with a particular focus on MDV-induced changes in host epigenome and disease predisposition. We use MHC-independent MD resistant line 6₃ and susceptible chicken line 7₂ as the experimental models. The overall goal of this dissertation project was to identify MDV-induced miRNAs and understand how MDV infection changes global methylation level in host genome. Two specific aims were pursued to achieve the overall goal. Specific aim 1: To identify MDV-induced miRNA expression signatures in line 6₃ and line 7₂ and investigate the roles of differentially expressed miRNAs in MDV disease development; Specific aim 2: To compare MDV infection induced changes in global methylation levels in line 6₃ and line 7₂. The results from this dissertation work provide important information about the roles of miRNAs and DNA methylation in mediating MD resistance or susceptibility.

MicroRNAs

Chicken MD resistant lines 6₃ and susceptible 7₂ have been extensively used to study the genetic mechanisms by which animals show striking differences in response to MDV infection. So far, the difference in miRNA expression profiles before and after MDV infection in these two lines has not been documented. We hypothesized

that MDV infection induces a significantly different changes in miRNA expression in lines 6₃ and 7₂ and these infection responsive miRNAs have functional roles in mediating MD resistance or susceptibility. MiRNA microarray experiment showed that prior to MDV infection, line 6₃ and line 7₂ had similar miRNA expression signatures, however, after MDV infection, these two lines were found to have dramatic difference in miRNA expression levels. As expected, MDV did not induce a significant change in miRNAs expression in line 6₃ but repressed 58 and increased 6 of host miRNAs in line 7₂. While the virus originated miRNAs were not expressed in line 6₃, 10 MDV miRNAs were highly expression in line 7₂ after MDV infection. Both host and viral miRNAs potentially regulated immune response by targeting important genes in host tissues such as oncogenes and tumor suppressors. Bioinformatics analysis revealed that differentially expressed miRNAs *gga-mib-15b* and *gga-let-7i* may target *ATF2* and *DNMT3a*, respectively. *ATF2* is the transcriptional activator that interacts with MDV oncoprotein Meq. *DNMT3a* is the *de novo* DNA methyltransferase that establish methylation patterns. Further analysis found that *ATF2* and *DNMT3a* transcription levels did not differ from two lines after MDV infection; however, their protein levels were increased in infected line 7₂ but not in infected line 6₃. Luciferase reporter assays proved that chicken miRNA *gga-mir-15* and *gga-let-7i* controlled *ATF2* and *DNMT3a* expression through the interaction within the coding regions. Interestingly, when DF-1 cells were transfected with *gga-mib-15b* or *gga-let-7i* overexpression vector, relative to control cells, cells containing overexpression vectors were found to have reduced level of MDV oncoprotein Meq and limited MDV genome copies following MDV infection,

indicating miRNAs have functional roles in preventing MDV infection at the cellular level. In summary, these projects provide functional data for the first time that miRNA play pivotal roles in mediating MDV-host interaction.

DNA methylation

DNMTs are important enzymes required for DNA methylation. Three different *DNMTs* (*DNMT1*, *DNMT3a*, and *DNMT3b*) have been identified in chicken. *DNMT1* transcript level was higher in line 7₂ than that in line 6₃. In both lines, MDV infection did not change *DNMT1* expression; however, *DNMT3a* and *DNMT3b* are different stories. *DNMT3a* and *DNMT3b* mRNA abundances were similar in line 6₃ and line 7₂ before MDV challenge. Following MDV infection, *DNMT3a* was down-regulated in line 6₃, no change was observed in line 7₂. Strikingly, *DNMT3b* was consistent in line 6₃ but showed a significant increase in line 7₂. Changes in *DNMT3a* and *DNMT3b* transcript abundances may contribute to different global methylation patterns in line 6₃ and line 7₂. Therefore we hypothesized that MDV induced changes in *DNMTs* transcription result in methylation changes in line 6₃ and line 7₂ and different methylation patterns might be related to MD resistance and susceptibility. A comprehensive chicken methylome was delineated by using a high throughput method termed Methyl-MAPS, which covered over 20% of CpGs with low, high or intermediate methylation in chicken genomes. The sequencing results and 5mC dot blot demonstrated that the methylation levels were higher in line 7₂ than in line 6₃ before MDV infection, which was coordinated well with higher *DNMT1* mRNA in line 7₂. MDV infection reduced the methylation level approximately 38% in line 6₃,

presumably caused by the repressed *DNMT3a*, and the methylation were slightly increased ~6% in infected line 7₂, corresponding well with the enhanced *DNMT3b* expression. The passive demethylation through DNMTs was likely to be the only reason reducing the methylation in line 6₃ since the active methylation via 5hmC was silenced in both lines. The decreased methylation in infected line 6₃ was largely due to the hypomethylation of CpG islands, repetitive DNA and gene regions. Based on the methylation variations, we identified the infection induced differential methylation regions (iDMRs) in line 6₃ and in line 7₂, and these iDMRs might regulate genes and pathways with different functions in the two lines. More importantly, we found the methylation inhibitor 5'AZA restricted MDV replication or spread in the infected DF-1 cells, suggesting the function of DNA methylation in MDV infection. Collectively, these studies provided the most detailed chicken methylome and discovered the involvement of DNA methylation in MD resistance and susceptibility. Taken together, all the results supported the notion that the pre-established methylation patterns and MDV infection driven methylation alterations are indispensable for MD resistance and susceptibility in line 6₃ and line 7₂.

Conclusions

This dissertation project has advanced our understanding on MD resistance and susceptibility through two aspects: miRNA and DNA methylation. The maintenance of chicken miRNA expression at the proper levels might contribute to MD resistance. The host miRNAs play antiviral functions through limiting viral propagation. The inherited DNA methylation differences were presumably one of the

causative factors for the MD resistance and susceptibility. The methylation profiles determined transcriptional activation and silencing after infection, which sequentially drove the methylation variations and influenced the disease outcomes. Moreover, DNA methylation and miRNAs were regulated mutually. Cellular miRNAs were identified to target DNA methyltransferase, which was indispensable for maintaining and spreading methylation. And DNA methylation might regulate miRNA expression as controlling gene transcription. Both miRNAs and DNA methylation, together with other genetic and epigenetic elements, such as SNPs, DNA copy number variations and histone modifications, provide the foundation for disease predisposition.

Future Directions

The present study proved the antiviral function of miRNAs through overexpression of a single miRNA using the retroviral vector. Further work is required to clarify the contribution of the miRNA target genes in this process. Although the functions of many genes have been clearly identified in model systems using transgenic and knockout approaches, in chickens, it is very challengeable. One way to investigate the gene function is to knockdown the gene of interest using RNA interference (RNAi). The knockdown of miRNA target genes can be accomplished by RNAi using the same retroviral vector in the DF-1 cells [221]. Short hairpin RNAs (shRNAs) can be synthesized to match the transcripts and introduced into the retroviral vector [222]. The infection of the target gene deficient cells could characterize the function of the miRNA target genes in responses to MDV.

It has been shown that the combination of multiple miRNAs and small

interfering RNAs (siRNAs) avoided the viral escape [188, 191]. Therefore, the construction of a retroviral vector that expresses the multiple miRNA simultaneously might further repress the viral replication by targeting more host and viral genes. Meanwhile, elucidating the regulation of viral genome by the cellular miRNAs is an important part to understand the crosstalk between host and virus. It has been shown that human miRNAs promoted hepatitis C virus translation by binding at the 5'UTR of the viral RNA [185]. Thus, compared to the host genes, cellular miRNAs use different mechanisms to regulate foreign RNA expression. The interaction between MDV and chicken miRNAs will be illustrated by the identification of cellular miRNA binding sites on viral transcripts, which may further uncover the mechanism of antiviral function of cellular miRNAs.

A functional test in the present study was done *in vitro*. Similar *in vivo* studies are necessary to understand the role of miRNAs in pathological conditions after MDV infection. The attempt to overexpress miRNAs in chicken was not successfully achieved by using ALV based vector, due to the extremely lower transfer efficiency in the germ line cells, which requires other delivery methods [223, 224]. The tissue-specific knockdown of gene expression by lentiviral vector has been successfully demonstrated in a mammalian system [225]. Using the lentiviral vector is a promising approach to stably express miRNAs in specific tissues in chickens. Together with vaccination, this would allow the development of new methods to improve the current protective strategy.

The other accomplishment of this study is the identification of MDV induced differential methylation regions (iDMRs). DNA methylation has a large impact on

gene expression regulation by influencing the transcription factor binding [226]. Therefore, a motif search in the constitutive or infection specific iDMRs would allow identification of the transcriptional factors involved in MD resistance and susceptibility. Transcription factor binding motifs were enriched in the lineage-specific and normal or cancer cell specific hypomethylated regions, indicating the possibility of identifying *trans* acting factors in regions with DNA methylation changes [227, 228]. Additionally, histone modifications regulate gene activation. Our lab has profiled the active gene marker histone 3 lysine 4 trimethylation (H3K4me3) and the silencing gene marker histone 3 lysine 27 trimethylation (H3K27me3) in MD resistant line 6₃ and MD susceptible line 7₂ before and after infection. The combination of the histone modification profiles and DNA methylation profiles with gene expression would provide more information about the epigenetic variations induced by MDV infection, and also about the feedback of epigenetic alterations to disease resistance through switching on/off the gene expression.

Finally, the present study uncovered a role of inherited DNA methylation patterns in MD resistance and susceptibility in chickens. Thus, we attempted to test the feasibility of finding DNA methylation patterns as biomarkers to select MD resistant chickens. DNA methylation has gained more attentions from the biomarker discovery field since it is able to be measured quantitatively compared to other epigenetic markers. Biomarker discovery in cancer includes five phases, identification of markers, clinical detection, longitude study, screening study, and lastly case control study [229]. In humans, several studies have revealed that DNA methylation was used as the marker for the disease risk evaluation, prognosis and

early diagnosis [230, 231]. The current study was the first step in characterizing the involvement of DNA methylation in MD resistance and susceptibility. More sophisticated analyses are required to delineate the regulatory functions of DNA methylation in MD predisposition in chickens, and to apply the discoveries in genetic or epigenetic selection of resistant chickens.

Appendices

Appendix I. Differentially expressed chicken microRNAs between infected and noninfected Line7₂ groups

Name	logFC	P.Value	FDR
<i>gga-miR-99a</i>	1.760595	3.29E-06	5.92E-05
<i>gga-miR-181a</i>	1.949209	4.76E-06	6.91E-05
<i>gga-miR-181b</i>	1.741941	5.12E-06	6.91E-05
<i>gga-miR-103</i>	1.350569	1.18E-05	0.000148
<i>gga-miR-128</i>	1.263305	1.93E-05	0.000223
<i>gga-miR-455</i>	1.273726	5.08E-05	0.000549
<i>gga-let-7b</i>	1.241415	5.84E-05	0.000591
<i>gga-miR-10b</i>	1.214064	0.000101	0.000915
<i>gga-miR-456</i>	1.166798	0.000113	0.000915
<i>gga-miR-1b</i>	1.208345	0.000166	0.00128
<i>gga-miR-107</i>	1.260672	0.000174	0.001283
<i>gga-miR-30a-3p</i>	1.744581	0.000225	0.001587
<i>gga-miR-100</i>	1.145376	0.000312	0.002104
<i>gga-let-7a/gga-let-7j</i>	1.325531	0.00036	0.002308
<i>gga-miR-146a</i>	-1.21913	0.00037	0.002308
<i>gga-miR-30d</i>	1.087841	0.0004	0.0024
<i>gga-miR-147</i>	-1.01843	0.000542	0.003135
<i>gga-miR-17-3p</i>	1.220382	0.000676	0.003776
<i>gga-miR-218</i>	1.116341	0.000703	0.003795
<i>gga-miR-9</i>	1.110438	0.000789	0.004124
<i>gga-miR-138</i>	0.809944	0.001534	0.00751
<i>gga-let-7f</i>	0.795792	0.001566	0.00751
<i>gga-miR-199</i>	0.762491	0.001576	0.00751
<i>gga-miR-124a</i>	0.923271	0.001945	0.009004
<i>gga-miR-18b</i>	0.836313	0.002905	0.01286
<i>gga-miR-125b</i>	0.870999	0.002937	0.01286
<i>gga-miR-153</i>	1.453438	0.003084	0.013146
<i>gga-miR-221</i>	0.782907	0.003887	0.016148
<i>gga-miR-30c</i>	0.703324	0.004367	0.017688
<i>gga-miR-92</i>	0.864246	0.004583	0.018108
<i>gga-miR-133b</i>	0.920419	0.00512	0.019748
<i>gga-miR-204/gga-miR-211</i>	0.860571	0.006747	0.025417
<i>gga-miR-30a-5p</i>	0.708035	0.007139	0.026286
<i>gga-let-7c</i>	0.74543	0.007522	0.027077
<i>gga-miR-30b</i>	0.576117	0.008145	0.027771
<i>gga-miR-199*</i>	0.97806	0.008242	0.027771

<i>gga-miR-302b*</i>	-0.78133	0.008365	0.027771
<i>gga-miR-181a*</i>	0.908167	0.0092	0.029596
<i>gga-let-7k</i>	1.067455	0.009317	0.029596
<i>gga-miR-140</i>	0.616854	0.009505	0.029611
<i>gga-miR-193</i>	0.772655	0.010378	0.031715
<i>gga-miR-27b</i>	0.814612	0.011326	0.033361
<i>gga-miR-148a</i>	0.927259	0.011542	0.03339
<i>gga-miR-126</i>	0.979227	0.012862	0.036554
<i>gga-let-7i</i>	0.54566	0.013985	0.039062
<i>gga-miR-33</i>	0.785207	0.014266	0.039171
<i>gga-miR-466</i>	-1.39321	0.014926	0.040066
<i>gga-miR-126*</i>	0.818411	0.015086	0.040066
<i>gga-miR-34a</i>	0.508048	0.015553	0.040638
<i>gga-miR-18a</i>	0.766642	0.015945	0.041002
<i>gga-miR-15b</i>	0.530495	0.016677	0.041865
<i>gga-miR-375</i>	0.66711	0.016798	0.041865
<i>gga-miR-223</i>	-0.69745	0.018769	0.04551
<i>gga-let-7g</i>	0.576923	0.018822	0.04551
<i>gga-miR-190</i>	0.667463	0.021096	0.050258
<i>gga-miR-7</i>	-0.59965	0.0216	0.050714
<i>gga-miR-184</i>	-0.79159	0.025407	0.058799
<i>gga-miR-499</i>	0.604568	0.025957	0.059226
<i>gga-miR-17-5p</i>	0.643931	0.032926	0.073068
<i>gga-miR-21</i>	-0.70144	0.033677	0.073726
<i>gga-miR-122</i>	0.701345	0.039442	0.084073
<i>gga-miR-205b</i>	-0.53455	0.040507	0.085223
<i>gga-miR-26a</i>	0.658442	0.04147	0.086131
<i>gga-miR-489</i>	0.750998	0.046173	0.094684

^A: logFC was computed as $\log_2\left(\frac{\text{non infectedLine7}_2}{\text{InfectedLine7}_2}\right)$

Appendix II. Differentially expressed chicken microRNAs between infected Line 6₃ and Line7₂ groups

Name	logFC	P.Value	FDR
<i>gga-miR-99a</i>	2.22393	2.71E-07	8.79E-06
<i>gga-miR-455</i>	1.594012	5.64E-06	9.14E-05
<i>gga-miR-100</i>	1.69626	8.07E-06	0.000119
<i>gga-miR-10b</i>	1.431896	2.15E-05	0.00029
<i>gga-let-7b</i>	1.293156	3.98E-05	0.000461
<i>gga-miR-181a</i>	1.49834	6.25E-05	0.000622
<i>gga-miR-125b</i>	1.390395	6.70E-05	0.000622
<i>gga-miR-181b</i>	1.334056	6.91E-05	0.000622
<i>gga-miR-147</i>	-1.26644	8.28E-05	0.000697
<i>gga-miR-199</i>	1.084724	8.60E-05	0.000697
<i>gga-miR-103</i>	1.088025	9.30E-05	0.000717
<i>gga-miR-107</i>	1.329872	0.000108	0.000799
<i>gga-let-7c</i>	1.150765	0.000329	0.00232
<i>gga-miR-153</i>	1.847916	0.000515	0.003361
<i>gga-miR-146a</i>	-1.17015	0.000519	0.003361
<i>gga-miR-128</i>	0.868683	0.000553	0.003445
<i>gga-miR-126*</i>	1.319732	0.000635	0.003808
<i>gga-miR-218</i>	1.123449	0.000668	0.003867
<i>gga-let-7f</i>	0.884625	0.0007	0.003908
<i>gga-miR-302b*</i>	-1.10584	0.000771	0.004163
<i>gga-miR-30a-3p</i>	1.437773	0.001082	0.005538
<i>gga-miR-199*</i>	1.306179	0.001181	0.0058
<i>gga-miR-1b</i>	0.921415	0.001487	0.006902
<i>gga-miR-456</i>	0.851689	0.001491	0.006902
<i>gga-miR-34a</i>	0.734018	0.001538	0.006923
<i>gga-miR-383</i>	1.117926	0.001627	0.007124
<i>gga-miR-30b</i>	0.731435	0.001693	0.007216
<i>gga-miR-30d</i>	0.868993	0.002237	0.009293
<i>gga-let-7k</i>	1.303096	0.002632	0.010603
<i>gga-miR-30c</i>	0.756482	0.002683	0.010603
<i>gga-let-7a/gga-let-7j</i>	0.996138	0.003125	0.012054
<i>gga-miR-193</i>	0.913973	0.003701	0.013626
<i>gga-miR-148a</i>	1.092814	0.004294	0.015457
<i>gga-miR-205b</i>	-0.81643	0.004549	0.01568
<i>gga-miR-122</i>	1.046192	0.004798	0.015976
<i>gga-miR-7</i>	-0.78138	0.004874	0.015976
<i>gga-miR-365</i>	0.653083	0.008264	0.025158
<i>gga-miR-200b</i>	1.649155	0.008472	0.025158
<i>gga-miR-200a</i>	1.683736	0.008649	0.025158

<i>gga-miR-26a</i>	0.901929	0.008696	0.025158
<i>gga-miR-27b</i>	0.835299	0.009832	0.027944
<i>gga-miR-184</i>	-0.92207	0.011634	0.032494
<i>gga-miR-126</i>	0.988679	0.012204	0.033508
<i>gga-miR-190</i>	0.71046	0.01536	0.041472
<i>gga-miR-124a</i>	0.657104	0.015924	0.04229
<i>gga-miR-142-5p</i>	-0.8538	0.017161	0.044128
<i>gga-miR-466</i>	-1.33813	0.018389	0.046548
<i>gga-miR-223</i>	-0.69342	0.019322	0.048068
<i>gga-let-7i</i>	0.511276	0.019583	0.048068
<i>gga-miR-138</i>	0.528106	0.021019	0.050823
<i>gga-miR-24</i>	0.57525	0.02276	0.054222
<i>gga-miR-429</i>	1.645703	0.025175	0.059107
<i>gga-miR-29b</i>	-0.6612	0.025809	0.059715
<i>gga-miR-133b</i>	0.683815	0.026171	0.059715
<i>gga-miR-499</i>	0.579396	0.031524	0.07093
<i>gga-miR-21</i>	-0.70396	0.033152	0.073569
<i>gga-miR-18b</i>	0.538932	0.033743	0.07387
<i>gga-miR-221</i>	0.524929	0.034307	0.074102
<i>gga-miR-215</i>	-0.7945	0.038339	0.079845
<i>gga-let-7g</i>	0.483645	0.042131	0.085316
<i>gga-miR-140</i>	0.448124	0.045048	0.090096
<i>gga-miR-204/gga-miR-211</i>	0.574843	0.049942	0.098665

^A: logFC was computed as $\log_2\left(\frac{\text{infectedLine6}_3}{\text{InfectedLine7}_2}\right)$

Appendix III. Differentially expressed MDV microRNAs in chickens of the infected Line 6₃ and Line7₂ groups

Name	logFC	P.Value	FDR
<i>mdv1-miR-M6</i>	-6.60394	1.65E-09	1.69E-07
<i>mdv1-miR-M8</i>	-7.54209	2.08E-09	1.69E-07
<i>mdv1-miR-M5</i>	-4.87375	2.78E-08	1.50E-06
<i>mdv1-miR-M3</i>	-5.11485	5.01E-08	1.58E-06
<i>mdv1-miR-M2</i>	-3.84215	5.60E-08	1.58E-06
<i>mdv1-miR-M4</i>	-6.64692	5.84E-08	1.58E-06
<i>mdv1-miR-M2*</i>	-3.62937	5.76E-07	1.33E-05
<i>mdv1-miR-M7</i>	-3.55253	2.22E-06	4.50E-05
<i>mdv1-miR-M1</i>	-3.92847	4.08E-06	6.61E-05
<i>mdv1-miR-M4*</i>	-2.50929	0.000102	0.000915

^A: logFC was computed as $\log_2\left(\frac{InfectedLine6_3}{InfectedLine7_2}\right)$

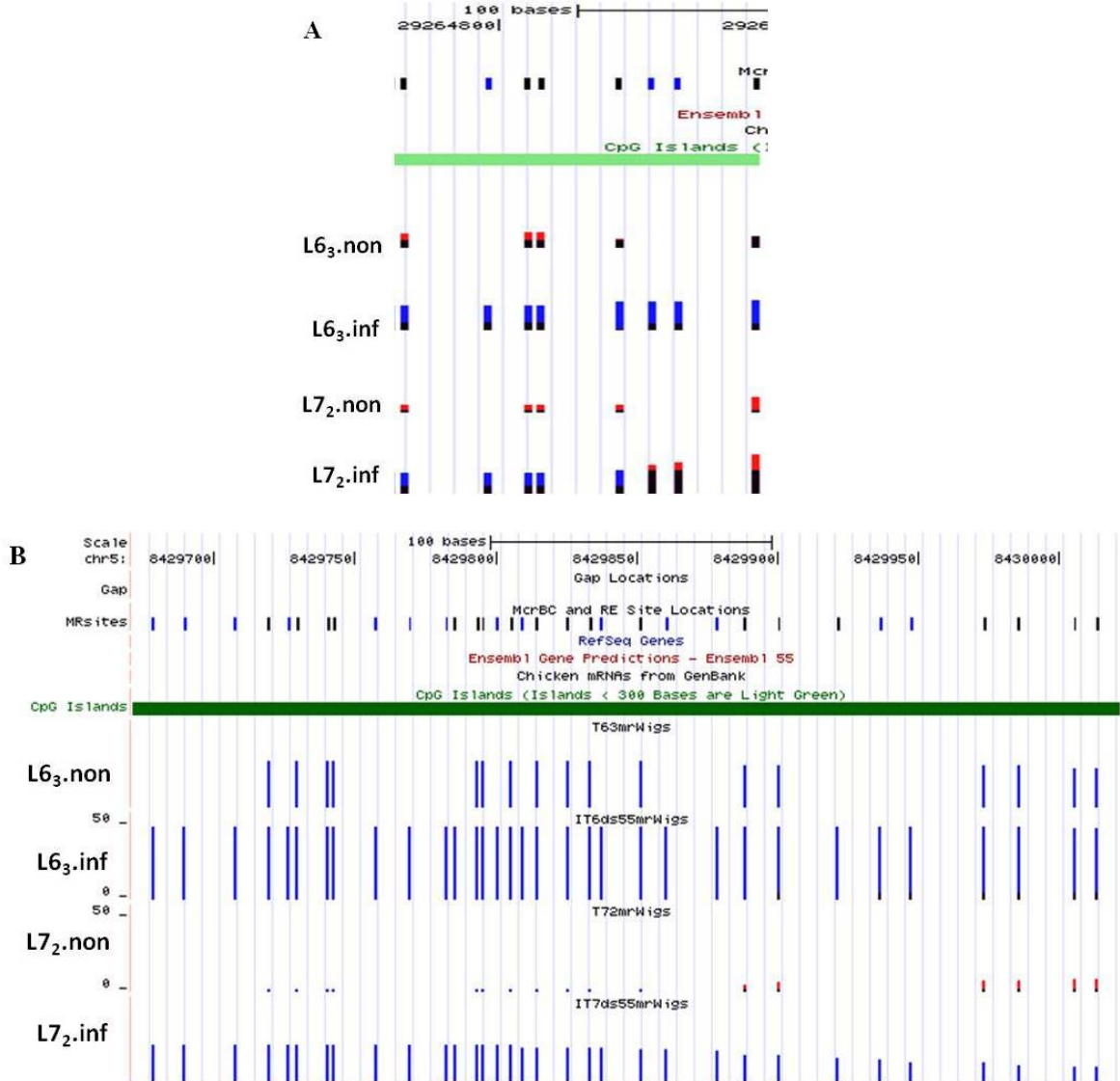
Appendix IV. Pathways predicted by IPA

Pathways	log(p-value)
HGF Signaling	-4.57
EGF Signaling	-4.17
T Cell Receptor Signaling	-4.09
ILK Signaling	-3.90
Neurotrophin/TRK Signaling	-3.88
Inositol Phosphate Metabolism	-3.80
IGF-1 Signaling	-3.44
Nitric Oxide Signaling in the Cardiovascular System	-3.32
Renal Cell Carcinoma Signaling	-3.21
B Cell Receptor Signaling	-3.11
Molecular Mechanisms of Cancer	-3.10
ERK/MAPK Signaling	-3.09
Ovarian Cancer Signaling	-3.09
FGF Signaling	-3.07
ERK5 Signaling	-3.06
Glioblastoma Multiforme Signaling	-3.04
Melanocyte Development and Pigmentation Signaling	-3.02
Protein Ubiquitination Pathway	-2.90
Role of Osteoblasts, Osteoclasts and Chondrocytes in Rheumatoid Arthritis	-2.88
Ceramide Signaling	-2.81
Hypoxia Signaling in the Cardiovascular System	-2.79
PKC θ Signaling in T Lymphocytes	-2.79
Regulation of IL-2 Expression in Activated and Anergic T Lymphocytes	-2.77
Colorectal Cancer Metastasis Signaling	-2.74
Glioma Invasiveness Signaling	-2.74
Wnt/ β -catenin Signaling	-2.71
Prostate Cancer Signaling	-2.68
Integrin Signaling	-2.68
SAPK/JNK Signaling	-2.64
Myc Mediated Apoptosis Signaling	-2.63
TGF- β Signaling	-2.59
BMP signaling pathway	-2.56
Cardiac Hypertrophy Signaling	-2.44
FAK Signaling	-2.43
RANK Signaling in Osteoclasts	-2.43
Leptin Signaling in Obesity	-2.42

NF- κ B Signaling	-2.39
Cholecystokinin/Gastrin-mediated Signaling	-2.38
Rac Signaling	-2.28
PI3K Signaling in B Lymphocytes	-2.27
Huntington's Disease Signaling	-2.23
HMGB1 Signaling	-2.18
RAN Signaling	-2.17
Renin-Angiotensin Signaling	-2.12
PDGF Signaling	-2.09
GNRH Signaling	-2.07
Role of NFAT in Cardiac Hypertrophy	-2.07
Aldosterone Signaling in Epithelial Cells	-2.05
LPS-stimulated MAPK Signaling	-2.01

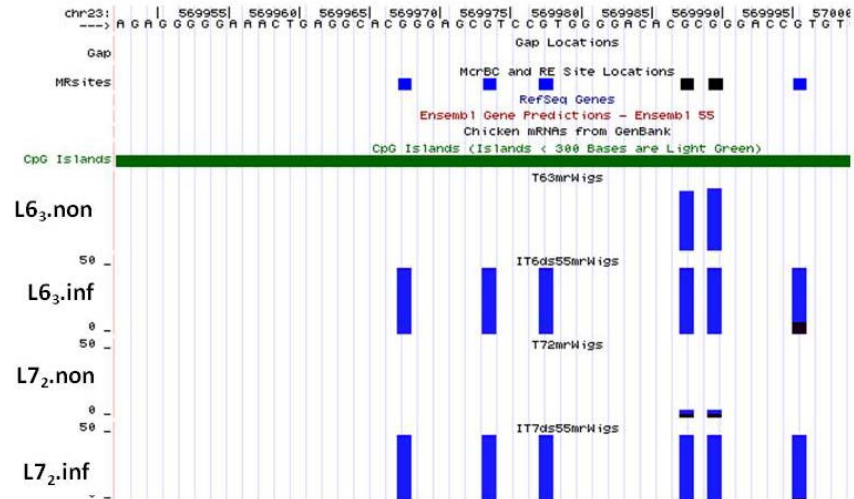
Appendix V The genome browser view of two CGI methylation.

The CGI upstream of *HDAC9* (A) was on chromosome 2: 29,264-29,264,968 and the CGI upstream of *FARI* (B) was on chromosome 5: 8,429,672-8,430,025. And the vertical blue, red and black bars represented the methylation of CpG sites.



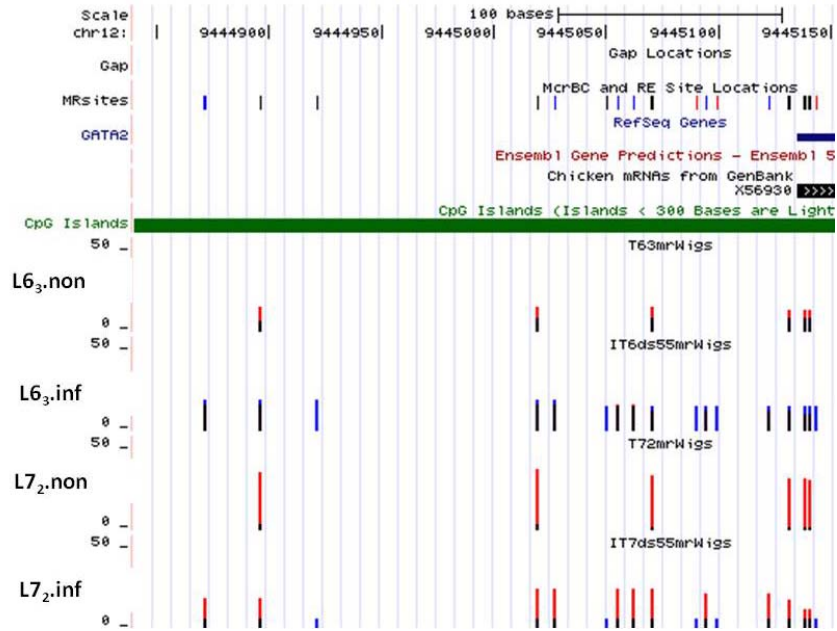
Appendix VI The genome browser view of *FABP3* CGI methylation.

The CGI upstream of *FABP3* on Chromosome 23 :569,948-570,011. The horizontal green bar indicated the position of CGI. And the vertical blue bars represented the methylation of CpG sites.



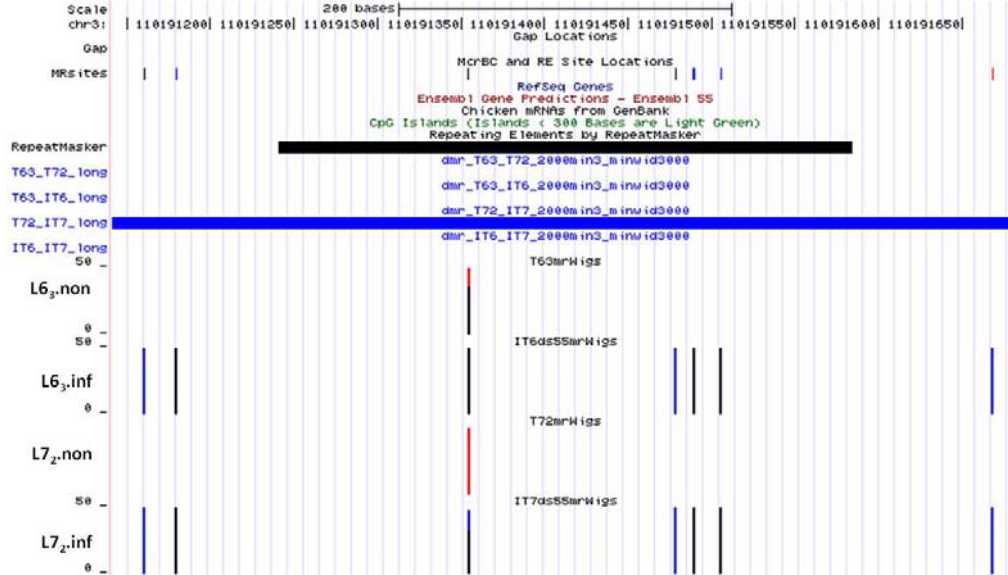
Appendix VII. The genome browser view of *GATA2* promoter methylation.

The 19 CpGs on *GATA2* promoter, located at chromosome 12: 9,444,841-9,445,317, showed different methylation. The horizontal green bar indicated the position of CGI. And the vertical red and blue bars represented the methylation of CpG sites.



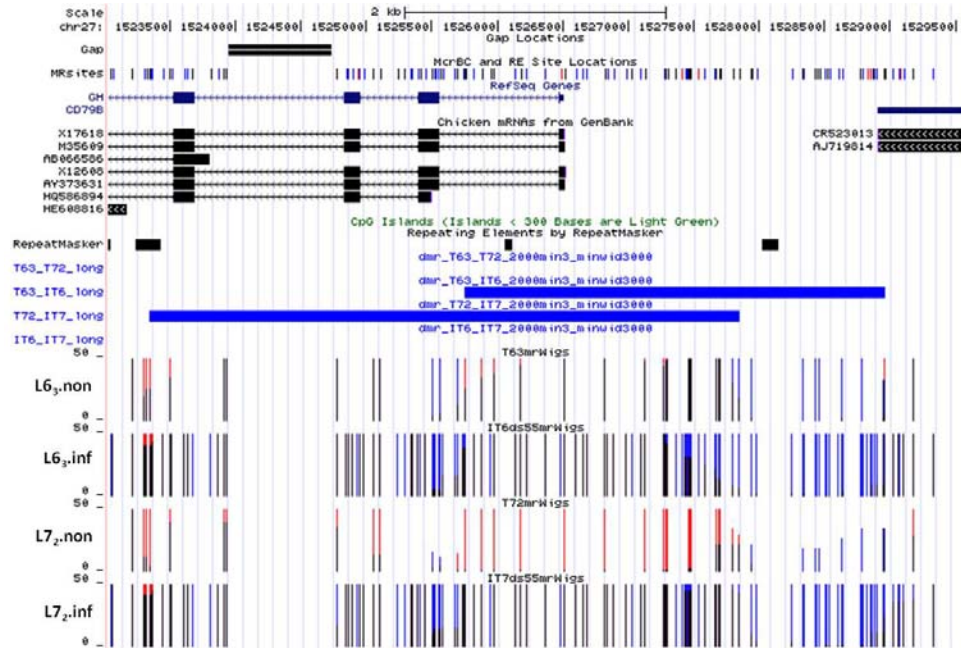
Appendix VIII The genome browser view of CR1-B methylation.

The CR1-B, on chromosome 3: 110,191,142-110,191,684, showed different methylation level in line 63 and line 72 after MDV infection. The horizontal blue bar indicated the position of infection induced differential methylation region (iDMR). And the vertical blue, red and black bars represented the methylation of CpG sites.



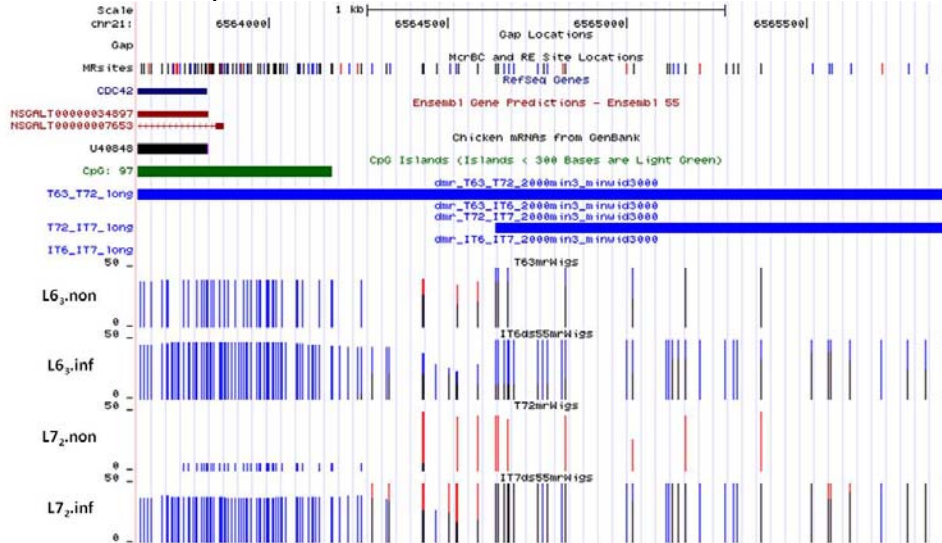
Appendix IX The genome browser view of *GH* DMR.

The horizontal blue bars indicated the position DMRs in 4 comparisons. And the vertical red and blue bars represented the methylation level of CpG sites.



Appendix X. The genome browser view of *CDC42* DMR.

The 19 CpGs upstream of *CDC42*, at chromosome 21: 6,564,439-6,565,113, were identified as iDMRs in line 7₂. The horizontal blue bars indicated the position iDMRs in 4 comparisons. And the vertical red and blue bars represented the methylation level of CpG sites.



Bibliography

1. Davison TF, Nair V: **Marek's disease: an evolving problem**. Amsterdam; Boston: Elsevier; 2004.
2. Grafodatskaya D, Choufani S, Ferreira JC, Butcher DT, Lou Y, Zhao C, Scherer SW, Weksberg R: **EBV transformation and cell culturing destabilizes DNA methylation in human lymphoblastoid cell lines**. *Genomics* 2010, **95**(2):73-83.
3. Luo J, Yu Y, Chang S, Tian F, Zhang H, Song J: **DNA Methylation Fluctuation Induced by Virus Infection Differs between MD-resistant and -susceptible Chickens**. *Front Genet* 2012, **3**:20.
4. Brown AC, Nair V, Allday MJ: **Epigenetic regulation of the latency-associated region of Marek's disease virus in tumor-derived T-cell lines and primary lymphoma**. *J Virol* 2012, **86**(3):1683-1695.
5. Tian F, Luo J, Zhang H, Chang S, Song J: **MiRNA expression signatures induced by Marek's disease virus infection in chickens**. *Genomics* 2012, **99**(3):152-159.
6. Triboulet R, Mari B, Lin YL, Chable-Bessia C, Bennasser Y, Lebrigand K, Cardinaud B, Maurin T, Barbry P, Baillat V *et al*: **Suppression of microRNA-silencing pathway by HIV-1 during virus replication**. *Science* 2007, **315**(5818):1579-1582.
7. Moore PS, Chang Y: **Why do viruses cause cancer? Highlights of the first century of human tumour virology**. *Nat Rev Cancer* 2010, **10**(12):878-889.
8. Ferrari R, Berk AJ, Kurdistani SK: **Viral manipulation of the host epigenome for oncogenic transformation**. *Nat Rev Genet* 2009, **10**(5):290-294.
9. Esquela-Kerscher A, Slack FJ: **Oncomirs - microRNAs with a role in cancer**. *Nat Rev Cancer* 2006, **6**(4):259-269.
10. Feng S, Jacobsen SE, Reik W: **Epigenetic reprogramming in plant and animal development**. *Science* 2010, **330**(6004):622-627.
11. Katada S, Imhof A, Sassone-Corsi P: **Connecting threads: epigenetics and metabolism**. *Cell* 2012, **148**(1-2):24-28.
12. Rodriguez-Paredes M, Esteller M: **Cancer epigenetics reaches mainstream oncology**. *Nat Med* 2011, **17**(3):330-339.
13. Villagra A, Cheng F, Wang HW, Suarez I, Glozak M, Maurin M, Nguyen D, Wright KL, Atadja PW, Bhalla K *et al*: **The histone deacetylase HDAC11 regulates the expression of interleukin 10 and immune tolerance**. *Nat Immunol* 2009, **10**(1):92-100.
14. Wilson CB, Rowell E, Sekimata M: **Epigenetic control of T-helper-cell differentiation**. *Nat Rev Immunol* 2009, **9**(2):91-105.
15. Suzuki MM, Bird A: **DNA methylation landscapes: provocative insights from epigenomics**. *Nat Rev Genet* 2008, **9**(6):465-476.
16. Shiota K, Kogo Y, Ohgane J, Imamura T, Urano A, Nishino K, Tanaka S, Hattori N: **Epigenetic marks by DNA methylation specific to stem, germ**

- and somatic cells in mice.** *Genes Cells* 2002, **7**(9):961-969.
17. Dudnikova E, Vlasov A, Norkina S, Kireev D, Witter RL: **Factors influencing the attenuation of serotype 1 Marek's disease virus by serial cell culture passage and evaluation of attenuated strains for protection and replication.** *Avian Dis* 2009, **53**(1):63-72.
 18. Witter RL: **Increased virulence of Marek's disease virus field isolates.** *Avian Dis* 1997, **41**(1):149-163.
 19. Osterrieder N, Kamil JP, Schumacher D, Tischler BK, Trapp S: **Marek's disease virus: from miasma to model.** *Nat Rev Microbiol* 2006, **4**(4):283-294.
 20. Tulman ER, Afonso CL, Lu Z, Zsak L, Rock DL, Kutish GF: **The genome of a very virulent Marek's disease virus.** *J Virol* 2000, **74**(17):7980-7988.
 21. Brown AC, Baigent SJ, Smith LP, Chattoo JP, Petherbridge LJ, Hawes P, Allday MJ, Nair V: **Interaction of MEQ protein and C-terminal-binding protein is critical for induction of lymphomas by Marek's disease virus.** *Proc Natl Acad Sci U S A* 2006, **103**(6):1687-1692.
 22. Barrow AD, Burgess SC, Baigent SJ, Howes K, Nair VK: **Infection of macrophages by a lymphotropic herpesvirus: a new tropism for Marek's disease virus.** *J Gen Virol* 2003, **84**(Pt 10):2635-2645.
 23. Baigent SJ, Ross LJ, Davison TF: **Differential susceptibility to Marek's disease is associated with differences in number, but not phenotype or location, of pp38+ lymphocytes.** *J Gen Virol* 1998, **79** (Pt 11):2795-2802.
 24. Hunt HD, Lupiani B, Miller MM, Gimeno I, Lee LF, Parcels MS: **Marek's disease virus down-regulates surface expression of MHC (B Complex) Class I (BF) glycoproteins during active but not latent infection of chicken cells.** *Virology* 2001, **282**(1):198-205.
 25. Koppers-Lalic D, Reits EA, Rensing ME, Lipinska AD, Abele R, Koch J, Marcondes Rezende M, Admiraal P, van Leeuwen D, Bienkowska-Szewczyk K *et al*: **Varicelloviruses avoid T cell recognition by UL49.5-mediated inactivation of the transporter associated with antigen processing.** *Proc Natl Acad Sci U S A* 2005, **102**(14):5144-5149.
 26. Jarosinski KW, Hunt HD, Osterrieder N: **Down-regulation of MHC class I by the Marek's disease virus (MDV) UL49.5 gene product mildly affects virulence in a haplotype-specific fashion.** *Virology* 2010, **405**(2):457-463.
 27. Davison TF, Nair V: **Marek's disease : an evolving problem.** Amsterdam ; Boston: Elsevier; 2004.
 28. Burnside J, Bernberg E, Anderson A, Lu C, Meyers BC, Green PJ, Jain N, Isaacs G, Morgan RW: **Marek's disease virus encodes MicroRNAs that map to meq and the latency-associated transcript.** *J Virol* 2006, **80**(17):8778-8786.
 29. Delecluse HJ, Hammerschmidt W: **Status of Marek's disease virus in established lymphoma cell lines: herpesvirus integration is common.** *J Virol* 1993, **67**(1):82-92.
 30. Delecluse HJ, Schuller S, Hammerschmidt W: **Latent Marek's disease virus can be activated from its chromosomally integrated state in herpesvirus-transformed lymphoma cells.** *Embo J* 1993, **12**(8):3277-3286.

31. Bumstead N, Sillibourne J, Rennie M, Ross N, Davison F: **Quantification of Marek's disease virus in chicken lymphocytes using the polymerase chain reaction with fluorescence detection.** *J Virol Methods* 1997, **65**(1):75-81.
32. Suchodolski PF, Izumiya Y, Lupiani B, Ajithdoss DK, Lee LF, Kung HJ, Reddy SM: **Both homo and heterodimers of Marek's disease virus encoded Meq protein contribute to transformation of lymphocytes in chickens.** *Virology* 2010, **399**(2):312-321.
33. Levy AM, Gilad O, Xia L, Izumiya Y, Choi J, Tsalenko A, Yakhini Z, Witter R, Lee L, Cardona CJ *et al*: **Marek's disease virus Meq transforms chicken cells via the v-Jun transcriptional cascade: a converging transforming pathway for avian oncoviruses.** *Proc Natl Acad Sci U S A* 2005, **102**(41):14831-14836.
34. Huguier S, Baguet J, Perez S, van Dam H, Castellazzi M: **Transcription factor ATF2 cooperates with v-Jun to promote growth factor-independent proliferation in vitro and tumor formation in vivo.** *Mol Cell Biol* 1998, **18**(12):7020-7029.
35. Levy AM, Izumiya Y, Brunovskis P, Xia L, Parcels MS, Reddy SM, Lee L, Chen HW, Kung HJ: **Characterization of the chromosomal binding sites and dimerization partners of the viral oncoprotein Meq in Marek's disease virus-transformed T cells.** *J Virol* 2003, **77**(23):12841-12851.
36. Liu HC, Cheng HH, Tirunagaru V, Sofer L, Burnside J: **A strategy to identify positional candidate genes conferring Marek's disease resistance by integrating DNA microarrays and genetic mapping.** *Anim Genet* 2001, **32**(6):351-359.
37. Heidari M, Huebner M, Kireev D, Silva RF: **Transcriptional profiling of Marek's disease virus genes during cytolytic and latent infection.** *Virus Genes* 2008, **36**(2):383-392.
38. Yu Y, Luo J, Mitra A, Chang S, Tian F, Zhang H, Yuan P, Zhou H, Song J: **Temporal transcriptome changes induced by MDV in Marek's disease-resistant and -susceptible inbred chickens.** *BMC Genomics* 2011, **12**:501.
39. Venugopal K, Payne LN: **Molecular pathogenesis of Marek's disease-recent developments.** *Avian Pathol* 1995, **24**(4):597-609.
40. Burgess SC, Young JR, Baaten BJ, Hunt L, Ross LN, Parcels MS, Kumar PM, Tregaskes CA, Lee LF, Davison TF: **Marek's disease is a natural model for lymphomas overexpressing Hodgkin's disease antigen (CD30).** *Proc Natl Acad Sci U S A* 2004, **101**(38):13879-13884.
41. Xing Z, Schat KA: **Expression of cytokine genes in Marek's disease virus-infected chickens and chicken embryo fibroblast cultures.** *Immunology* 2000, **100**(1):70-76.
42. Thantrige-Don N, Read LR, Abdul-Careem MF, Mohammadi H, Mallick AI, Sharif S: **Marek's disease virus influences the expression of genes associated with IFN-gamma-inducible MHC class II expression.** *Viral Immunol* 2010, **23**(2):227-232.
43. Rath NC, Parcels MS, Xie H, Santin E: **Characterization of a spontaneously transformed chicken mononuclear cell line.** *Vet Immunol Immunopathol* 2003, **96**(1-2):93-104.

44. Abdul-Careem MF, Haq K, Shanmuganathan S, Read LR, Schat KA, Heidari M, Sharif S: **Induction of innate host responses in the lungs of chickens following infection with a very virulent strain of Marek's disease virus.** *Virology* 2009, **393**(2):250-257.
45. Kodama H, Mikami T, Inoue M, Izawa H: **Inhibitory effects of macrophages against Marek's disease virus plaque formation in chicken kidney cell cultures.** *J Natl Cancer Inst* 1979, **63**(5):1267-1271.
46. Haffer K, Sevoian M, Wilder M: **The role of the macrophages in Marek's disease: in vitro and in vivo studies.** *Int J Cancer* 1979, **23**(5):648-656.
47. Lee LF, Witter RL: **Humoral immune responses to inactivated oil-emulsified Marek's disease vaccine.** *Avian Dis* 1991, **35**(3):452-459.
48. Omar AR, Schat KA: **Syngeneic Marek's disease virus (MDV)-specific cell-mediated immune responses against immediate early, late, and unique MDV proteins.** *Virology* 1996, **222**(1):87-99.
49. Ghiasi H, Kaiwar R, Nesburn AB, Wechsler SL: **Baculovirus expressed herpes simplex virus type 1 glycoprotein C protects mice from lethal HSV-1 infection.** *Antiviral Res* 1992, **18**(3-4):291-302.
50. Ghiasi H, Kaiwar R, Nesburn AB, Wechsler SL: **Expression of herpes simplex virus type 1 glycoprotein I in baculovirus: preliminary biochemical characterization and protection studies.** *J Virol* 1992, **66**(4):2505-2509.
51. Gavora JS, Grunder AA, Spencer JL, Gowe RS, Robertson A, Speckmann GW: **An assessment of effects of vaccination on genetic resistance to Marek's disease.** *Poult Sci* 1974, **53**(3):889-897.
52. von Krosigk CM, McClary CF, Vielitz E, Zander DV: **Selection for resistance to Marek's disease and its expected effects on other important traits in white leghorn strain crosses.** *Avian Dis* 1972, **16**(1):11-19.
53. Hepkema BG, Blankert JJ, Albers GA, Tilanus MG, Egberts E, van der Zijpp AJ, Hensen EJ: **Mapping of susceptibility to Marek's disease within the major histocompatibility (B) complex by refined typing of White Leghorn chickens.** *Anim Genet* 1993, **24**(4):283-287.
54. Briles WE, Briles RW, Taffs RE, Stone HA: **Resistance to a malignant lymphoma in chickens is mapped to subregion of major histocompatibility (B) complex.** *Science* 1983, **219**(4587):977-979.
55. Hartmann W: **Evaluation of "major genes" affecting disease resistance in poultry in respect to their potential for commercial breeding.** *Prog Clin Biol Res* 1989, **307**:221-231.
56. Bacon LD, Hunt HD, Cheng HH: **A review of the development of chicken lines to resolve genes determining resistance to diseases.** *Poult Sci* 2000, **79**(8):1082-1093.
57. Gallatin WM, Longenecker BM: **Expression of genetic resistance to an oncogenic herpesvirus at the target cell level.** *Nature* 1979, **280**(5723):587-589.
58. Powell PC, Lee LF, Mustill BM, Rennie M: **The mechanism of genetic resistance to Marek's disease in chickens.** *Int J Cancer* 1982, **29**(2):169-174.

59. Kuhnlein U, Ni L, Weigend S, Gavora JS, Fairfull W, Zadworny D: **DNA polymorphisms in the chicken growth hormone gene: response to selection for disease resistance and association with egg production.** *Anim Genet* 1997, **28**(2):116-123.
60. Heidari M, Sarson AJ, Huebner M, Sharif S, Kireev D, Zhou H: **Marek's disease virus-induced immunosuppression: array analysis of chicken immune response gene expression profiling.** *Viral Immunol* 2010, **23**(3):309-319.
61. Chen C, Li H, Xie Q, Shang H, Ji J, Bai S, Cao Y, Ma Y, Bi Y: **Transcriptional profiling of host gene expression in chicken liver tissues infected with oncogenic Marek's disease virus.** *J Gen Virol* 2011, **92**(Pt 12):2724-2733.
62. Kano R, Konnai S, Onuma M, Ohashi K: **Microarray analysis of host immune responses to Marek's disease virus infection in vaccinated chickens.** *J Vet Med Sci* 2009, **71**(5):603-610.
63. Sarson AJ, Parvizi P, Lepp D, Quinton M, Sharif S: **Transcriptional analysis of host responses to Marek's disease virus infection in genetically resistant and susceptible chickens.** *Anim Genet* 2008, **39**(3):232-240.
64. Sarson AJ, Abdul-Careem MF, Zhou H, Sharif S: **Transcriptional analysis of host responses to Marek's disease viral infection.** *Viral Immunol* 2006, **19**(4):747-758.
65. Kaiser P, Underwood G, Davison F: **Differential cytokine responses following Marek's disease virus infection of chickens differing in resistance to Marek's disease.** *J Virol* 2003, **77**(1):762-768.
66. Winter J, Jung S, Keller S, Gregory RI, Diederichs S: **Many roads to maturity: microRNA biogenesis pathways and their regulation.** *Nat Cell Biol* 2009, **11**(3):228-234.
67. Lee Y, Kim M, Han J, Yeom KH, Lee S, Baek SH, Kim VN: **MicroRNA genes are transcribed by RNA polymerase II.** *Embo J* 2004, **23**(20):4051-4060.
68. Han J, Lee Y, Yeom KH, Nam JW, Heo I, Rhee JK, Sohn SY, Cho Y, Zhang BT, Kim VN: **Molecular basis for the recognition of primary microRNAs by the Drosha-DGCR8 complex.** *Cell* 2006, **125**(5):887-901.
69. Bartel DP: **MicroRNAs: genomics, biogenesis, mechanism, and function.** *Cell* 2004, **116**(2):281-297.
70. Luciano DJ, Mirsky H, Vendetti NJ, Maas S: **RNA editing of a miRNA precursor.** *Rna* 2004, **10**(8):1174-1177.
71. Yang W, Chendrimada TP, Wang Q, Higuchi M, Seeburg PH, Shiekhattar R, Nishikura K: **Modulation of microRNA processing and expression through RNA editing by ADAR deaminases.** *Nat Struct Mol Biol* 2006, **13**(1):13-21.
72. Blow MJ, Grocock RJ, van Dongen S, Enright AJ, Dicks E, Futreal PA, Wooster R, Stratton MR: **RNA editing of human microRNAs.** *Genome Biol* 2006, **7**(4):R27.
73. Kim VN: **Small RNAs: classification, biogenesis, and function.** *Mol Cells* 2005, **19**(1):1-15.

74. Schwarz DS, Hutvagner G, Du T, Xu Z, Aronin N, Zamore PD: **Asymmetry in the assembly of the RNAi enzyme complex.** *Cell* 2003, **115**(2):199-208.
75. Khvorova A, Reynolds A, Jayasena SD: **Functional siRNAs and miRNAs exhibit strand bias.** *Cell* 2003, **115**(2):209-216.
76. He L, Hannon GJ: **MicroRNAs: small RNAs with a big role in gene regulation.** *Nat Rev Genet* 2004, **5**(7):522-531.
77. Kim VN, Han J, Siomi MC: **Biogenesis of small RNAs in animals.** *Nat Rev Mol Cell Biol* 2009, **10**(2):126-139.
78. Krol J, Loedige I, Filipowicz W: **The widespread regulation of microRNA biogenesis, function and decay.** *Nat Rev Genet*, **11**(9):597-610.
79. Chuang JC, Jones PA: **Epigenetics and microRNAs.** *Pediatr Res* 2007, **61**(5 Pt 2):24R-29R.
80. Song JJ, Smith SK, Hannon GJ, Joshua-Tor L: **Crystal structure of Argonaute and its implications for RISC slicer activity.** *Science* 2004, **305**(5689):1434-1437.
81. Diederichs S, Haber DA: **Dual role for argonautes in microRNA processing and posttranscriptional regulation of microRNA expression.** *Cell* 2007, **131**(6):1097-1108.
82. Brodersen P, Voinnet O: **Revisiting the principles of microRNA target recognition and mode of action.** *Nat Rev Mol Cell Biol* 2009, **10**(2):141-148.
83. Lewis BP, Shih IH, Jones-Rhoades MW, Bartel DP, Burge CB: **Prediction of mammalian microRNA targets.** *Cell* 2003, **115**(7):787-798.
84. Stark A, Brennecke J, Russell RB, Cohen SM: **Identification of Drosophila MicroRNA targets.** *PLoS Biol* 2003, **1**(3):E60.
85. Yekta S, Shih IH, Bartel DP: **MicroRNA-directed cleavage of HOXB8 mRNA.** *Science* 2004, **304**(5670):594-596.
86. Guo H, Ingolia NT, Weissman JS, Bartel DP: **Mammalian microRNAs predominantly act to decrease target mRNA levels.** *Nature*, **466**(7308):835-840.
87. Giraldez AJ, Mishima Y, Rihel J, Grocock RJ, Van Dongen S, Inoue K, Enright AJ, Schier AF: **Zebrafish MiR-430 promotes deadenylation and clearance of maternal mRNAs.** *Science* 2006, **312**(5770):75-79.
88. Liu J, Valencia-Sanchez MA, Hannon GJ, Parker R: **MicroRNA-dependent localization of targeted mRNAs to mammalian P-bodies.** *Nat Cell Biol* 2005, **7**(7):719-723.
89. Vasudevan S, Tong Y, Steitz JA: **Switching from repression to activation: microRNAs can up-regulate translation.** *Science* 2007, **318**(5858):1931-1934.
90. Vasudevan S, Tong Y, Steitz JA: **Cell-cycle control of microRNA-mediated translation regulation.** *Cell Cycle* 2008, **7**(11):1545-1549.
91. Lytle JR, Yario TA, Steitz JA: **Target mRNAs are repressed as efficiently by microRNA-binding sites in the 5' UTR as in the 3' UTR.** *Proc Natl Acad Sci U S A* 2007, **104**(23):9667-9672.
92. Duursma AM, Kedde M, Schrier M, le Sage C, Agami R: **miR-148 targets human DNMT3b protein coding region.** *Rna* 2008, **14**(5):872-877.
93. Sethupathy P, Corda B, Hatzigeorgiou AG: **TarBase: A comprehensive**

- database of experimentally supported animal microRNA targets.** *Rna* 2006, **12**(2):192-197.
94. Xiao C, Rajewsky K: **MicroRNA control in the immune system: basic principles.** *Cell* 2009, **136**(1):26-36.
 95. Chen CZ, Li L, Lodish HF, Bartel DP: **MicroRNAs modulate hematopoietic lineage differentiation.** *Science* 2004, **303**(5654):83-86.
 96. Koralov SB, Muljo SA, Galler GR, Krek A, Chakraborty T, Kanellopoulou C, Jensen K, Cobb BS, Merkenschlager M, Rajewsky N *et al*: **Dicer ablation affects antibody diversity and cell survival in the B lymphocyte lineage.** *Cell* 2008, **132**(5):860-874.
 97. Ventura A, Young AG, Winslow MM, Lintault L, Meissner A, Erkeland SJ, Newman J, Bronson RT, Crowley D, Stone JR *et al*: **Targeted deletion reveals essential and overlapping functions of the miR-17 through 92 family of miRNA clusters.** *Cell* 2008, **132**(5):875-886.
 98. Baltimore D, Boldin MP, O'Connell RM, Rao DS, Taganov KD: **MicroRNAs: new regulators of immune cell development and function.** *Nat Immunol* 2008, **9**(8):839-845.
 99. Wu H, Neilson JR, Kumar P, Manocha M, Shankar P, Sharp PA, Manjunath N: **miRNA profiling of naive, effector and memory CD8 T cells.** *PLoS One* 2007, **2**(10):e1020.
 100. Li QJ, Chau J, Ebert PJ, Sylvester G, Min H, Liu G, Braich R, Manoharan M, Soutschek J, Skare P *et al*: **miR-181a is an intrinsic modulator of T cell sensitivity and selection.** *Cell* 2007, **129**(1):147-161.
 101. Liston A, Lu LF, O'Carroll D, Tarakhovskiy A, Rudensky AY: **Dicer-dependent microRNA pathway safeguards regulatory T cell function.** *J Exp Med* 2008, **205**(9):1993-2004.
 102. Calin GA, Croce CM: **MicroRNA signatures in human cancers.** *Nat Rev Cancer* 2006, **6**(11):857-866.
 103. Volinia S, Calin GA, Liu CG, Ambs S, Cimmino A, Petrocca F, Visone R, Iorio M, Roldo C, Ferracin M *et al*: **A microRNA expression signature of human solid tumors defines cancer gene targets.** *Proc Natl Acad Sci U S A* 2006, **103**(7):2257-2261.
 104. Meng F, Henson R, Lang M, Wehbe H, Maheshwari S, Mendell JT, Jiang J, Schmittgen TD, Patel T: **Involvement of human micro-RNA in growth and response to chemotherapy in human cholangiocarcinoma cell lines.** *Gastroenterology* 2006, **130**(7):2113-2129.
 105. Chan JA, Krichevsky AM, Kosik KS: **MicroRNA-21 is an antiapoptotic factor in human glioblastoma cells.** *Cancer Res* 2005, **65**(14):6029-6033.
 106. Johnson SM, Grosshans H, Shingara J, Byrom M, Jarvis R, Cheng A, Labourier E, Reinert KL, Brown D, Slack FJ: **RAS is regulated by the let-7 microRNA family.** *Cell* 2005, **120**(5):635-647.
 107. Grosshans H, Johnson T, Reinert KL, Gerstein M, Slack FJ: **The temporal patterning microRNA let-7 regulates several transcription factors at the larval to adult transition in C. elegans.** *Dev Cell* 2005, **8**(3):321-330.
 108. He L, Thomson JM, Hemann MT, Hernando-Monge E, Mu D, Goodson S, Powers S, Cordon-Cardo C, Lowe SW, Hannon GJ *et al*: **A microRNA**

- polycistron as a potential human oncogene.** *Nature* 2005, **435**(7043):828-833.
109. O'Donnell KA, Wentzel EA, Zeller KI, Dang CV, Mendell JT: **c-Myc-regulated microRNAs modulate E2F1 expression.** *Nature* 2005, **435**(7043):839-843.
 110. Castellano L, Giamas G, Jacob J, Coombes RC, Lucchesi W, Thiruchelvam P, Barton G, Jiao LR, Wait R, Waxman J *et al*: **The estrogen receptor-alpha-induced microRNA signature regulates itself and its transcriptional response.** *Proc Natl Acad Sci U S A* 2009, **106**(37):15732-15737.
 111. Brodersen P, Voinnet O: **The diversity of RNA silencing pathways in plants.** *Trends Genet* 2006, **22**(5):268-280.
 112. Otsuka M, Jing Q, Georgel P, New L, Chen J, Mols J, Kang YJ, Jiang Z, Du X, Cook R *et al*: **Hypersusceptibility to vesicular stomatitis virus infection in Dicer1-deficient mice is due to impaired miR24 and miR93 expression.** *Immunity* 2007, **27**(1):123-134.
 113. Pedersen IM, Cheng G, Wieland S, Volinia S, Croce CM, Chisari FV, David M: **Interferon modulation of cellular microRNAs as an antiviral mechanism.** *Nature* 2007, **449**(7164):919-922.
 114. Lecellier CH, Dunoyer P, Arar K, Lehmann-Che J, Eyquem S, Himber C, Saib A, Voinnet O: **A cellular microRNA mediates antiviral defense in human cells.** *Science* 2005, **308**(5721):557-560.
 115. Huang J, Wang F, Argyris E, Chen K, Liang Z, Tian H, Huang W, Squires K, Verlinghieri G, Zhang H: **Cellular microRNAs contribute to HIV-1 latency in resting primary CD4+ T lymphocytes.** *Nat Med* 2007, **13**(10):1241-1247.
 116. Pfeffer S, Sewer A, Lagos-Quintana M, Sheridan R, Sander C, Grasser FA, van Dyk LF, Ho CK, Shuman S, Chien M *et al*: **Identification of microRNAs of the herpesvirus family.** *Nat Methods* 2005, **2**(4):269-276.
 117. Pfeffer S, Zavolan M, Grasser FA, Chien M, Russo JJ, Ju J, John B, Enright AJ, Marks D, Sander C *et al*: **Identification of virus-encoded microRNAs.** *Science* 2004, **304**(5671):734-736.
 118. Ghosh Z, Mallick B, Chakrabarti J: **Cellular versus viral microRNAs in host-virus interaction.** *Nucleic Acids Res* 2009, **37**(4):1035-1048.
 119. Burnside J, Ouyang M, Anderson A, Bernberg E, Lu C, Meyers BC, Green PJ, Markis M, Isaacs G, Huang E *et al*: **Deep sequencing of chicken microRNAs.** *BMC Genomics* 2008, **9**:185.
 120. Yao Y, Zhao Y, Xu H, Smith LP, Lawrie CH, Watson M, Nair V: **MicroRNA profile of Marek's disease virus-transformed T-cell line MSB-1: predominance of virus-encoded microRNAs.** *J Virol* 2008, **82**(8):4007-4015.
 121. Zhao Y, Yao Y, Xu H, Lambeth L, Smith LP, Kgosana L, Wang X, Nair V: **A functional MicroRNA-155 ortholog encoded by the oncogenic Marek's disease virus.** *J Virol* 2009, **83**(1):489-492.
 122. Zhao Y, Xu H, Yao Y, Smith LP, Kgosana L, Green J, Petherbridge L, Baigent SJ, Nair V: **Critical role of the virus-encoded microRNA-155 ortholog in the induction of Marek's disease lymphomas.** *PLoS Pathog* 2011, **7**(2):e1001305.

123. Muylkens B, Coupeau D, Dambrine G, Trapp S, Rasschaert D: **Marek's disease virus microRNA designated Mdv1-pre-miR-M4 targets both cellular and viral genes.** *Arch Virol* 2010, **155**(11):1823-1837.
124. Xu S, Xue C, Li J, Bi Y, Cao Y: **Marek's disease virus type 1 microRNA miR-M3 suppresses cisplatin-induced apoptosis by targeting Smad2 of the transforming growth factor beta signal pathway.** *J Virol* 2010, **85**(1):276-285.
125. Hicks JA, Trakooljul N, Liu HC: **Discovery of chicken microRNAs associated with lipogenesis and cell proliferation.** *Physiol Genomics* 2009.
126. Hicks JA, Tembhurne PA, Liu HC: **Identification of microRNA in the developing chick immune organs.** *Immunogenetics* 2009, **61**(3):231-240.
127. Trakooljul N, Hicks JA, Liu HC: **Characterization of miR-10a mediated gene regulation in avian splenocytes.** *Gene* 2012, **500**(1):107-114.
128. Guillon-Munos A, Dambrine G, Richerieux N, Coupeau D, Muylkens B, Rasschaert D: **The chicken miR-150 targets the avian orthologue of the functional zebrafish MYB 3'UTR target site.** *BMC Mol Biol* 2010, **11**:67.
129. Lambeth LS, Yao Y, Smith LP, Zhao Y, Nair V: **MicroRNAs 221 and 222 target p27Kip1 in Marek's disease virus-transformed tumour cell line MSB-1.** *J Gen Virol* 2009, **90**(Pt 5):1164-1171.
130. Lister R, Pelizzola M, Dowen RH, Hawkins RD, Hon G, Tonti-Filippini J, Nery JR, Lee L, Ye Z, Ngo QM *et al*: **Human DNA methylomes at base resolution show widespread epigenomic differences.** *Nature* 2009, **462**(7271):315-322.
131. Ehrlich M, Gama-Sosa MA, Huang LH, Midgett RM, Kuo KC, McCune RA, Gehrke C: **Amount and distribution of 5-methylcytosine in human DNA from different types of tissues of cells.** *Nucleic Acids Res* 1982, **10**(8):2709-2721.
132. Gardiner-Garden M, Frommer M: **CpG islands in vertebrate genomes.** *J Mol Biol* 1987, **196**(2):261-282.
133. Lin IG, Tomzynski TJ, Ou Q, Hsieh CL: **Modulation of DNA binding protein affinity directly affects target site demethylation.** *Mol Cell Biol* 2000, **20**(7):2343-2349.
134. Williams K, Christensen J, Pedersen MT, Johansen JV, Cloos PA, Rappsilber J, Helin K: **TET1 and hydroxymethylcytosine in transcription and DNA methylation fidelity.** *Nature* 2010, **473**(7347):343-348.
135. Wu SC, Zhang Y: **Active DNA demethylation: many roads lead to Rome.** *Nat Rev Mol Cell Biol* 2010, **11**(9):607-620.
136. Lehnertz B, Ueda Y, Derijck AA, Braunschweig U, Perez-Burgos L, Kubicek S, Chen T, Li E, Jenuwein T, Peters AH: **Suv39h-mediated histone H3 lysine 9 methylation directs DNA methylation to major satellite repeats at pericentric heterochromatin.** *Curr Biol* 2003, **13**(14):1192-1200.
137. Brinkman AB, Gu H, Bartels SJ, Zhang Y, Matarese F, Simmer F, Marks H, Bock C, Gnirke A, Meissner A *et al*: **Sequential ChIP-bisulfite sequencing enables direct genome-scale investigation of chromatin and DNA methylation cross-talk.** *Genome Res* 2012.
138. Vire E, Brenner C, Deplus R, Blanchon L, Fraga M, Didelot C, Morey L, Van

- Eynde A, Bernard D, Vanderwinden JM *et al*: **The Polycomb group protein EZH2 directly controls DNA methylation.** *Nature* 2006, **439**(7078):871-874.
139. Kawasaki H, Taira K: **Induction of DNA methylation and gene silencing by short interfering RNAs in human cells.** *Nature* 2004, **431**(7005):211-217.
140. Waterland RA, Jirtle RL: **Transposable elements: targets for early nutritional effects on epigenetic gene regulation.** *Mol Cell Biol* 2003, **23**(15):5293-5300.
141. Jirtle RL, Skinner MK: **Environmental epigenomics and disease susceptibility.** *Nat Rev Genet* 2007, **8**(4):253-262.
142. Anway MD, Cupp AS, Uzumcu M, Skinner MK: **Epigenetic transgenerational actions of endocrine disruptors and male fertility.** *Science* 2005, **308**(5727):1466-1469.
143. Nan X, Ng HH, Johnson CA, Laherty CD, Turner BM, Eisenman RN, Bird A: **Transcriptional repression by the methyl-CpG-binding protein MeCP2 involves a histone deacetylase complex.** *Nature* 1998, **393**(6683):386-389.
144. Bell AC, West AG, Felsenfeld G: **The protein CTCF is required for the enhancer blocking activity of vertebrate insulators.** *Cell* 1999, **98**(3):387-396.
145. Heindel JJ, McAllister KA, Worth L, Jr., Tyson FL: **Environmental epigenomics, imprinting and disease susceptibility.** *Epigenetics* 2006, **1**(1):1-6.
146. Bibikova M, Chudin E, Wu B, Zhou L, Garcia EW, Liu Y, Shin S, Plaia TW, Auerbach JM, Arking DE *et al*: **Human embryonic stem cells have a unique epigenetic signature.** *Genome Res* 2006, **16**(9):1075-1083.
147. Danbara M, Kameyama K, Higashihara M, Takagaki Y: **DNA methylation dominates transcriptional silencing of Pax5 in terminally differentiated B cell lines.** *Mol Immunol* 2002, **38**(15):1161-1166.
148. Richardson B: **DNA methylation and autoimmune disease.** *Clin Immunol* 2003, **109**(1):72-79.
149. Javierre BM, Fernandez AF, Richter J, Al-Shahrour F, Martin-Subero JJ, Rodriguez-Ubreva J, Berdasco M, Fraga MF, O'Hanlon TP, Rider LG *et al*: **Changes in the pattern of DNA methylation associate with twin discordance in systemic lupus erythematosus.** *Genome Res* 2012, **20**(2):170-179.
150. Schwartz DA: **The importance of gene-environment interactions and exposure assessment in understanding human diseases.** *J Expo Sci Environ Epidemiol* 2006, **16**(6):474-476.
151. Meshorer E, Misteli T: **Chromatin in pluripotent embryonic stem cells and differentiation.** *Nat Rev Mol Cell Biol* 2006, **7**(7):540-546.
152. Bollati V, Schwartz J, Wright R, Litonjua A, Tarantini L, Suh H, Sparrow D, Vokonas P, Baccarelli A: **Decline in genomic DNA methylation through aging in a cohort of elderly subjects.** *Mech Ageing Dev* 2009, **130**(4):234-239.
153. Rakyan VK, Down TA, Balding DJ, Beck S: **Epigenome-wide association studies for common human diseases.** *Nat Rev Genet* 2011, **12**(8):529-541.

154. Bobetsis YA, Barros SP, Lin DM, Weidman JR, Dolinoy DC, Jirtle RL, Boggess KA, Beck JD, Offenbacher S: **Bacterial infection promotes DNA hypermethylation.** *J Dent Res* 2007, **86**(2):169-174.
155. Paschos K, Smith P, Anderton E, Middeldorp JM, White RE, Allday MJ: **Epstein-barr virus latency in B cells leads to epigenetic repression and CpG methylation of the tumour suppressor gene Bim.** *PLoS Pathog* 2009, **5**(6):e1000492.
156. Kalla M, Gobel C, Hammerschmidt W: **The lytic phase of epstein-barr virus requires a viral genome with 5-methylcytosine residues in CpG sites.** *J Virol* 2012, **86**(1):447-458.
157. Corcoran DL, Pandit KV, Gordon B, Bhattacharjee A, Kaminski N, Benos PV: **Features of mammalian microRNA promoters emerge from polymerase II chromatin immunoprecipitation data.** *PLoS One* 2009, **4**(4):e5279.
158. Ozsolak F, Poling LL, Wang Z, Liu H, Liu XS, Roeder RG, Zhang X, Song JS, Fisher DE: **Chromatin structure analyses identify miRNA promoters.** *Genes Dev* 2008, **22**(22):3172-3183.
159. Han L, Witmer PD, Casey E, Valle D, Sukumar S: **DNA methylation regulates MicroRNA expression.** *Cancer Biol Ther* 2007, **6**(8):1284-1288.
160. Saito Y, Liang G, Egger G, Friedman JM, Chuang JC, Coetzee GA, Jones PA: **Specific activation of microRNA-127 with downregulation of the proto-oncogene BCL6 by chromatin-modifying drugs in human cancer cells.** *Cancer Cell* 2006, **9**(6):435-443.
161. Weber B, Stresemann C, Brueckner B, Lyko F: **Methylation of human microRNA genes in normal and neoplastic cells.** *Cell Cycle* 2007, **6**(9):1001-1005.
162. Fabbri M, Garzon R, Cimmino A, Liu Z, Zanesi N, Callegari E, Liu S, Alder H, Costinean S, Fernandez-Cymering C *et al*: **MicroRNA-29 family reverts aberrant methylation in lung cancer by targeting DNA methyltransferases 3A and 3B.** *Proc Natl Acad Sci U S A* 2007, **104**(40):15805-15810.
163. Lujambio A, Calin GA, Villanueva A, Ropero S, Sanchez-Cespedes M, Blanco D, Montuenga LM, Rossi S, Nicoloso MS, Faller WJ *et al*: **A microRNA DNA methylation signature for human cancer metastasis.** *Proc Natl Acad Sci U S A* 2008, **105**(36):13556-13561.
164. Lujambio A, Esteller M: **How epigenetics can explain human metastasis: a new role for microRNAs.** *Cell Cycle* 2009, **8**(3):377-382.
165. Lindsay MA: **microRNAs and the immune response.** *Trends Immunol* 2008, **29**(7):343-351.
166. Lu J, Getz G, Miska EA, Alvarez-Saavedra E, Lamb J, Peck D, Sweet-Cordero A, Ebert BL, Mak RH, Ferrando AA *et al*: **MicroRNA expression profiles classify human cancers.** *Nature* 2005, **435**(7043):834-838.
167. Davison TF, Nair V: **Marek's disease : an evolving problem.** Amsterdam ; Boston: Elsevier; 2004.
168. Abdul-Careem MF, Hunter BD, Nagy E, Read LR, Sanei B, Spencer JL, Sharif S: **Development of a real-time PCR assay using SYBR Green**

- chemistry for monitoring Marek's disease virus genome load in feather tips. *J Virol Methods* 2006, **133**(1):34-40.**
169. Zehner ZE, Paterson BM: **Characterization of the chicken vimentin gene: single copy gene producing multiple mRNAs.** *Proc Natl Acad Sci U S A* 1983, **80**(4):911-915.
170. Smyth GK: **Linear models and empirical bayes methods for assessing differential expression in microarray experiments.** *Stat Appl Genet Mol Biol* 2004, **3**:Article3.
171. Smyth GK, Speed T: **Normalization of cDNA microarray data.** *Methods* 2003, **31**(4):265-273.
172. Eisen MB, Spellman PT, Brown PO, Botstein D: **Cluster analysis and display of genome-wide expression patterns.** *Proc Natl Acad Sci U S A* 1998, **95**(25):14863-14868.
173. Lee LF, Powell PC, Rennie M, Ross LJ, Payne LN: **Nature of genetic resistance to Marek's disease in chickens.** *J Natl Cancer Inst* 1981, **66**(4):789-796.
174. Burgess SC, Davison TF: **Identification of the neoplastically transformed cells in Marek's disease herpesvirus-induced lymphomas: recognition by the monoclonal antibody AV37.** *J Virol* 2002, **76**(14):7276-7292.
175. Persengiev SP, Green MR: **The role of ATF/CREB family members in cell growth, survival and apoptosis.** *Apoptosis* 2003, **8**(3):225-228.
176. Liu H, Kohane IS: **Tissue and process specific microRNA-mRNA co-expression in mammalian development and malignancy.** *PLoS One* 2009, **4**(5):e5436.
177. Sayed D, Abdellatif M: **MicroRNAs in development and disease.** *Physiol Rev* 2011, **91**(3):827-887.
178. Farh KK, Grimson A, Jan C, Lewis BP, Johnston WK, Lim LP, Burge CB, Bartel DP: **The widespread impact of mammalian MicroRNAs on mRNA repression and evolution.** *Science* 2005, **310**(5755):1817-1821.
179. Shkumatava A, Stark A, Sive H, Bartel DP: **Coherent but overlapping expression of microRNAs and their targets during vertebrate development.** *Genes Dev* 2009, **23**(4):466-481.
180. Bhoumik A, Ronai Z: **ATF2: a transcription factor that elicits oncogenic or tumor suppressor activities.** *Cell Cycle* 2008, **7**(15):2341-2345.
181. Bhoumik A, Gangi L, Ronai Z: **Inhibition of melanoma growth and metastasis by ATF2-derived peptides.** *Cancer Res* 2004, **64**(22):8222-8230.
182. Garzon R, Liu S, Fabbri M, Liu Z, Heaphy CE, Callegari E, Schwind S, Pang J, Yu J, Muthusamy N *et al*: **MicroRNA-29b induces global DNA hypomethylation and tumor suppressor gene reexpression in acute myeloid leukemia by targeting directly DNMT3A and 3B and indirectly DNMT1.** *Blood* 2009, **113**(25):6411-6418.
183. Braconi C, Huang N, Patel T: **MicroRNA-dependent regulation of DNA methyltransferase-1 and tumor suppressor gene expression by interleukin-6 in human malignant cholangiocytes.** *Hepatology* 2010, **51**(3):881-890.
184. Scaria V, Hariharan M, Maiti S, Pillai B, Brahmachari SK: **Host-virus**

- interaction: a new role for microRNAs.** *Retrovirology* 2006, **3**:68.
185. Henke JI, Goergen D, Zheng J, Song Y, Schuttler CG, Fehr C, Junemann C, Niepmann M: **microRNA-122 stimulates translation of hepatitis C virus RNA.** *Embo J* 2008, **27**(24):3300-3310.
186. Roberts AP, Lewis AP, Jopling CL: **miR-122 activates hepatitis C virus translation by a specialized mechanism requiring particular RNA components.** *Nucleic Acids Res* 2011, **39**(17):7716-7729.
187. Yao Y, Zhao Y, Smith LP, Lawrie CH, Saunders NJ, Watson M, Nair V: **Differential expression of microRNAs in Marek's disease virus-transformed T-lymphoma cell lines.** *J Gen Virol* 2009, **90**(Pt 7):1551-1559.
188. Chen M, Payne WS, Hunt H, Zhang H, Holmen SL, Dodgson JB: **Inhibition of Marek's disease virus replication by retroviral vector-based RNA interference.** *Virology* 2008, **377**(2):265-272.
189. Li SD, Chono S, Huang L: **Efficient oncogene silencing and metastasis inhibition via systemic delivery of siRNA.** *Mol Ther* 2008, **16**(5):942-946.
190. ter Brake O, Berkhout B: **A novel approach for inhibition of HIV-1 by RNA interference: counteracting viral escape with a second generation of siRNAs.** *J RNAi Gene Silencing* 2005, **1**(2):56-65.
191. ter Brake O, t Hooft K, Liu YP, Centlivre M, von Eije KJ, Berkhout B: **Lentiviral vector design for multiple shRNA expression and durable HIV-1 inhibition.** *Mol Ther* 2008, **16**(3):557-564.
192. Kim JH, Dhanasekaran SM, Prensner JR, Cao X, Robinson D, Kalyana-Sundaram S, Huang C, Shankar S, Jing X, Iyer M *et al*: **Deep sequencing reveals distinct patterns of DNA methylation in prostate cancer.** *Genome Res* 2011, **21**(7):1028-1041.
193. Feinberg AP, Tycko B: **The history of cancer epigenetics.** *Nat Rev Cancer* 2004, **4**(2):143-153.
194. Brown AC, Nair V, Allday MJ: **Epigenetic regulation of the latency-associated region of Marek's disease virus in tumor-derived T-cell lines and primary lymphoma.** *J Virol* 2011, **86**(3):1683-1695.
195. Bock C, Tomazou EM, Brinkman AB, Muller F, Simmer F, Gu H, Jager N, Gnirke A, Stunnenberg HG, Meissner A: **Quantitative comparison of genome-wide DNA methylation mapping technologies.** *Nat Biotechnol* 2010, **28**(10):1106-1114.
196. Edwards JR, O'Donnell AH, Rollins RA, Peckham HE, Lee C, Milekic MH, Chanrion B, Fu Y, Su T, Hibshoosh H *et al*: **Chromatin and sequence features that define the fine and gross structure of genomic methylation patterns.** *Genome Res* 2010, **20**(7):972-980.
197. Robertson KD, Uzvolgyi E, Liang G, Talmadge C, Sumegi J, Gonzales FA, Jones PA: **The human DNA methyltransferases (DNMTs) 1, 3a and 3b: coordinate mRNA expression in normal tissues and overexpression in tumors.** *Nucleic Acids Res* 1999, **27**(11):2291-2298.
198. Feinberg AP, Gehrke CW, Kuo KC, Ehrlich M: **Reduced genomic 5-methylcytosine content in human colonic neoplasia.** *Cancer Res* 1988, **48**(5):1159-1161.
199. Mizuno S, Chijiwa T, Okamura T, Akashi K, Fukumaki Y, Niho Y, Sasaki H:

- Expression of DNA methyltransferases DNMT1, 3A, and 3B in normal hematopoiesis and in acute and chronic myelogenous leukemia.** *Blood* 2001, **97**(5):1172-1179.
200. Leonard S, Wei W, Anderton J, Vockerodt M, Rowe M, Murray PG, Woodman CB: **Epigenetic and transcriptional changes which follow Epstein-Barr virus infection of germinal center B cells and their relevance to the pathogenesis of Hodgkin's lymphoma.** *J Virol* 2011, **85**(18):9568-9577.
201. Kim GD, Ni J, Kelesoglu N, Roberts RJ, Pradhan S: **Co-operation and communication between the human maintenance and de novo DNA (cytosine-5) methyltransferases.** *Embo J* 2002, **21**(15):4183-4195.
202. Ostler KR, Davis EM, Payne SL, Gosalia BB, Exposito-Cespedes J, Le Beau MM, Godley LA: **Cancer cells express aberrant DNMT3B transcripts encoding truncated proteins.** *Oncogene* 2007, **26**(38):5553-5563.
203. Li Q, Li N, Hu X, Li J, Du Z, Chen L, Yin G, Duan J, Zhang H, Zhao Y *et al*: **Genome-wide mapping of DNA methylation in chicken.** *PLoS One* 2011, **6**(5):e19428.
204. Laird PW: **Principles and challenges of genomewide DNA methylation analysis.** *Nat Rev Genet* 2010, **11**(3):191-203.
205. Singh H: **Teeing up transcription on CpG islands.** *Cell* 2009, **138**(1):14-16.
206. Feschotte C: **Transposable elements and the evolution of regulatory networks.** *Nat Rev Genet* 2008, **9**(5):397-405.
207. Jordan IK, Rogozin IB, Glazko GV, Koonin EV: **Origin of a substantial fraction of human regulatory sequences from transposable elements.** *Trends Genet* 2003, **19**(2):68-72.
208. Huda A, Jordan IK: **Epigenetic regulation of Mammalian genomes by transposable elements.** *Ann N Y Acad Sci* 2009, **1178**:276-284.
209. Slotkin RK, Martienssen R: **Transposable elements and the epigenetic regulation of the genome.** *Nat Rev Genet* 2007, **8**(4):272-285.
210. Esteller M: **Epigenetics in cancer.** *N Engl J Med* 2008, **358**(11):1148-1159.
211. Consortium ICGS: **Sequence and comparative analysis of the chicken genome provide unique perspectives on vertebrate evolution.** *Nature* 2004, **432**(7018):695-716.
212. Lee SH, Eldi P, Cho SY, Rangasamy D: **Control of chicken CR1 retrotransposons is independent of Dicer-mediated RNA interference pathway.** *BMC Biol* 2009, **7**:53.
213. Liu HC, Kung HJ, Fulton JE, Morgan RW, Cheng HH: **Growth hormone interacts with the Marek's disease virus SORF2 protein and is associated with disease resistance in chicken.** *Proc Natl Acad Sci U S A* 2001, **98**(16):9203-9208.
214. Duncan MC, Peifer M: **Regulating polarity by directing traffic: Cdc42 prevents adherens junctions from crumbling' aPart.** *J Cell Biol* 2008, **183**(6):971-974.
215. Karin M, Cao Y, Greten FR, Li ZW: **NF-kappaB in cancer: from innocent bystander to major culprit.** *Nat Rev Cancer* 2002, **2**(4):301-310.
216. Blanc M, Hsieh WY, Robertson KA, Watterson S, Shui G, Lacaze P,

- Khondoker M, Dickinson P, Sing G, Rodriguez-Martin S *et al*: **Host defense against viral infection involves interferon mediated down-regulation of sterol biosynthesis.** *PLoS Biol* 2011, **9**(3):e1000598.
217. Cairns RA, Harris IS, Mak TW: **Regulation of cancer cell metabolism.** *Nat Rev Cancer* 2011, **11**(2):85-95.
218. Lucas A, Dai E, Liu LY, Nation PN: **Atherosclerosis in Marek's disease virus infected hypercholesterolemic roosters is reduced by HMGCoA reductase and ACE inhibitor therapy.** *Cardiovasc Res* 1998, **38**(1):237-246.
219. Fabricant CG, Fabricant J, Minick CR, Litrenta MM: **Herpesvirus-induced atherosclerosis in chickens.** *Fed Proc* 1983, **42**(8):2476-2479.
220. Fynan EF, Ewert DL, Block TM: **Latency and reactivation of Marek's disease virus in B lymphocytes transformed by avian leukosis virus.** *J Gen Virol* 1993, **74** (Pt 10):2163-2170.
221. Smith CA, Roeszler KN, Ohnesorg T, Cummins DM, Farlie PG, Doran TJ, Sinclair AH: **The avian Z-linked gene DMRT1 is required for male sex determination in the chicken.** *Nature* 2009, **461**(7261):267-271.
222. Paddison PJ, Caudy AA, Bernstein E, Hannon GJ, Conklin DS: **Short hairpin RNAs (shRNAs) induce sequence-specific silencing in mammalian cells.** *Genes Dev* 2002, **16**(8):948-958.
223. Rapp JC, Harvey AJ, Speksnijder GL, Hu W, Ivarie R: **Biologically active human interferon alpha-2b produced in the egg white of transgenic hens.** *Transgenic Res* 2003, **12**(5):569-575.
224. Bosselman RA, Hsu RY, Boggs T, Hu S, Bruszewski J, Ou S, Kozar L, Martin F, Green C, Jacobsen F *et al*: **Germline transmission of exogenous genes in the chicken.** *Science* 1989, **243**(4890):533-535.
225. Lois C, Hong EJ, Pease S, Brown EJ, Baltimore D: **Germline transmission and tissue-specific expression of transgenes delivered by lentiviral vectors.** *Science* 2002, **295**(5556):868-872.
226. Kim J, Kollhoff A, Bergmann A, Stubbs L: **Methylation-sensitive binding of transcription factor YY1 to an insulator sequence within the paternally expressed imprinted gene, Peg3.** *Hum Mol Genet* 2003, **12**(3):233-245.
227. Hodges E, Molaro A, Dos Santos CO, Thekkat P, Song Q, Uren PJ, Park J, Butler J, Rafii S, McCombie WR *et al*: **Directional DNA methylation changes and complex intermediate states accompany lineage specificity in the adult hematopoietic compartment.** *Mol Cell* 2011, **44**(1):17-28.
228. Gebhard C, Benner C, Ehrich M, Schwarzfischer L, Schilling E, Klug M, Dietmaier W, Thiede C, Holler E, Andreesen R *et al*: **General transcription factor binding at CpG islands in normal cells correlates with resistance to de novo DNA methylation in cancer cells.** *Cancer Res* 2010, **70**(4):1398-1407.
229. Pepe MS, Etzioni R, Feng Z, Potter JD, Thompson ML, Thornquist M, Winget M, Yasui Y: **Phases of biomarker development for early detection of cancer.** *J Natl Cancer Inst* 2001, **93**(14):1054-1061.
230. Kim M, Long TI, Arakawa K, Wang R, Yu MC, Laird PW: **DNA methylation as a biomarker for cardiovascular disease risk.** *PLoS One*

2010, **5**(3):e9692.

231. Anglim PP, Alonzo TA, Laird-Offringa IA: **DNA methylation-based biomarkers for early detection of non-small cell lung cancer: an update.** *Mol Cancer* 2008, **7**:81.